UNIVERSITY OF CALIFORNIA,
IRVINE

Fully Integrated Molecular Diagnostic CD Platform Based on Thermal Control

DISSERTATION

submitted in partial satisfaction of the requirements
for the degree of

DOCTOR OF PHILOSOPHY

in Biomedical Engineering

by

Ling Xuan Kong

Dissertation Committee:
Professor Marc Madou, Chair
Professor William Tang
Professor James Brody

2015

DEDICATION

To my father, who encouraged me to study a subject that I love in depth, and to his father, who taught me everything about discipline, ethics, and honor.

Table of Contents

List of Figures

List of Tables

ACKNOWLEDGMENTS

First and foremost, I would like to thank Professor Marc Madou for giving me the opportunity to be a part of his group. During my graduate study, I gained an invaluable amount of knowledge and experience. I have always been appreciative of Professor Madou's unique and inspiring insight on problem solving and future outlook.

I would also like to thank Dr. Lawrence Kulinsky, Dr. Régis Peytavi, and Dr. Horacio Kido for their expertise. They have given me guidance in essentially every relevant aspect and I cannot imagine doing my research without their help.

I would like to thank my committee members, Professor William Tang and Professor James Brody, as well as Professor Lorenzo Valdevit and Dr Ping Wang, for advising me on my graduate work.

I would like to acknowledge my collaborators in Canada, including Dr. Michel Bergeron and Dr. Gale Stewart at Centre de Recherche en Infectiologie; Dr. Teodor Veres (especially hosting me when I visited Montréal), Dr. Liviu Clime, Dr. Emmanuel Roy, and Maxence Mounier at the National Research Council; and David Béliveau-Viel at Centre d'optique, photonique et laser. I have learned a lot from our collaboration and appreciate any guidance and materials that I received.

I am thankful for Dr. Kameel Abi-Samra for his guidance when I joined the lab. He taught me everything essential for my field and was patient enough to include me in every aspect of his projects. While I was careful in my experimental design, Kameel was efficient and motivated. We were great lab partners, and became good friends.

I am extremely fortunate to have Alexandra Perebikovsky as a lab partner starting 2012. Though I was initially her research mentor, her quickness to learn, unique outlook on different projects and scientific problems, and unbeatable level of curiosity have taught me a tremendous amount. She was there through all of my ups and downs. We have become close friends and I look up to her in countless ways.

I would also like to Kshama Parate, who has been a great lab partner and friend. She has been extremely supportive and motivational during the publication process for my first first-author journal article. I would also like to thank Jacob Moebius for being supportive and tremedously helpful wherever he was able to contribute, and I would like to thank Tae-Hyeong Kim for our first collaboration.

Next, I would like to thank Dr. José Manuel Rodríguez-Delgado, Sunshine Holmberg, and Sergey Shaboyan. My work would not have been possible without them. I would like to thank Matias Vazquez for his advice on my work. I would also like to thank Amin Kazemzadeh (Kewmars) and M. Mahdi Aeinehvand for our mini-collaborations. Additionally, I would like to thank Bryce Kubo, Kimberly Sarrisin, Jigar Shah, Shilpa Jagannath, Lijie Chen, Yangdy Chen, Thai Nguyen, and Sepehr Zomorodian for their contribution. I would like to thank all of the friends I made in and out of the BioMEMS Lab throughout my graduate studies.

Finally, I would like to recognize Transon Nguyen and Siavash Ahrar for their academic and life advice, for being patient, and for being amazing friends.

I would like to acknowledge the National Institute of Health for funding me under grant 1R01AI089541-01.

I would like to acknowledge SAGE Publications, Springer Science+Business Media, The Royal Society of Chemistry, Elsevier, The Electrochemical Society, The International Society for Advancement of Cytometry, The American Chemical Society, and PLOS One for allowing me to reuse their published material.

CURRICULUM VITAE

Ling Xuan Kong

EDUCATION

Doctor of Philosophy in Biomedical Engineering **2015**
University of California, Irvine *Irvine, CA*

Bachelor of Science in Biomedical Engineering **2010**
University of California, Irvine *Irvine, CA*

RESEARCH EXPERIENCE

Graduate Student Researcher **2010-2015**
BioMEMS Laboratory with Prof. Marc Madou *University of California, Irvine*

Undergraduate Research Assistant **2009-2010**
Hearing and Speech Lab with Prof. Fan-Gang Zeng *University of California, Irvine*

Undergraduate Research Assistant **2007-2009**
Dr. Hans Keirstead's Lab *University of California, Irvine*

PEER-REVIEWED JOURNAL PUBLICATIONS

L. X. Kong, K. Parate, K. Abi-Samra, and M. Madou, "Multifunctional wax valves for liquid handling and incubation on a microfluidic CD," *Microfluid. Nanofluidics*, Oct. 2014.

L. X. Kong, A. Perebikovsky, J. Moebius, L. Kulinsky, and M. Madou, "Lab-on-a-CD: a fully integrated molecular diagnostic system," *J. Assoc. Lab. Autom.* May 2015. Accepted for publication.

K. Abi-Samra, L. Clime, L. Kong, R. Gorkin, T.-H. Kim, Y.-K. Cho, and M. Madou, "Thermo-pneumatic pumping in centrifugal microfluidic platforms," *Microfluid. Nanofluidics*, vol. 11, no. 5, pp. 643652, Jun. 2011.

CONFERENCE PUBLICATIONS

L. Kong, J. M. Rodriguez, A. Perebikovsky, J. Moebius, R. Mitchell, L. Kulinsky, and M. Madou, "Novel heating and cooling techniques on a centrifugal fluidic platform for polymerase chain reaction," in *Microtechnologies in Medicine and Biology*, 2013.

ABSTRACT OF THE DISSERTATION

Fully Integrated Molecular Diagnostic CD Platform Based on Thermal Control

By

Ling Xuan Kong

Doctor of Philosophy in Biomedical Engineering

University of California, Irvine, 2015

Professor Marc Madou, Chair

Centrifugal microfluidics, or compact disc (CD) microfluidics, has been gaining popularity in the lab-on-a-chip field as an advanced diagnostic platform over the last fifteen years. The lab-on-a-disc (LoD) platform embodies advantages of the lab-on-a-chip platform, including small volumes, fast reaction times, low power consumption, and portability; it also has other unique advantages, including embedded fluid pump operation and ease of automation and multiplexing. These advantages make the lab-on-a-disc diagnostic system attractive due to its capability for rapid disease diagnosis. In clinical diagnostics, rapid nucleic acid biomarker detection generally has been a challenge especially due to the rigorous thermocycling required to bring the biomarker quantity up to a delectable level. This work follows the development of a diagnostic microfluidic disc that utilizes polymerase chain reaction for DNA amplification and a DNA microarray that allows for visual detection of numerous target biomarkers. The assay begins with a sample volume that undergoes preparation, thermocycling, post-processing, and detection, so a number of challenges must be addressed; these challenges include precise fluid manipulation, application of heat, and storage and release of reagents. Along the way, modular fluid-handling techniques, including the thermo-pneumatic pump (TPP) and the multifunctional wax valves (MWV), were implemented to reduce the complexity and cost of the overall hardware system. This system would not only be capable of nucleic acid amplification but also specialized multiplexed biomarker amplification and

detection. It is anticipated that this platform will provide a foundation for the development of other fully-integrated LoD systems for rapid disease diagnosis in the near future.

Chapter 1

Introduction

The field of centrifugal microfluidics has experienced tremendous growth over the last fifteen years, especially in applications such as lab-on-disc (LoD) diagnostics. The strength of LoD systems is in its potential for integrated sample-to-answer analysis systems. This chapter highlights the technologies necessary to develop the next generation of these systems. In addition to outlining valving and other fluid-handling operations, this chapter discusses the recent advances and future outlook in four categories of LoD processes: reagent storage, sample preparation, nucleic acid amplification, analyte detection strategies. Lastly, the need for true sample-to-answer diagnostic systems is briefly discussed, including the current availability and need of commercial systems that are capable of rapid and effective molecular diagnostics, an assay that improves turnaround times for clinical diagnostics.

1.1 Characteristics of the Centrifugal Microfluidic Platform

Centrifugal microfluidic devices, also called lab-on-a-disc (LoD) systems, comprise a subcategory of lab-on-a-chip (LoC) devices. LoC platforms have advantages such as reduced cost, the use of smaller amounts of materials and reagents, faster reaction times due to small liquid volumes and diffusion distances, portability, and programmability. While LoD systems incorporate the same advantages as miniature chip-based systems, their superiority lies in their inherent simplicity. A simple motor generates several pseudo forces on the platform: the centrifugal force, which acts as a liquid pump and generates a force gradient affecting fluids differently at varying radial positions, the Coriolis force, which allows for direction-specific liquid pumping control, and the Euler force, which can be used to create turbulence during mixing. The disc rotation facilitates multiplexing of several assays on a single disc, separating components of a sample by density, eliminating trapped bubbles, and allowing liquids to be pumped without direct contact with external hardware (see expanded list in Table 1.1). A comprehensive comparison of the characteristics of different microfluidic platforms can be found in the dissertation by Jia [1].

While many different assays, such as enzyme-linked immunosorbent assay (ELISA) and blood chemistry panels, have already been automated on the lab-on-a-disc platform, there is a demand for a wider range of fully integrated assays that require precisely controlled operational parameters. Therefore, this chapter emphasizes molecular diagnostic assays techniques, which can be especially challenging to implement on centrifugal microfluidic platforms and have not been adequately covered in previous reviews [2–6].

This paper first provides a background of the physical effects of the centrifugal microfluidic system before introducing the most common fabrication methods used for prototyping and mass production of microfluidic discs. Operations such as valving, pumping, mixing,

Table 1.1: Advantageous and disadvantageous characteristics Lab-on-Chip and Lab-on-Disc platforms. Generally, advantages of the LoC platform are also present on the LoD platform.

Lab-on-a-Chip (LoC) Advantages	**Lab-on-a-Disc (LoD)** Advantages
• Reduced material cost • Reduced reagent volume and cost • Smaller diffusion distances and faster mixing • Portable and programmable • Time-saving and labor-saving Disadvantages • Tubing is required for fluid pumping • Difficulty handling larger volumes • Bubble formation • Difficult to multiplex	• Uses only a motor to pump fluids (allows for closed fluidic network) • Pumps fluids of a variety of physicochemical properties • Able to work with a wide range of volumes • Multiplexing of several assays on one disc • Easy to mix and meter fluids • Density-based separation • Eliminates trapped bubbles Disadvantages • Unidirectional nature of liquid flow • Difficulty working with very small volumes (<1 nanoliter)

and volume definition are important for sequencing the different fluidic processes in any on-disc assay. Therefore, a large section of this chapter is devoted to techniques that perform fluid-handling tasks on a LoD platform (Section 1.4).

Molecular diagnostic assays need to include storage and dispensation of reagents, efficient sample preparation, nucleic acid amplification, and rapid detection, all seamlessly integrated on a fluidic platform. This chapter examines the current state-of-the-art in all of the assay steps outlined above and provides the future outlook for point-of-care molecular diagnostics on a CD.

1.2 Physics Framework

The LoD platform utilizes centrifugal, Coriolis, and Euler forces to manipulate liquid flow on the disc (see Figure 1.1). These three forces are pseudo forces—fictitious forces with respect to a rotating, or non-inertial, frame of reference.

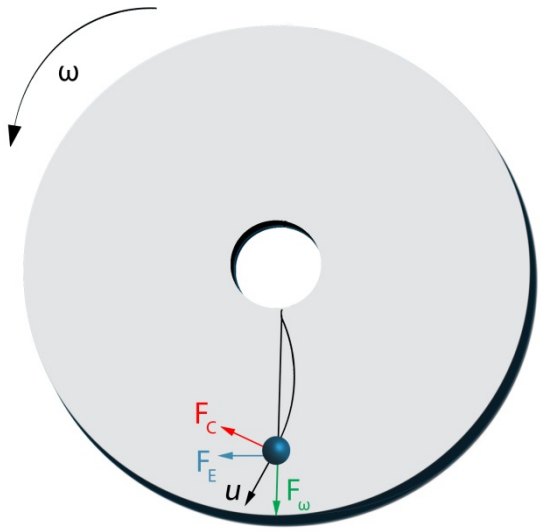

Figure 1.1: Schematic of forces present on a rotating platform. F_ω is the centrifugal force, F_C is the Coriolis force, which is perpendicular to the velocity vector, and F_E is the Euler force, which is perpendicular to the centrifugal force. The particle can represent a unit volume of liquid.

Although each of the pseudo forces has its respective characteristics and applications, the main driving force for fluids on a disc is the centrifugal force, which propels liquid radially outward from the center of the disc, forcing it through channels and chambers. The centrifugal force acting on each unit volume of liquid, also referred to as a "particle", is represented by eq. (1.1):

$$\vec{F_\omega} = \rho\vec{\omega}(\vec{\omega} \times \vec{r}) \tag{1.1}$$

where ρ is the liquid density, $\vec{r}$ is the average distance of the liquid from the center of the disc, and $\vec{\omega}$ is the angular velocity in rad/s.

The Coriolis force is perpendicular to the velocity vector of the moving particle shown in Figure 1.1. The force per unit volume is:

$$\vec{F_c} = -2\rho\vec{\omega} \times \vec{u} \tag{1.2}$$

where ρ is the liquid density, $\vec{\omega}$ is the angular velocity in rad/s, and $\vec{u}$ is the velocity vector of the particle moving on the disc. The Coriolis force is used in applications for particle separation (refer to Section 1.6.1) and in flow-switching techniques [7].

The Euler force is perpendicular to the centrifugal force and opposite to the direction of angular acceleration. This force is only generated when the angular velocity changes with respect to time, and the force per unit volume is:

$$\vec{F_e} = -\rho\frac{d\vec{\omega}}{dt} \times \vec{r} \tag{1.3}$$

where ρ is the liquid density, $\frac{d\vec{\omega}}{dt}$ is the change in angular velocity per unit time, and $\vec{r}$ is the average distance of the liquid from the center of the disc. Generally, the Euler force is applied during oscillation of disc angular velocity for mixing.

In most cases, only the centrifugal force is utilized for liquid propulsion. Liquid flow characteristics are dependent on the liquid's properties (e.g. density and viscosity), its radial location on the disc, the angular velocity of the disc, and the geometry of the microfluidic features. This flow rate was characterized by Madou *et al.* and Duffy *et al.*, who derived the flow rates of liquids on a LoD platform from basic centrifuge theory [8, 9]. The average velocity of the liquid on a spinning platform is given by eq. (1.4):

$$\vec{U} = \frac{D_b^2\rho\vec{\omega^2}\bar{r}\,\Delta r}{32\mu L} \tag{1.4}$$

where D_b is the hydraulic diameter of the channel (defined as $4A/P$, where A is the cross-sectional area and P is the wetted perimeter), ρ is the liquid density, $\vec{\omega}$ is the angular velocity of the disc, $\bar{r}$ is the average distance of the liquid in the channel from the center of the disc, Δr is the radial extent of the liquid, μ is the viscosity of the liquid, and L is the length of the liquid column in the microchannel.

The volumetric flow rate (Q) is defined in eq. (1.5):

$$Q = \vec{U} \cdot \vec{A} \tag{1.5}$$

Flow rates achieved experimentally by Duffy *et al.* exhibited no systematic deviation from the theoretical model and ranged from 5 nl/s to 0.1 ml/s depending on a combination of factors including rotational speeds of the disc (400-1,600 revolutions per minute, or RPM), channel widths (20-500 μm), and channel depths (16-340 μm) [9]. Since this early work, higher rotational speeds and greater variation in channel width and depth have been used to achieve flow rates that are significantly higher [6].

Furthermore, Duffy *et al.* tested the flow rates of different liquids to verify the effectiveness of the centrifugal pumping mechanism when pumping liquids with a variety of physicochemical properties such as pH, ionic strength, and conductivity [9].

1.3 CD Fabrication

Successful adoption and utilization of LoD systems depend on inexpensive and reliable solutions for manufacturing disposable CDs. Common materials used for microfluidic discs include, but are not limited to, polycarbonate, poly(methyl methacrylate) (PMMA), cyclic olefin polymer (COP), polydimethylsiloxane (PDMS), and polyurethane. Often, optical de-

tection requires optical grade materials, which can be costly. The materials listed can be used for rapid prototyping by molding, 3D printing, laminating, and CNC machining, and some can be injection molded for mass production. For rapid prototyping purposes, microfluidic discs are generally made from layers of adhesives and hard plastics (see Figure 1.2) [10]. Features can be cut into polycarbonate, PMMA, or COP sheets using a milling machine [10, 11]. PDMS and polyurethane features can be molded using, for example, a wax or SU-8 mold [9, 12]. PMMA can be cut using a laser, while COP and other polymers in thin sheet form can also be embossed or micro-thermoformed [12, 13].

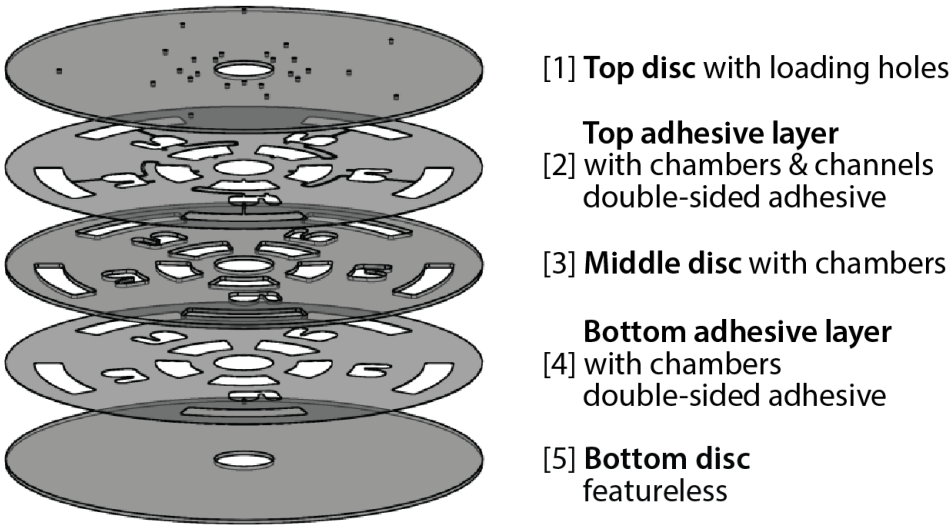

Figure 1.2: Five-layer disc assembly method. Layers 1, 3, and 5 are typically made from a hard plastic material. Layers 2 and 4 are typically made using a double-sided adhesive.

Other bonding techniques, such as laser bonding [14], solvent bonding [15], thermal bonding [16], or ultrasonic bonding [17], have been used to bond CD layers together, and these approaches can be scaled up for mass production. Most materials utilized for CD microfluidics are sufficiently hydrophobic for use in hydrophobic burst valves, which are spin frequency-controlled valves. In certain cases where the disc surfaces need to be more hydrophilic, the material must be surface treated using oxygen plasma or a surfactant. However, oxygen plasma treatment adds to the cost of fabrication, and both plasma or surfactant treatment often result in devices with short shelf lives [18–21].

New solutions to produce more permanent surface treatments that are also compatible with reagents and samples used on the CD are becoming available. Kitsara *et al.* spun coat poly(vinyl alcohol) (PVA) and (hydroxypropyl)methyl cellulose (HPMC) on poly(methyl methacrylate) (PMMA) surfaces, demonstrating a contact angle change from 68° to 22° and 27°, respectively, that lasted for more than 60 days. This surface treatment was tested on a CD device with serial siphon valves as previously designed by Siegrist *et al* [10], and a sandwich immunoassay was implemented to validate the biocompatibility of the treatment [22].

1.3.1 Future Outlook for CD Fabrication

While many of the works described in the centrifugal microfluidic field use so-called subtractive manufacturing methods, where material is removed to create desired features, the focus has begun shifting to rapid prototyping using additive manufacturing methods such as 3D printing. Despite the geometric distortions that typically accompany 3D printing, Moore *et al.* showed that the experimental burst frequencies, or spin frequencies at or above which liquids pass through a burst valve, on microfluidic discs fabricated using this method were comparable to theoretical burst frequencies, proving that traditional CD functions can be implemented on 3D printed disks with similar results for prototyping purposes [23]. This implies that 3D printing harbors further potential for CD microfluidics research. Furthermore, prototyping in CD microfluidics generally uses layers of different materials, making transfer to injection molding in mass manufacturing difficult because fluidic behavior may change with respect to disc materials. While 3D printing cannot be used for mass manufacturing, it can be used to study fluidic behavior in microfluidic discs with homogeneous material composition.

Although the cost for a high resolution 3D printer is still high, its advantages over other manufacturing techniques described here include quick fabrication time (<30 minutes) and ease of fabrication requiring only computer aided drafting (CAD) knowledge. Additionally, 3D printing is appropriate for low-resource environments, where microfluidic diagnostics can be produced and utilized. Additive manufacturing modules can also be a part of sophisticated, portable manufacturing platforms such as desktop integrated manufacturing platforms (DIMPs) for prototyping or research purposes [24].

1.4 Fluid-Handling Techniques

1.4.1 Valving Techniques

Effective valving technologies lie at the heart of sample-to-answer assays, keeping a liquid volume isolated from the rest of the system during various operations such as sample lysis and mixing, ensuring accurate aliquoting, and preventing unwanted transfer of liquids during temperature changes. These are just a few examples of the function of valves on a microfluidic CD.

Valving techniques on centrifugal microfluidic platforms can be classified into three different categories: passive, active, and semi-active. Passive valves do not utilize any forces besides those present on the spinning disc for actuation. The actuation of a passive valve is dependent on the interplay between the surface tension between the liquid and the material and centrifugal force acting on the liquid in the disc. The most common passive valves are burst valves [9, 25]. When the disc's angular velocity is sufficiently high, the centrifugal force overcomes the surface tension of the liquid, allowing it to burst into the next chamber. For this reason, the angular velocity of the disc at which the valve breaks is called the burst frequency. Some passive valves are actuated by decreasing the rotational speed

of the disc, examples of which being the pneumatic pump (refer to Section 1.4.2) and the siphon valve [3]. Another type of passive valve, the Coriolis valve, is actuated by changing the direction of disc rotation [7]. Although passive valves are simple to fabricate, some types require a hydrophilic surface treatment step, usually plasma treatment [3]. This surface treatment is reversible and generally limits the shelf-life of the device to a range of days to weeks [18–21], while current diagnostic devices remain on the shelf for many months before use. In addition, variations in the manufacturing process can change the burst frequency from device to device, making it difficult to implement a reliable protocol [22].

Active valves require an external actuation mechanism, resulting in higher reliability and robustness than passive valves. The operation of these valves is independent of or only partially dependent on the angular velocity of the disc. Examples of external actuators include heat sources, lasers, and magnets. The main disadvantage of active valving is the need for additional hardware, adding complexity and cost to the platform.

This work defines another type of valving: semi-active valving. Semi-active valves are disc angular velocity-dependent valves that offer a higher level of control than passive valves, yet are simple to fabricate and do not involve surface treatments. They usually integrate additional, inexpensive materials, such as paper, in order to perform valving tasks.

In the context of valves, it is important to distinguish between liquid valves and vapor valves. When liquid passive valves are "closed," they do not prevent vapor exchange within the disc's fluidic network. In contrast, a closed vapor valve seals off both liquid and vapor, but allows them to pass upon opening. Certain vapor valves have long enough shelf-lives and can be used for liquid reagent storage on the disc, eliminating the need to manually add reagents before running an assay and increasing the commercial value of the microfluidic device.

1.4.2 Passive Valves

Passive valves remain an advantageous valving technique because of their simplicity and ease of fabrication. Capillary valves were the first type of passive valve to be investigated on LoD platforms and are dependent on the interaction between the liquids and the disc materials. When the centrifugal force exerted on a volume of liquid overcomes the capillary force exerted on that liquid by the surrounding materials, the liquid is pushed through the fluidic features from the center of the disc outward (Figure 1.3A). Thio *et al.* analyzed several existing models for predicting the burst frequencies of capillary valves and examined convex menisci that extended beyond the channel opening, taking into consideration the angle with which a channel opens into a larger reservoir. Adjusting the equation parameters to more closely simulate previous experimental conditions has yielded improvements on the agreement between theoretical and experimental data [26].

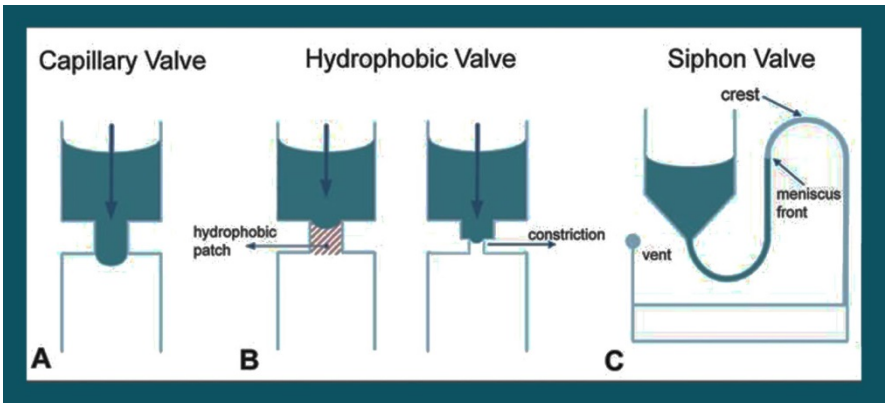

Figure 1.3: Passive valving techniques on a microfluidic disc. A) A capillary valve using hydrophilic microchannel. B) Hydrophobic valves use either a hydrophobic patch on the microchannel (left) or a constriction (right). C) A hydrophilic siphon valve. (Adapted from Reference [3], ©2006, with permission of Annual Reviews; and reproduced from Reference [2], ©2010, with permission of the Royal Society of Chemistry.)

Another type of passive valve, the hydrophobic valve, is also dependent on the interaction of the liquid with the materials of the disc and uses a hydrophobic patch or a constriction in the channel to stop liquid flow (Figure 1.3B) [3, 27–30]. An advantage of hydrophobic

valves is that they do not require hydrophilic surface treatments, which can be costly and ineffective, as discussed in the previous section.

The siphon valve addresses the challenge of process timing in a microfluidic system. A siphon valve, together with an adjacent liquid-containing reservoir, again exploits the interplay of capillary forces and centrifugal forces. At initial high angular velocities of the disc, the liquid level in the channel remains below the crest of the siphon. When the angular velocity is sufficiently reduced, capillary forces dominate, and the liquid fills the siphon, priming the valve (Figure 1.3C). When the angular velocity of the disc is increased again, the hydrostatic pressure difference now aids in the complete emptying of the adjacent reservoir.

In 2011, Gorkin *et al.* enhanced this technique by pumping one liquid through a passive valve to release a second liquid stored in an adjacent chamber. The second liquid's storage chamber is connected to the first liquid's downstream hydrophobic channel by a hydrophobic siphon. When the first channel is burst, a negative pressure is created, which pulls the second liquid over the hydrophobic siphon, draining that chamber due to the hydrostatic pressure in the siphon. This technique does not require any surface treatments and can be used when two liquids need to be pumped sequentially [31].

Another modification of the siphon valve is the micropulley valve developed by Soroori *et al* [32]. For this method to work, a sample liquid is introduced into a loading chamber, which is connected to a transfer chamber where the sample liquid will drain. A second working liquid is loaded in a chamber where a channel connects the top of the transfer chamber to the top of the working liquid's loading chamber. The channels and chamber between the two liquids are ventless. Under high centrifugal force, the working liquid bursts and begins to flow into a collection chamber. The working liquid column and the air connecting the two volumes behave like the weight and rope of a pulley system, respectively. As the working liquid column height decreases, the expanding air creates a negative pressure that pulls the sample liquid, against the centrifugal force, toward the center of the disc [32].

Passive Pneumatic Valves

The centrifugal force points radially outward from the center of a microfluidic disc, making the implementation of more complex LoD systems problematic as liquids cannot be pumped back to the center of the disc. To overcome this problem, methods were developed for pumping liquids against the centrifugal force, extending the path length of the fluidic network. In one case, Gorkin *et al.* utilized an air compression chamber to pump fluids back toward the center of the disc [33]. Liquid was centrifuged at 7,000 RPM to trap and compress air, storing pneumatic energy. When the disc's angular velocity was lowered, the trapped air quickly expanded, pushing liquid back toward the center of the disc. This cycle of high and low angular velocities can be repeated to act as a reciprocating pump. A connecting siphon in a pristine disc can now offer the same function as a siphon valve [3].

Taking advantage of pneumatic reciprocating pumping, Noroozi *et al.* embedded an immunoassay array in a special mixing chamber connected to the air compression chamber of a pneumatic pump. When the disc was spun at high angular velocities, the liquid sample compressed the trapped air and passed over the array in one direction. When the angular velocity was decreased, the sample was pumped out from the mixing unit in the reverse direction. Noroozi *et al.* compared the efficiency of reciprocating flow, flow through, and passive diffusion methods when forming antigen-antibody complexes between human IgG antigens and goat anti-human IgG antibodies. Reciprocating flow was found to be the most efficient method, because it reuses the same sample volume, using only a fraction of the volume required for a flow-through assay. Reciprocating the sample volume also introduces chaotic advection, reducing the reaction time compared to when passive diffusion is used [34].

Pneumatic pumping was further improved with the implementation of the latex micro-balloon pump introduced by Aeinehvand *et al* (see Figure 1.4). The micro-balloon comsists of a highly elastic latex rubber sheet directly integrated into the CD. As the CD was spun at

a high angular velocity, air trapped by a liquid volume expanded the elastic sheet outwards. When the CD's angular velocity was lowered, the latex sheet relaxed to its original shape and the compressed air was released. While Gorkin *et al.*'s pneumatic pump requires a very high operational angular velocity, adding a balloon feature to the pneumatic pump lowers the required working angular velocity to 1,500 RPM or less, which also lowers the power required for pumping and relaxes the demands on the sealing quality of the CD parts. A high disc angular velocity may also prematurely open valves in other parts of the microfluidic disc, so the low actuation angular velocity in this technology is advantageous [35]. The micro-balloon pump was also used for assisted siphon priming and liquid transfer. Latex, however, can be more difficult to work with than other prototyping materials.

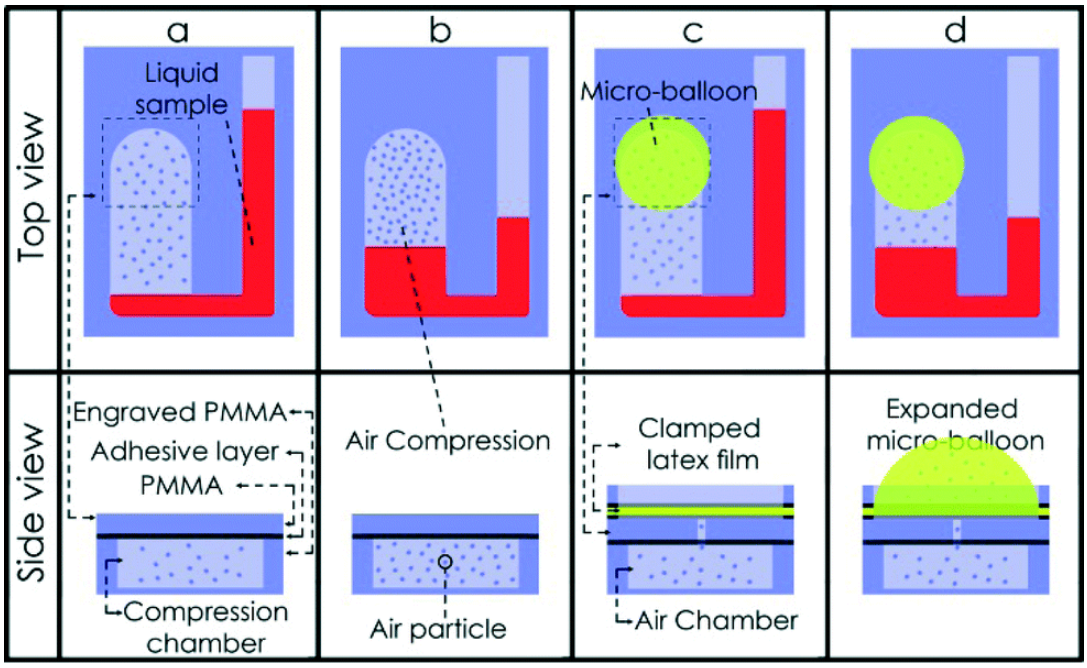

Figure 1.4: Aeinehvand *et al.* integrated sheets of latex rubber to improve Gorkin et al's pneumatic pumping technique by lowering the disc angular velocity required for compression. At low angular velocities, the liquid is at the same height without and with the microballoon in (a) and (c) respectively. In the regular air compression chamber (b), the air has a higher pressure when very high centrifugal force is exerted (Gorkin et al.). In the case with the micro-balloon (d), the micro-balloon is pushed outwards under high centrifugal force. The angular velocity in the latter case (c,d) is much lower than in the case without the microballoon (a,b). (Reproduced from Reference [35] with permission of The Royal Society of Chemistry.)

Zehnle *et al.* also used a compression chamber to increase the distance over which a fluidic pump can send liquid toward the center of the disc [36, 37]. The group was able to pump a variety of liquid types from a compression chamber near the rim of a disc to a collection chamber located close to the center of the disc by designing channel geometries to have the appropriate fluidic resistances. A channel with a larger cross sectional area has a lower fluidic resistance, so the group designed the channel that feeds liquid into the compression chamber to be much smaller than the channel through which the same liquid exits the compression chamber. Although this technique does not guarantee complete liquid volume transfer to the center of the disc, a majority of that volume can be successfully transferred without any external actuation mechanisms or specialized fabrication steps, making this technique useful where a longer fluidic path is required to perform a more complicated assay. A variation on this technique enables thermocycling of the sample liquid, such as in nucleic acid amplification, without overpressure [38].

The complexity of many of today's assays cannot be handled by passive valves alone due to the low reliability of their burst frequencies, one cause of which may be manufacturing inconsistencies. Additionally, passive valves are generally not vapor-tight barriers. The latter characteristic makes the passive valve unsuitable for reagent storage due to the loss or exchange of vapors over time. As a result, other liquid-handling techniques must often be used in conjunction with passive valves to achieve a higher level of fluidic control.

1.4.3 Active Valves

Paraffin Wax valves on the CD

Paraffin wax has been a preferred method of vapor valving in chip-based microfluidics due to its biocompatibility and simplicity of operation. It is a phase-change valve, and its convenience and utility are well known [39, 40]. Only a heat source is required to actuate a paraffin

wax valve. Abi-Samra *et al.* used an infrared lamp to serially open valves made of different melting temperature-paraffin waxes on a CD [41]. The advantage of this technique is that all valves on the same radius of a disc can be actuated at the same time during spinning by positioning the non-contact heat source above the desired radial location of the disc.

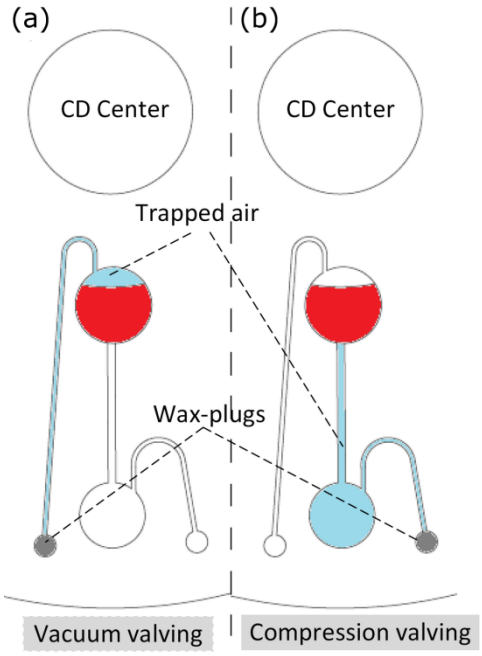

Figure 1.5: Vacuum- and Compression- Valves developed by Al-Faqheri *et al* [42]. (a) The design for vacuum valving. When wax blocks the source chamber vent hole, air is trapped above the sample, preventing liquid flow (b) The design for compression valving. When wax blocks the destination chamber vent hole, air is trapped below the sample, preventing liquid flow.

Paraffin valves were also used by Al-Faqheri *et al.* to achieve vacuum- and compression-controlled valving on a disc [42]. The design (see Figure 1.5) consisted of source and destination chambers and corresponding vent holes. Vacuum valving was achieved by blocking the source chamber vent hole with paraffin wax, which caused the trapped air above the sample to form a negative pressure that prevented liquid flow to the destination chamber. Melting the wax opened the valve, allowing the liquid to flow to the destination chamber. Compression valving was achieved in a similar manner. In this case, paraffin wax was utilized to block the vent hole connected to the destination chamber, compressing the trapped air beneath the sample and preventing liquid from entering the chamber. When heat was applied to melt

the wax, the fluidic pathway was vented to allow liquid flow. Since the paraffin wax does not provide a physical barrier directly below the liquid, its disadvantage is that under high enough centrifugal force, liquid can prematurely enter the downstream chamber. However, it provides yet another method of on-disc liquid control, and by designing the wax valve to be distant enough from the sample chamber, unnecessary heating of sample and reagents during an assay can be prevented.

Another example of paraffin wax valves, demonstrated on a CD by Park *et al.*, used iron oxide nanoparticles mixed in with the paraffin wax. These valves were actuated by laser irradiation so that the nanoparticles acted as nano-heaters [43]. In this technique, called laser irradiated ferrowax microvalves (LIFMs), as the valves are actuated by a small laser light spot, the probability of exposing the sample to excessive heat is significantly reduced. The disadvantages are that disc rotation must be stopped to actuate the valve and that the valve actuation process is serial.

Active Pneumatic Valves

Active pressure-based fluidic techniques provide a simple mechanism to actuate a built-in on-disc pump by expanding an air pocket. Unlike the techniques described in Section 1.4.2 [31–33], active valving and pumping techniques involve external actuation mechanisms and provide more control in fluid handling.

Abi-samra *et al.* demonstrated thermo-pneumatic pumping which involves heating a ventless chamber of air on a disc. As the air volume thermally expanded, it pushed out liquid in an adjacent chamber [44]. The angular velocity of the disc had to be kept low enough to allow the force generated through thermal expansion to overcome the centrifugal force exerted on the liquid being pumped while high enough to create a uniform meniscus in the liquid reservoir on which the expanding air can exert pressure. The pumping ability

is characterized by the following factors: the amount of temperature change of the air (in accordance with Charles' Law), the size of the ventless chamber, and the location of the liquid on the disc. A heat source, such as an infrared lamp, is the only piece of external hardware required for pump actuation. The thermo-pneumatic pump is further discussed in Section 2.1.

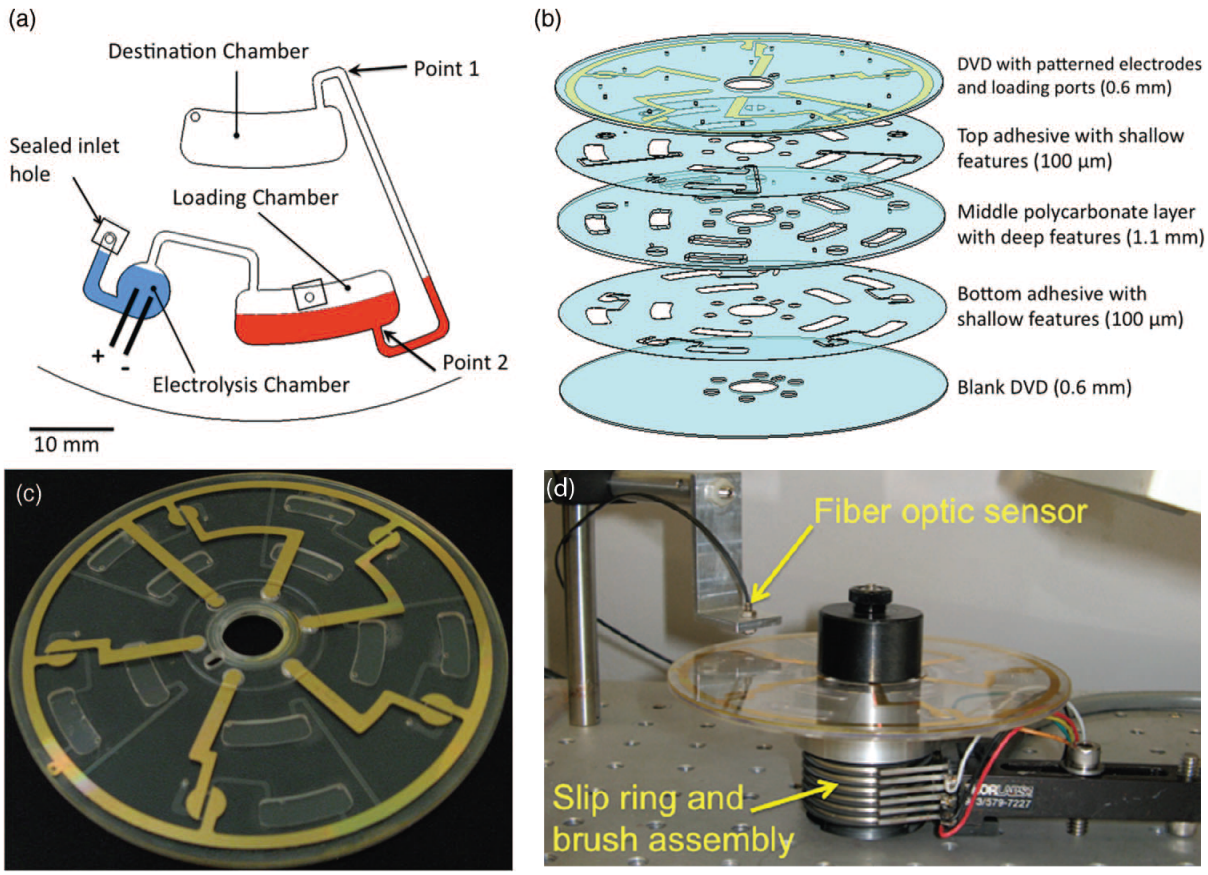

Figure 1.6: (a) Noroozi *et al.* developed an electrolysis pump which can be integrated onto the centrifugal microfluidic platform. When a current is sent through the electrolysis chamber (blue liquid), a gas is generated, pushing the red liquid in the loading chamber toward the destination chamber. (b) The assembly scheme is shown. The top polycarbonate layer includes an etched layer of gold to form the electrode geometry. (c) The assembled disc is shown. (d) The slip ring used to bring electricity to the microfluidic disc is shown. (Adapted from reference [45], ©2011, by permission of The Electrochemical Society.)

Pumping using electrolysis was implemented by Noroozi *et al.* as shown in Figure 1.6 [45]. A slip ring-and-brush assembly was used to provide electricity to the CD, and a current was sent through an electrolyte solution using embedded planar gold electrodes. The current

generates hydrogen gas at the cathode and oxygen gas at the anode, pumping liquid out of the chamber. Unlike the case of the thermo-pneumatic pump, where the temperature change limits the volume of liquid that can be pumped, a small amount of electrolyte in the electrolysis pump produces a large volume of gas. This method allows for pumping regardless of its radial distance from the CD center, which is useful when more on-disc real-estate is required for an assay.

Laser-actuated Valves on the CD

Optofluidic valves, implemented using plastic sheets and a laser printer, are advantageous because they are easy to fabricate with existing commercial equipment. Garcia-Cordero *et al.* printed valves as black dots onto a thin plastic sheet sandwiched between two layers of plastic containing overlapping fluidic channels (see Figure 1.7). The valves were printed in the overlapping region of the channels in the two plastic layers, and pierced by a 671 nm, 500 mW laser. Due to laser light absorption by the dark pigment, only the valve material directly adjacent to the printed dot was melted, opening the fluidic pathway [46]. Accidental piercing anywhere else on the device is avoided due to the strict requirement of light absorption for valve piercing. A laser from a commercial optical CD drive can be used to perform serial valve piercing, leveraging existing technology and simplifying the hardware development process. Furthermore, since the valve is liquid- and vapor-tight, and must be opened using a laser to enable liquid and vapor exchange, this technology is high in utility and reliability.

Magnetic Valving and Pumping on the CD

Magnetism as a valving solution on the CD has recently been explored by several groups because of its reliability and versatility. Burger *et al.* utilized external magnets to produce

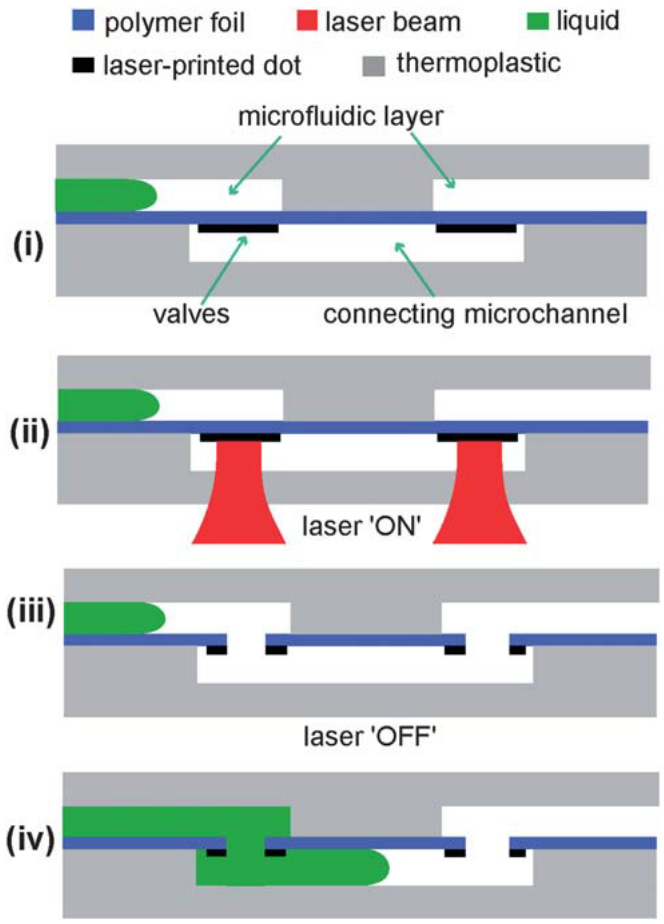

Figure 1.7: Garcia-Cordero *et al.* used a 671 nm, 500 mW laser to pierce valves which consist of black dots printed on thin plastic sheets. The operation sequence is as follows: (i) the construction of the valves before piercing is shown, (ii) laser beams are positioned on the valves to pierce them, (iii) a path is open for liquid flow (from left, green), and (iv) liquid flows through the connecting channels. (Reproduced from Reference [46] with permission of The Royal Society of Chemistry.)

a reversible liquid flow inside a microfluidic CD made of a soft silicone elastomeric material, polydimethylsiloxane (PDMS) [47, 48]. An on-disc magnet was attached to the top of one chamber while a connecting chamber contained a V-cup array for particle trapping. The V-cup array chamber was filled with a stationary bulk liquid and a microbead solution was added via a loading hole. A stationary external magnet was located below the disc at the same radius as the on-disc magnet. While the disc is spinning, the on-disc magnet periodically aligned with the external magnet, pushing the chamber ceiling downwards, and propelling the liquid into the V-cup array chamber and toward the center of the disc. The induced hydrodynamic lift forces dislodged the trapped micro-particles. Once the two magnets were no longer aligned, the chamber ceiling relaxed, causing a reciprocating flow from the V-cup array to the compression chamber. The behavior of the on-disc magnet was determined by the angular velocity of the CD. A higher angular velocity allowed capture by the centrifugal force and a lower angular velocity released the captured particles. Integrating an optical tweezer module enabled the transport of individual stain-identified cells to a separate chamber for analysis, useful when experiments on individual cells are necessary [49].

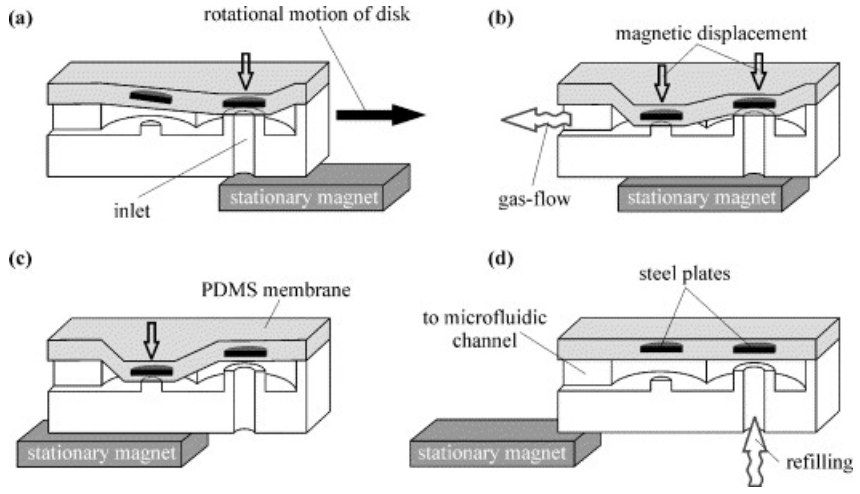

Figure 1.8: a) In the gas micropump by Haeberle *et al.*, one embedded steel plate is attracted to the magnet, sealing off gas in a chamber. b) As the disc rotates, both steel plates are actuated, pushing the gas toward the left. c-d) The steel plates are released, refilling the chamber with gas. (Reprinted from Reference [50], ©2007, with permission from Elsevier.)

This same magnetic-pumping mechanism was applied by Haeberle *et al.* to develop the centrifugo-magnetically actuated gas micropump, which utilizes two valves [50]. Two steel plates, each to control a single valve, were directly integrated into a top PDMS layer of a CD. These plates were positioned adjacent to each other but at the same radial distance from the disc center, enabling them to be actuated by a single mounted external magnet. As the disc was spinning, the plates passed over the magnet, and the PDMS ceiling was pulled down, closing the valves sequentially and pressurizing the gas in the chamber. Once the steel plates were no longer above the magnets, the valves were opened, allowing the pressure difference to equalize (see Figure 1.8). The pressurized gas can be used for pumping liquid streams or for the introduction of ambient air into a liquid sample to implement multi-phase flow.

Although this technique was used as a fluid pump by the two groups listed above, the amount of liquid that the pump can transfer is generally limited and depends on the volume capacity of the pump. Another major drawback is that the disc requires the use of a soft chamber wall, limiting the material choices. However, in fully integrated systems, this technology can be used to perform other functions such as mixing and requires no external electrical power.

1.4.4 Semi-active Valves

Although only a limited number of approaches have been demonstrated in the category of semi-active valves, these valves can be highly practical due to their low cost and ease of implementation. Passive valves, such as capillary valves, may have a spectrum of possible burst frequencies instead of one absolute burst frequency. Semi-active valves reduce the dependence on the reproducibility of the native surfaces of devices by using an alternative material or a delay mechanism. In systems where the fluid-handling tasks become more

complex, semi-active valves can be added to achieve more robust control than passive valving techniques alone.

Dissolvable Film Valves

Valving using biocompatible dissolvable films was first introduced by Gorkin *et al.* in 2012 [51]. In this approach, two chambers were connected with a pneumatic chamber containing a commercially available dissolvable film tab in between as shown in Figure 1.9. Under low disc angular frequencies, a trapped air pocket prevented the liquid in the upstream chamber from entering the pneumatic chamber and wetting the dissolvable film. Once a high enough angular frequency was reached, liquid entered the pneumatic chamber, dissolved the dissolvable film (DF), and passed into the downstream chamber. With the dissolvable film, the pneumatic chamber allowed for more control over the bursting event, since the angular velocity of the disc must be sufficiently high for liquid from the upstream chamber to enter the pneumatic chamber and begin the valve-opening process by dissolving the film in that chamber. Although this valve is not vapor-tight, it provides considerably more control than capillary valves and is tunable in that films with different dissolution rates can be chosen.

A hydrophobic membrane valve can be used in conjunction with dissolvable film to selectively flow aqueous and organic solutions into different chambers [52–56]. Dissolvable films have also been used in combination with paper microfluidics to implement timed fluidic control [57] and has also been demonstrated in clinical applications, including a fluorescence-linked immunoassay and a liver assay panel [58, 59].

The Paper Siphon

Another type of semi-active valving is established by using paper strips inserted into the CD to perform the function of hydrophilic siphons. Although this type of valving is controlled

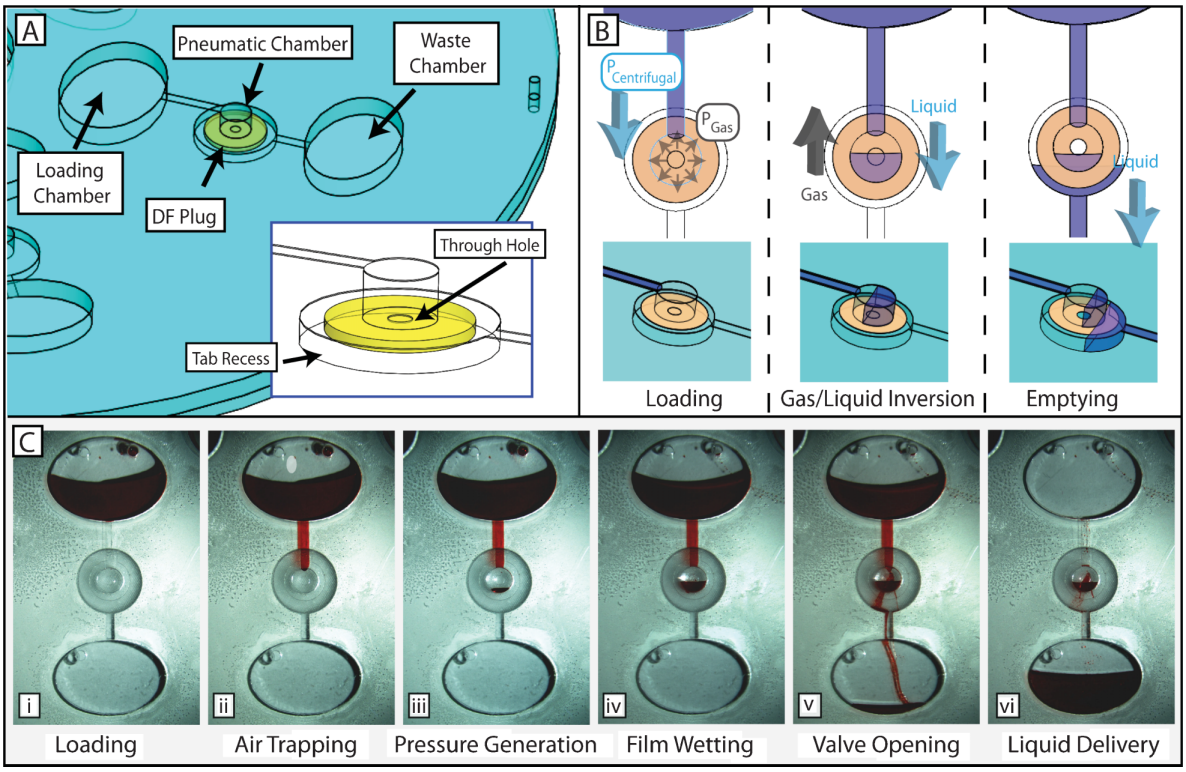

Figure 1.9: (A) Gorkin *et al.* developed a valving technique using dissolvable films (DF) and a pneumatic chamber before the DF as a barrier. Air is trapped in the pneumatic chamber before valve actuation. (B) At high rotational frequencies of the disc, the liquid breaks into the pneumatic chamber and makes contact with the DF. The dissolution process then begins and the duration of the valve opening process is dependent on the properties of the DF. When the film is dissolved, the chamber empties. (C) Experimental images show sample loading at 500 RPM to 3,500 RPM (i-ii), increasing disc angular velocity to 4,000 RPM to overcome air pressure and burst the capillary valve (iii), and dissolution of the DF valve and liquid transfer (iv-vi). (Reproduced from Reference [51] with permission of The Royal Society of Chemistry.)

by disc angular velocity, the wicking ability of the paper offers a higher level of fluidic control than traditional passive valving. The principle of paper microfluidics on a CD is based on the interplay of capillary forces, which allow liquid to wick through the paper, and centrifugal force, which pushes liquid only toward the outer edge of the disc. Godino *et al.* utilized chromatographic paper in a siphon to achieve a high level of control over blood plasma flow [60]. Aliquoted whole blood sample was spun on a disc to separate blood plasma from the red blood cell pellet. The disc was spun at 375 RPM for 5 minutes to allow the plasma to wick up the paper siphon before it was accelerated to 2,250 RPM to collect plasma on

the other end of the paper siphon. This process was repeated until 10 μL of blood plasma was collected. Both dissolvable films and paper microfluidics have been combined in the development of another technology which involves event-based valve actuation [57]. In this case, the wicking of a liquid across a paper strip opens dissolvable film valves in a desired sequence that determines the fluidic operation.

Graphene Oxide Membrane Valve

Gaughran *et al.* used graphene oxide membranes for flow control of aqueous and organic phases in microfluidic disc [61]. The group assembled a 10 μm thick graphene oxide membrane with pressure-sensitive adhesive before assembling it into an 8-layer disc. Characterization demonstrated that the membrane is permeable to water but impermeable to air, isopropanol, and ethanol.

Check Valves

Check valves are valves that allow fluid to flow in only one direction. Al-Faqheri *et al.* implemented several check valves, each incorporating a latex membrane (side views of these valves are seen in Figure 1.10). As shown in Figures 1.10a1-a3 and 1.10b1-b3, a latex membrane in a cavity separates the inlet and outlet channels for each terminal check valve (TCV). A 0.5 mm diameter hole, cut into the latex membrane and offset from the fluid channels, allows or denies fluid flow depending on the direction in which pressure is exerted. Figure 1.10a2 shows that when a positive pressure is exerted, a latex membrane placed next to the inlet is distended, allowing fluid to access the hole and to flow through the TCV. In Figure 1.10a3, the negative pressure contracts the latex membrane, closing off the hole and preventing fluid flow. The TCV can be placed next to the outlet to reverse the actuation and blocking mechanisms, as shown in Figure 1.10b1-b3. The bridge check valve (BCV)

consists of a latex membrane with the inlet and outlet channels on one side and an air exchange hole on the other side (see Figure 1.10c1). Positive pressure actuates the valve and allows fluid to flow through (see Figure 1.10c2). Negative pressure causes valve blocking, preventing fluid flow (see Figure 1.10c3). A BCV can be combined with a thermo-pneumatic pump (described in Section 1.4.3) for an active valve. Al-Faqheri *et al.* also describes a microfluidic disc with a TCV, a BCV, a thermo-pneumatic pump to demonstrate "liquid swapping" for applications such as immunoassays [62].

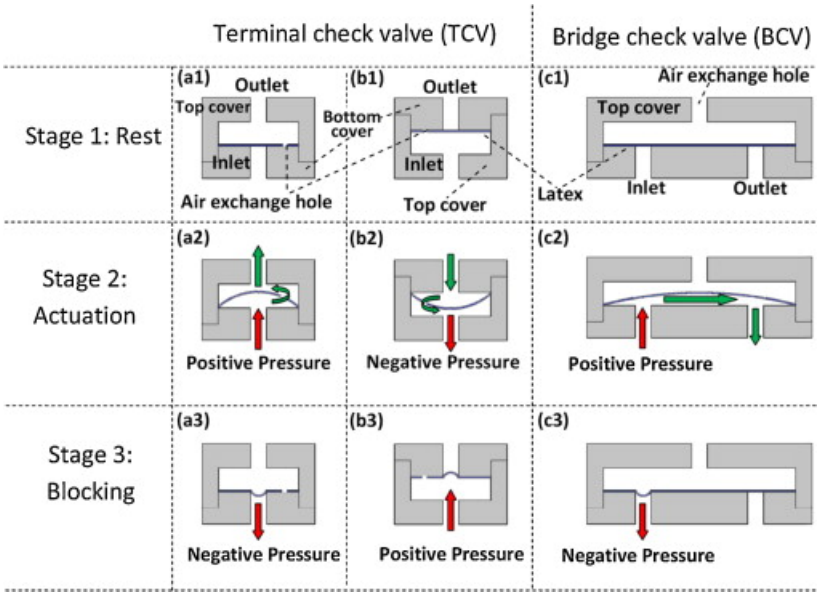

Figure 1.10: Al-Faqheri *et al.* implemented terminal check valves (TCV) and bridge check valves (BCV) by incorporating a latex membrane layer in the disc fabrication process. In a TCV (a1-a3 and b1-b3), the inlet and the outlet channels were separated by a latex membrane. The latex membrane contains a hole, offset from the adjacent channel, which controls fluid flow depending on the pressure is exerted. When a positive pressure is exerted on the valve where the latex membrane is next to the inlet (a2), fluid flows through the TCV. When a negative pressure is exerted (a3), fluid flow is blocked. When the latex membrane is placed next to the outlet (b1-b3), the actuation and blocking mechanisms are reversed. A BCV (c1) has inlet and outlet channels on one side of a latex membrane and an air exchange hole on the other side. Positive pressure actuates the valve (c2) while negative pressure causes valve blocking (c3). (Reprinted from Reference [62] ©2015, with permission from Elsevier.)

Similarly, Carpentras *et al.* proposed a theoretical model for controlling liquid flow through a channel by using a magnetic ball as a movable plug actuated by an external

magnetic field [63]. Various channel geometries and materials were tested for both the valve and the movable plug, and an ideal geometry, a conical PDMS valve seat, was proposed. While this valve has not yet been used in an application, flow control that is independent of heat or chemicals is useful in temperature- or contamination-sensitive molecular diagnostic assays.

1.4.5 Volume Definition

Volume definition, in some cases called aliquoting, is used to obtain the appropriate volumes of reagents and samples for downstream analysis. Although the simplest way to define volumes is with the use of an overflow chamber [6], many other techniques have been utilized on the disc. For example, volume definition can be performed by placing a body of liquid inside a chamber with two channels: an overflow channel at the top, and a collection channel, which opens after overflow is complete, at the bottom [64]. Volume splitting was implemented by Andersson and Ekstrand, who created a zigzag hydrophilic channel design that geometrically defines a series of volumes before sending each fraction to perform its respective test [65]. This feature can be used to vary the concentrations of the reagents to automatically synthesize different nanoparticles, as shown by Park *et al.* in applications that synthesizes nanoparticles of various colors [66] and anisotropic metallic nanoparticles [67]. Optimization of this technique with other functional units in a system can yield high-throughput synthesis of a great variety of nanoparticles for biological or chemical assays.

Decanting from a sample volume, such as a fractionated whole blood sample, has been explored and demonstrated by several groups [64, 68–72]. Whole blood fractionation techniques are useful when blood plasma is required for its components. The most common way to decant blood plasma from a fractionated whole blood sample is to use a hydrophilic

siphon that leads from the bottom of the plasma layer to a collection chamber. At lower , plasma flows out through the siphon, similar to the mechanism of a siphon valve.

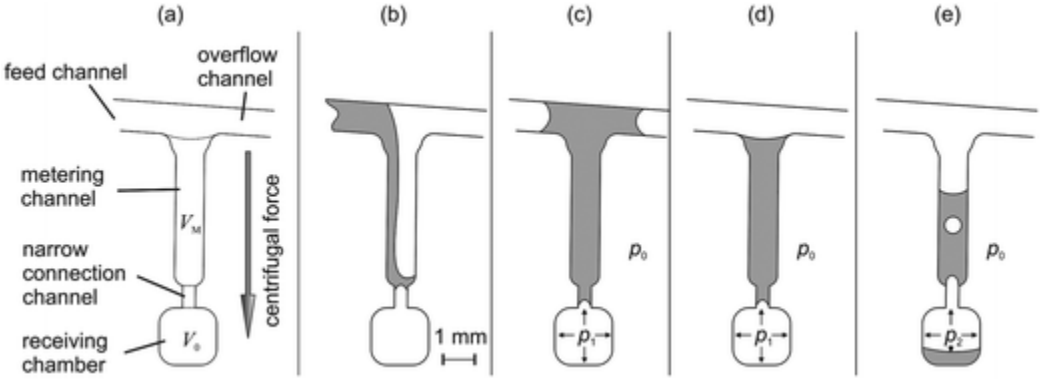

Figure 1.11: Mark *et al.* implemented a fluidic feature that essentially incorporates two volumes—V_M for metering and V_0 for receiving the final volume of liquid (a). Liquid first flows through the feed channel at the top and begins filling the metering channel, which has the volume V_M (b). When filling finishes (c), the angular frequency of the disc is increased, forming the top meniscus shown in (d), and defining the desired liquid volume. Meanwhile, V_0 remains empty because a much higher centrifugal force is required to overcome the air pressure in this unvented chamber. When the angular frequency is again increased to be sufficiently high, liquid finally enters the receiving chamber while air bubbles exit through the top (e). (Reproduced from Reference [73] with permission of The Royal Society of Chemistry.)

One of the more commonly used techniques for volume definition in complex assays was demonstrated by Mark *et al.*, who divided a liquid sample into smaller volumes [73]. The feature that this team implemented is shown in Figure 1.11 and allows a stream of liquid to enter the volume V_M, while the volume of the unvented chamber below, V_0, remains empty. The channel between the two chambers prevents the liquid from entering V_0 at low spin frequencies because of the air pressure in the chamber. At high spin frequencies, the surface tension is broken, overcoming the high pressure in the chamber and allowing the liquid to enter V_0. This technique has been analyzed in detail [74] and is especially useful for performing real-time PCR because defined liquid volumes can undergo thermocycling at high centrifugation speeds with reduced evaporation and no risk for unwanted liquid transfer [13, 75–77].

1.4.6 Mixing

Mixing of reagents and samples is a critical step in any μTAS, particularly in molecular diagnostic processes, where fully automated fluidic processes in a closed system are crucial for avoiding contamination. While necessary, mixing is challenging due to the low Reynolds numbers and laminar flow regime present in microfluidic devices [78,79]. In microfluidic chips, liquid streams are generally confined to narrow channels, allowing for only diffusive mixing. On the other hand, in microfluidic discs, separate liquid streams are usually transferred into a large chamber, inducing both convective and diffusive mixing. While this phenomenon makes the centrifugal microfluidic platform inherently better for mixing, various passive and active mixing techniques have been developed to further speed up the process. Here, a variety of mixing techniques for liquid-handling in LoD assays is presented.

Researchers have optimized on-disc mixing by incorporating various micromixers onto microfluidic devices. While passive micromixers utilize special microchannel geometries to induce advection during liquid handling and minimize diffusion times, active micromixers utilize additional hardware or integrated structures to homogenize liquids. One of the simplest passive mixers on a CD is the modified centrifugal force-based serpentine micromixer (CSM), as first simulated by La *et al.* [80] and further optimized by Kuo and Li [81]. A serpentine channel was incorporated into a microfluidic CD design, and the combination of Coriolis force and the channel geometry induced chaotic advection and diffusion in the sample, effectively mixing it. This phenomemon was modeled to show that as the bending channel width was increased, the mixing between two adjacent solution streams increased. Kuo and Li used the CSM method to mix reagents with plasma after separation by sedimentation, demonstrating the potency of this mixing technique in sample preparation [81].

Using the same principle demonstrated by Kuo and Li, Aguirre *et al.* increased chaotic advection by adding an alternating directional flow pattern to the existing CSM. The mixing

unit changed the bulk flow direction resulting in a phenomena called "flipping." This method was effective in mixing fluorescent tags with targeted cancer cells in a blood sample [82].

Other passive mixing methods utilize droplets as microreaction chambers [82] or bubbles to promote chaotic advection [83]. Droplet formation on a disc, where the small diameter of the microreaction chambers significantly reduces the diffusion distance of any reactants, has been realized by Haeberle *et al* [82]. Bubble mixing using T-junctions has not yet been integrated on a disc, possibly due to the constraint of the disc's footprint size, but could be implemented in the future.

A more effective passive mixing technique is flow reciprocation, which utilizes less on-disc real estate than serpentine channels and can be used for sample hybridization. In 2009, Noroozi *et al.* designed a reciprocating flow mixer which utilized both centrifugal force and the pneumatic pressure generated in a ventless compression chamber to effectively and quickly mix two liquids together [84]. This technique can handle significantly more liquid sample volume than droplet and serpentine mixing. In 2011, Noroozi *et al.* integrated this technology into a multiplexed LoD immunoassay to improve *Burkholderia* detection, illustrating the impact this mechanism can have on sample preparation [34]. Furthermore, Aeinehvand *et al.* incorporated a microballoon for flow reciprocation [85]. The microballoon mixer required a smaller disc footprint than the reciprocating flow mixer by Noroozi *et al.* and reduced mixing time from 170 minutes of diffusive mixing to less than 23 seconds.

While effective, some drawbacks to passive mixing for more complicated assays include inefficient use of on-disc real estate, long mixing times, and ineffective mixing of very viscous samples. Active mixing techniques include electro-osmotic mixing [86], ultrasonic manipulation of a piezoelectric diaphragm [87], and magnetic mixing [88]. Electro-osmotic mixing has not been implemented on a CD due to its dependence on the sample's pH and ironic strength [89]. Mixing using piezoelectric actuation also has not yet been implemented on a microfluidic disc but could be developed in the future for suitable platforms.

Active mixing using magnetic beads is simple and effective and has been demonstrated on a microfluidic disc by Grumman *et al* [90]. In this technique, termed batch-mode mixing, a series of permanent magnets were placed at alternating radial distances underneath the mixing chamber, while magnetic microbeads were placed inside the mixing chamber. As the disc was spun, the beads inside the chamber are attracted to each permanent magnet, inducing turbulent mixing by means of the Stokes drag force. To further increase mixing, a shaking protocol was implemented, periodically changing the frequency of rotation to induce phases of acceleration and deceleration. This technique creates shear forces that stimulate an advective current during acceleration and deceleration of the disc. This alteration between spinning speeds induces lateral movement of the magnetic beads in the mixing chamber, increasing the mixing area of the beads and drastically reducing mixing time from seven minutes via diffusive mixing to less than one second. The mechanical lysis method developed by Kido *et al.* works using the same principle as the batch-mode mixing technique [11]. In addition to lysis, it also performs mixing and sample homogenization in the same chamber, and has been demonstrated in a nucleic acid extraction system developed by Siegrist *et al* [91].

1.4.7 Future Outlook for Fluid Handling Techniques on the CD

Although some of the valves described in the valving sections are yet to be used in fully integrated systems on a disc, the availability of an array of different valve options is important for the advancement of new, complex assays. The characteristics of the major CD valving options detailed above are summarized in Table 1.2 below. When choosing a valve for a particular application, many of the factors listed in the table need to be considered for a balanced solution between reliability, complexity, and cost. Active valves tend to be more reliable, while passive valves tend to be lower in complexity and more cost-effective. A valve may also share external hardware with other features on the disc to lower the overall

hardware cost. An example is the multifunctional wax valves technology developed by Kong *et al.*, where a single heat source was used for release of a liquid encapsulated in paraffin wax, incubation of the liquid, and thermo-pneumatic transfer of the liquid to a collection chamber (see discussion of thermo-pneumatic pump in Section 1.4.3, and discussion of multifunctional wax valves in Section 2.2) [92].

Although it may seem attractive to utilize a combination of several fluid-handling techniques in novel sample-to-answer assays, the resulting complexity will often be too high. Reducing such complexity can promote the development of multi-step assays on a CD. For example, the most effective mixing techniques utilize additional mechanical components, such as magnetic beads to create turbulent mixing. The use of these extra components allows for other operations such as lysis (as discussed in Section 1.6.4) in the same fluidic chamber, reducing design complexity and the use of on-disc real estate. Evidently, the need for simpler, lower cost, and more reliable fluid-handling options is always present.

Table 1.2: Characteristics and examples of passive, active, and semi-active valves. Each type of valve has its trade-off in complexity, cost, and reliability.

	Passive valving	**Active valving**	**Semi-active valving**
Vapor tight	No	Sometimes	No
Has moving parts	No	Sometimes	Sometimes
Liquid/surface-dependent	Yes	No	Sometimes
External Hardware	No	Sometimes	Sometimes
Angular velocity-dependent	Yes	No	Yes
Reliability	Low	High	Medium
Cost	Low	High	Low
Examples	Capillary [26]; siphon [10, 31]; micropulley [32]; pneumatic [33–35]	Wax [41, 92]; thermo-pneumatic [44]; electrolysis [45]; magnetic [50]; laser [43, 46]	Dissolvable films [51]; paper siphon [60]; check valves [62, 63]

1.5 Reagent Storage

One of the more neglected, yet critical aspects of CD microfluidics is long term, vapor-tight reagent storage and on-demand release of both liquid and solid or dried reagents on microfluidic discs. For a microfluidic assay to be effective, reagent storage must have the following characteristics:

1. Long term storage for up to 12-18 months. The quantity and integrity of the reagent must remain sufficient for its respective application before the end of the storage period.
2. On-demand release of reagents.
3. Low cost fabrication and ease of implementation.
4. Capability to effectively store both lyophilized and liquid reagents on the same disc.

The simplest method of reagent storage is to either dry or lyophilize reagents, turning them into easily resuspendable pellets [93]. However, this method is not vapor-tight and may require specified storage conditions. Kim *et al.* developed an effective method of encapsulating lyophilized reagents in paraffin wax [94]. Heating the wax-encapsulated reagents not only released the reagent but created a "hot start" effect for enzymes.

While this works well for solid reagents, some assays use liquid biological reagents or combinations of both liquid and dry reagents. To address the need for liquid reagent storage, Van Oordt *et al.* demonstrated an effective storage solution which uses pouches made from an aluminum foil composite [95]. These aluminum pouches, illustrated in Figure 1.12, were fabricated with a frangible seal. As the disc was spun at a sufficiently high angular velocity, this seal was broken by the hydrostatic pressure from the liquid inside the pouch. The pouches were sealed using ultrasonic welding and the strength of the seal was tuned so different seals could open at different disc spin rates. A second frangible seal can be imple-

mented on each pouch to demonstrate separate storage of liquid and dried reagents. These pouches were tested to have a volume loss of 0.4% after 42 days at 70°C, which is equivalent to 2 years at room temperature. In addition to the long-term vapor-tight storage of liquids, this technology can also serve as a semi-active valve.

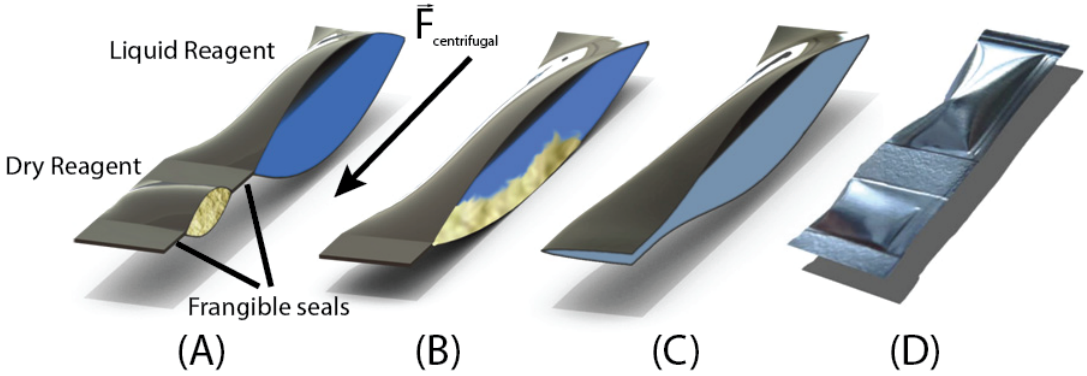

Figure 1.12: Miniature aluminum pouches, used for storing solid and liquid on microfluidic CDs, were made by van Oordt *et al* using ultrasonic welding and can be tuned to open at a desirable burst frequency (From left to right). (A) Reagents separated by a frangible seal and stored. (B) Frangible seal opens when experiencing a certain centrifugal force at a specific spin rate, and reagents are mixed. (C) Downstream frangible seal bursts at a different spin rate to release liquid for on-disc assay. (D) Photograph of a closed aluminum pouch. (Reproduced from Reference [95] with permission of The Royal Society of Chemistry.)

While aluminum pouches are well suited for storage due to their versatility and low cost, the best packages for long term storage of complex liquid biological reagents are bio-inert glass [96]. Despite the wide use of glass in most biological applications, cost, manufacturing, and safety challenges have prevented it from being used in microfluidic devices. For certain specialized assays, glass is necessary, and new techniques for integration of glass ampoules must be developed (See Appendix B for a novel technique for release of liquid reagent). On the other hand, plastic tubes have been successfully used in complex assays by companies such as GenePOC, who use plastic tubes sealed with a heat-sensitive material for nucleic acid (NA) amplification [97]. Certain active valves, such as the laser-pierceable polymer valves developed by Garcia-Cordero *et al.*, can also be used to store liquid reagents for up to 30 days with no significant evaporation [98].

1.5.1 Future Outlook for Reagent Storage

Reagent storage, which has been neglected in the field of CD microfluidics, remains one of the most critical components of a complete sample-to-answer system. Future work will focus on two aspects of reagent storage: the development of bio-inert, inexpensive materials for reagent encapsulation and the integration of simple reagent release mechanisms that take advantage of the forces present on a spinning disc.

1.6 Sample Preparation

In biological and chemical assays, a raw sample must go through a series of preparatory operations, which may include cell sorting or sample concentration, lysis of cells in assays requiring genomic material, sedimentation to isolate any precipitate from supernatant, or filtration [99]. Very few LoC and LoD devices, particularly those that perform molecular diagnostic assays, feature a completely integrated sample preparation system because modular solutions, where one fluidic feature or hardware component can be used for multiple functions, are rarely available. However, in order to develop a truly user-friendly and portable total analysis system, sample preparation is key. The physics already present on the rotating platform make it ideal for integration of multiple sample preparation steps on a single platform.

This section describes processes commonly used in clinical assays with a focus on nucleic acid processing. Particle sorting, sample purification, or sample concentration is utilized in any assay where a low quantity of the species of interest is present and needs to be further isolated, while sedimentation or filtration is used to separate components of different densities. Cell lysis is a specialized operation generally used for molecular diagnostic assays.

Purification of nucleic acids is required in certain molecular diagnostic assays [100]. A flow chart of the processes in a molecular diagnostic assay is shown in Figure 1.13.

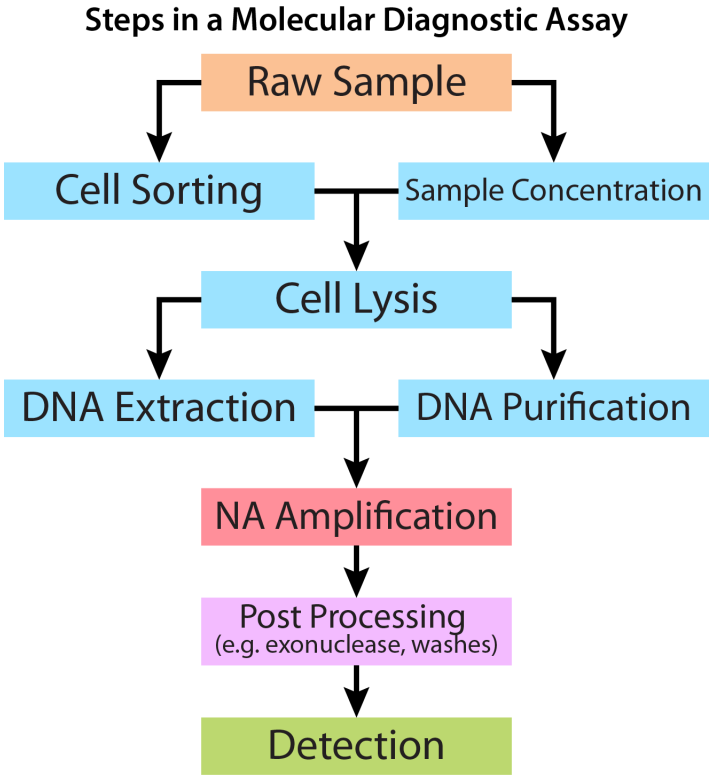

Figure 1.13: Steps in a typical molecular diagnostic assay.

1.6.1 Particle Sorting

Particle sorting is required when there is a low quantity of a target cell type amongst a population of cells. Such cases include separation of fetal cells from the mother's whole blood or separation of rare cancer cells from a tissue sample prior to nucleic acid analysis [99, 101]. The size range of particles that can be separated is inherently limited by the radial size of the disc. Even so, effective particle separation on a disc is possible, and is preferred because the motor for spinning the CD uses a small amount of power compared to any benchtop system.

Particle separation can use either passive methods that take advantage of the centrifugal force or active methods that incorporate external components. Aguirre *et al.* used Dean forces in serial serpentine flow-focusing channels to separate cell-bead complexes from blood [82]. Morijiri *et al.* separated particles of different densities and sizes using a rotational movement combined with a technique called pinched-flow fractionation. The fluidic structure was filled with a bulk buffer solution before the particles were introduced. As the disc rotated, the pinched segment focused particles onto the upper wall, while the centrifugal force drove the sedimentation of particles by their respective sizes and densities [102].

Besides utilizing pseudo forces present on a rotating platform, additional active components may be integrated for more effective particle separation. Recently, Kirby *et al.* utilized a set of three magnets on a CD platform to successfully simulate the isolation of rare bioparticles from background tissue cells [103]. A mixed particle suspension, including magnetic and non-magnetic particles of different sizes, was sent through a focusing channel where the centrifugal force, along with three permanent magnets located at different radial distances, separated particles according to their density, size and magnetic properties. Nearly 100% separation was achieved. This technique was used to separate MCF-7 cells of concentration as low as 1 target cell in 1 μL of whole blood with capture efficiencies of up to 88% (See Figure 1.14) [104]. A total of 18 μL of sample was processed on a disc within 10 minutes.

Glynn *et al.* used geometric designs, termed "size exclusion rail," to separate cells of different sizes [105]. Whole blood, spiked with HL60, colo794 and sk-mel28 cells, was sorted on the microfluidic disc. The different size-gaps in the geometric design allowed the passing of the appropriate sized cells into several bins. Each bin received cells of a certain size range, including components of blood, making this technique a simple and label-free manner for cell sorting.

Schaff *et al.* demonstrated sedimentation-based particle sorting, where two bead types (different sizes and densities), each type functionalized with a different capture antibody,

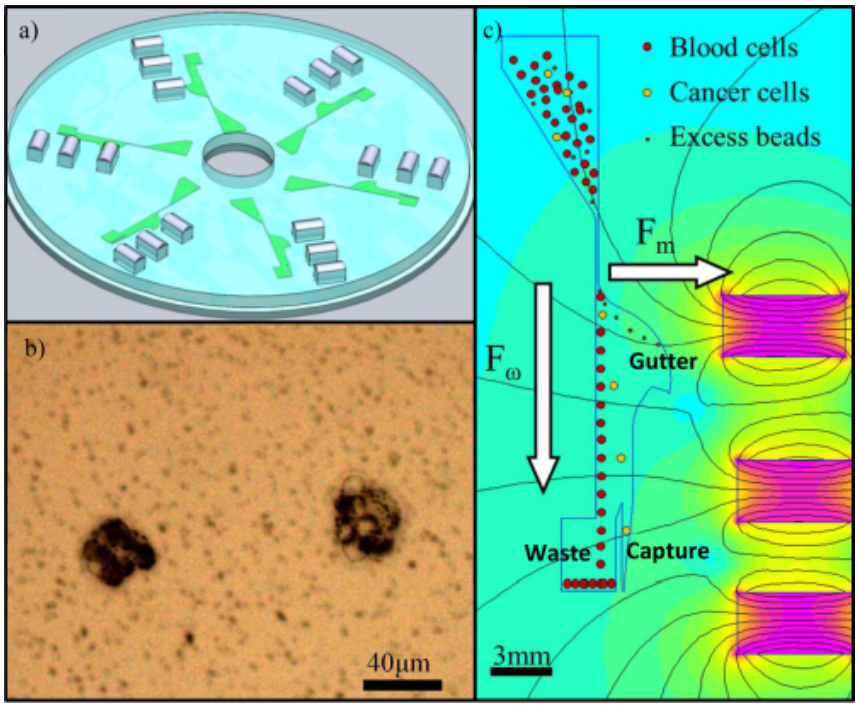

Figure 1.14: a) Schematic of a microfluidic disc, designed by Kirby *et al.*, that contains 6 multiplexed separation units. The microfluidic channels are green and next to the magnets, which are silver cylinders. b) Two clusters of MCF-7 cells, tagged with paramagnetic beads, are amongst beads (specks) in the background in this bright-field image from a microscope. c) A simulation of the separation unit that shows the separation trajectories for blood cells, magnetically-tagged cancer cells, and excess paramagnetic beads, which are separated into the "Waste", "Capture", and "Gutter" reservoirs, respectively. Centrifugal force is indicated by F_ω and the magnetic force is indicated by F_m. (Reproduced from Reference [104], ©2014 International Society for Advancement of Cytometry.)

sedimented into distinct layers when passing through a density medium. This process also separated the beads from any red blood cells present and provided a washing step for the beads [106]. Koh *et al.* performed a similar sedimentation step with only one bead type for the detection of botulinum toxin and achieved a lower limit of detection of 0.09 pg/mL [107].

1.6.2 Sample Purification and Concentration

The detection of low concentration components in many biological or chemical assays may require an initial step to concentrate or isolate the sample. Examples of components that

require such a process include proteins, environmental pollutants, and nucleic acids. The method of choice for concentration or purification often involves the use of a solid phase extraction column. Several methods have previously been used to extract compounds: the use of monolith in a microcolumn [108], *in situ* detection following collection of samples in the column [109, 110], and the use of hydrophobic membranes and dissolvable films for reagent flow control in silica bead-based RNA purification [52].

Moschou *et al.* discussed the implementation of such a unit on a microfluidic disc for the extraction of proteins [108]. The disc contained a microcolumn for separation, a fractionation channel to isolate the proteins from the rest of the sample volume, and an isolation chamber for optical detection of the proteins. The group prepared a monolithic column using *in situ* polymerization by microwaves for efficient sample extraction. Fluorescent analysis of the isolated analyte showed that at least 80% of the original 12.4 pmol sample was recovered.

Works from another group used a microfluidic CD design to detect and quantify elements in water samples [109] and an environmental pollutant [110]. Instead of elution using organic solvents, the authors analyzed the sample directly in the stationary phase of the column. Direct analysis of the column reduces loss of sample by wall adsorption and the amount of harmful organic solvents used for sample extraction. Using laser ablation, Lafleur and Salin found the limits of detection to be between 0.1 and 12 ng for Ni, Cu, V, and Co [109]. Lafleur *et al.* analyzed the column for fluorescein by fluorescence and absorbance and for anthracene by fluorescence. The limit of detection of fluorescein was 50 ng using both detection methods, and that of anthracene was 20 ng [110].

Dimov *et al.* introduced the use of hydrophobic membranes and dissolvable films for liquid reagent control in silica bead-based purification of RNA samples [52]. Although the system yielded considerably less RNA than benchtop methods, it was capable of purifying both mammalian and bacterial RNA.

Mamaev *et al.* built a fully contained and fully automated system that performs NA isolation and purification on up to 24 samples. The system incorporated lyophilized reagents, leak-proof inlets for sample input, outlets with standard micro test tubes for sample recovery, and hardware components that deliver heat, pressure, and spinning of the motor to perform valving and pumping. Experiments confirmed that the system was capable of isolating genomic material from *Bacillus thuringiensis* and *Mycobacterium tuberculosis* cells that were in the concentration range of 102 to 108 cells/mL and from hepatitis B and C viruses with concentrations of 102 to 107 particles/mL in plasma. Quantitative PCR was performed using the obtained *B. Thuringiensis* DNA, and the results amongst the replicates did not vary by more than 10%. The NA obtained from the automated system was compared to those obtained from the manual method, and the two sets of data were almost identical. These experiments confirmed that the platform was reliable for performing NA purification, and the authors project that when integrated with low-density hydrogel microarray technologies, the platform will be capable of analyzing viral and bacterial DNA and detecting genetic point mutations association with cancer or other conditions [111].

Despite the effectiveness of solid phase extraction for sample purification and concentration, a few challenges still prevent its widespread implementation on centrifugal microfluidic systems. One challenge is the requirement for liquid reagent storage for a fully automated assay. In the multi-step elution assays described, the reagents had to be manually introduced into the disc after each step [52,109]. A second challenge is the incompatibility of the reagents with the materials used to make the disc. For example, Moschou *et al.* observed that glycidal methacrylate and hexane, components used to create the microcolumn monolith precursor, caused deformation of the disc's PDMS layer [109]. In other cases, organic solvents, such as acetone or methanol, are sometimes the standard reagents for an assay. These solvents etch certain polymers such as polycarbonate or acrylic, limiting material choices.

1.6.3 Sedimentation and Filtration

Sedimentation and filtration are essential in assays where solid portions of the sample may disrupt the fluidic process. The inherent centrifugal force on a centrifugal microfluidic platform promotes convenient, built-in sedimentation and speedy filtration. Various aspects of these processes have thus been explored on a microfluidic disc.

One application of sedimentation, blood plasma separation, has been demonstrated in a variety of ways: by exploiting the density and size differences between cellular blood components and plasma [64, 68, 70, 112], by using curved microchannel geometries [113], and by using special finger-like structures during large volume blood plasma separation that increase the bonded area of the disc and therefore, structural integrity of the disc [69]. A technique for rapid separation of red blood cells from plasma by Kim *et al.* used inclined chamber walls in addition to centrifugal force, where a phenomenon called the Boycott Effect is observed [114]. According to the Boycott Effect, in a gravitational force field, particles suspended in a liquid settle toward the inclined wall, rather than the bottom, of a tilted container, shortening the total sedimentation distance and time. Kim *et al.* were able to separate red blood cells from plasma in whole blood up to eight times faster in inclined chambers than radial chambers. This effect was further described and mathematically analyzed by Schaflinger [115]. It was demonstrated on a disc in two cases—by Kim *et al.* using chambers with radial geometry [116] and by Kinahan *et al.* using chambers with spira mirabilis geometry [117]. Decreasing the width of the separation channels and increasing the inclination angle of channels from the radial direction increases the speed of the blood plasma separation process.

Sedimentation of soil samples has also been demonstrated by LaCroix-Fralish *et al.*, who integrated capillary tubes with very small inner diameters (ranging from 12 to 100 μm) that many microfluidic disc prototyping methods have not been able to accomplish [118]. The

capillary tube overreaches into the sample input reservoir, allowing sediments to fall around it and liquid to empty through the capillary tube.

Filtration is a necessary process for isolating components suspended in liquids and can be rapidly performed on a disc due to the presence of centrifugal force. Lee *et al.* used a polycarbonate membrane with 8-μm pores to filter MCF-7 cells from whole blood. On average, 3 mL of blood took 20 seconds to filter without significant radial sedimentation of red blood cells. The group was able to achieve 61% capture efficiency, while under different dilution factors, they achieve between 44% to 84% capture efficiency [101]. Karle *et al.* implemented an axial centrifugal filter on a disc to send liquid, termed permeate, down in the direction parallel to the spinning axis through a filter unit, while bacterial cells in the portion of the sample, termed retentate, avoided the filter and flowed toward the rim of the disc [119]. This strategy prevented the clogging of the filters. Templeton *et al.* sealed different types of filter paper onto polycarbonate layers to create leak-free filtration units and filtered soil from water in less than a minute using centrifugal force [119]. While filtration can isolate species suspended in solution that sedimentation cannot, sedimentation is generally preferred on the centrifugal microfluidic platform for two main reasons: sedimentation does not require any extra fabrication steps, while filtration may involve insertion of filtering units; moreover, filters can be clogged if the amount of precipitate is considerable.

1.6.4 Cell Lysis

For many biological samples, lysis is necessary for retrieving genomic or proteomic material from cells. The process usually involves breaking the outer membrane of the cells using one of two methods: physical means [11, 120, 121], such as laser-induced thermal shock [71] or sonication, or chemical means, which generally involves the use of detergents [2]. Many of

these processes can also perform sample homogenization to ensure that the biological sample is uniform in size and texture throughout.

Although a variety of methods can be used for sample lysis on the CD, bead beating, developed by Kido *et al.*, remains the most universally effective method, capable of lysing even the toughest samples [11]. To perform bead beating, a microfluidic disc is designed to contain glass beads as lysing media inside radially elongated fluidic chambers. A small ferromagnetic disc is free to move inside each chamber. The setup consists of several permanent magnets secured under the disc at alternating radial distances so that as the CD spins, the small ferromagnetic disc moves toward each permanent magnet as it passes them, sliding back and forth in the chamber to enhance the lysing process. This method was used to effectively lyse *Saccharomyces cerevisiae* cells, which are considered notoriously difficult to lyse.

1.6.5 Future Outlook for Sample Preparation

Sample preparation steps may include isolation of specific targets, sample purification, and handling of particles inside a liquid solution. The unique nature of the centrifugal platform makes it excellent at realizing many of these applications. Most techniques on this platform do not require any complex fabrication methods, surface treatments, or external hardware components and are capable of dealing with any sample type. To further simplify assays, one set of hardware can be used to accomplish multiple actions, such as the use of the bead beating setup for simultaneous mixing and lysis of a sample-reagent mixture.

Particle separation has not been integrated into a LoD system with other types of sample preparation units due to its large on-disc real estate requirements. However, with pending applications such as cell sorting for disease diagnosis and waste water analysis, sedimentation and particle sorting are subfields that continuously seek improvements for more efficient and

inexpensive solutions [122]. Future improvements will include the integration of compact particle separation units with other fluid-handling operation units.

To address the challenge of integrating multiple sample preparation steps on a disc with limited real-estate, a 3D architecture can be used to combine and organize different modules and reactor systems of the assay. The microfluidic disc created by Ukita *et al.* provided an elegant solution for performing various functions on a multi-layer stacked CD [123]. The different layers of the stack segregated the different steps of the assay, and provided several advantages: the increased reaction surface area improved immobilization of antibodies; the increased total thickness of the disc layers provided a longer optical path length for detection; a single reservoir of reagents on one layer dispensed reagents to multiple locations on multiple layers. The utilization of this 3D architecture is a possible solution for sophisticated sample-to-answer assays that require increased fluidic control.

1.7 Analyte Detection Strategies

Two methods of analyte detection have been used on LoD systems: optical detection and electrochemical detection. CD microfluidics, inspired by conventional CD players, has generally preferred optical detection schemes. While molecular diagnostic assays generally utilize fluorescent methods, colorimetric methods for the detection of other analytes are also described. Colorimetric methods for the detection of nucleic acid biomarkers have not yet been implemented on a disc and are discussed in Section 1.7.3. In addition, recent advances in microfabrication of electrodes have made electrochemical detection an attractive option for microfluidic devices. This section highlights the recent advances in these two detection schemes, and suggests potential future developments for LoD systems.

1.7.1 Optical Detection

Fluorescent Detection

Fluorescent detection methods, unlike colorimetric detection, do not depend on the optical pathlength of the sample, contributing to their enhanced lower detection limits. For example, Duffy *et al.* used fluorescence to detect 2000 times lower concentration of a substrate, p-nitrophenol phosphate, than using colorimetry in the same sample volume. Fluorescence has been successfully used in conjunction with the centrifugal microfluidic platform for a wide range of applications including solid phase extraction [110], analysis of PCR assays [123,124], and immunoassays [125, 126].

In molecular diagnostics, DNA microarray hybridization is commonly used in nucleic acid detection, particularly when high-throughput analysis is required. On a microfluidic disc, Peytavi *et al.* implemented a diagnostic microarray for the detection of the DNA of four staphylococcal species. Flow-through of the sample through the microarray was found to be a more effective method for the hybridization of the target DNA strands with the probes as opposed to passive hybridization [127, 128]. This has been the only DNA microarray integrated with fluidics on a CD. Burstein Technologies developed a viable strategy using a laser in a CD drive to detect hybridization on DNA microarray [2]. After Streptavidin-labeled microspheres were added to hybridized spots, positive spots reflected laser light back to the CD drive's optical sensor. Other fluorescent detection methods for nucleic acid targets have been discussed extensively by Epstein *et al* [129].

Riegger *et al.* enhanced the sensitivity of fluorescent signals by using detection antibodies tagged with special fluorescent polystyrene microspheres, called FluoSpheres®, that amplify a fluorescent signal by two orders of magnitude [127]. The efficiency of this disc-based

fluorescent assay was enhanced by rapidly hybridizing the sample and probe using centrifugal force and by detecting several biomarkers on one microfluidic CD.

Fluorescent detection is generally performed with a stationary disc, forcing the user to stop the disc and manually align it to the camera to perform detection. To solve this problem, Ukita and Takayama developed a stroboscopic optical setup to image fluorescent objects on a spinning platform [130].

The results for fluorescent imaging, traditionally obtained visually through a microscope, can be subjective. To automate fluorescent image analysis, Sundberg *et al.* implemented a digital PCR assay (described in Section 3.1.2 and shown in Figure 3.2). The disc was imaged by a fluorescent reader, which consisted of a light emitting diode, a band-pass filter, a lens, and a charge-coupled device (CCD) camera. While the acquired results were analyzed with ImageJ software [124], digital PCR assays involve more objective image analysis that can easily be fully programmed, implying that the entire assay can eventually be automated.

Moreover, due to the high cost of optical hardware, research groups have presented alternative cost-effective solutions. To substitute expensive glass lenses, Kuo *et al.* fabricated a microfluidic disc with a built-in PDMS lens for focusing the excitation source [131]. Lutz *et al.* described a microfluidic disc for isothermal amplification that was operated using a modified commercial thermocycler, the Rotor-Gene 2000 (Corbett Life Sciences, now Qiagen, Australia), which was also capable of reading real-time fluorescent signals [13]. Adapting an existing machine reduces the cost and eliminates the need to develop new hardware.

Colorimetric Detection

Colorimetry is a widely used technique in many biological and chemical assays for evaluating the concentration of specific analytes. The analyte concentration is determined by measuring the absorbance of light of specific wavelengths when a probe beam is passed through a

sample holding chamber of a specific thickness. Absorbance (A) is linearly proportional to the concentration of a substance in a solution (c) and the optical path length of the solution (l), according to the Beer-Lambert law shown in eq. (1.6):

$$A = \varepsilon l c \tag{1.6}$$

where ε is the molar absorptivity of the sample.

Since the optical path length in a microfluidic device is typically very short, the sensitivity of colorimetric detection can be severely compromised. Rather than sending a light beam perpendicular to the bulk surface of a disc, Grumann *et al.* designed parallel V-grooves on both sides of the detection chamber to guide a laser beam through the length of a fluidic chamber and parallel to the surface of the disc (see Figure 1.15). The geometry of the chamber is designed to take advantage of the principle of total internal reflection, ensuring that no light is lost, and the entire light beam is reflected throughout the path length of the sample. This setup achieved a five-fold increase in the pathlength. The disc can continue to rotate while the colorimetric assay is executed, requiring no disc alignment to optical hardware and enabling real-time detection. The enhanced sensitivity of the method has been shown to be comparable to standard colorimetric cuvette-based assays, such as those for alcohol, glucose, and hemoglobin levels in serum and whole blood [64, 121, 132, 133].

1.7.2 Electrochemical Detection

Electrochemical detection is an attractive alternative to optical detection because of its low cost, small equipment footprint, high sensitivity, specificity, and portability [134–136]. The most common type of electrochemical detection used in microfluidic systems is amperometric detection [134, 137, 138]. In amperometric detection, the current produced with either the reduction or oxidation of an electroactive species is monitored.

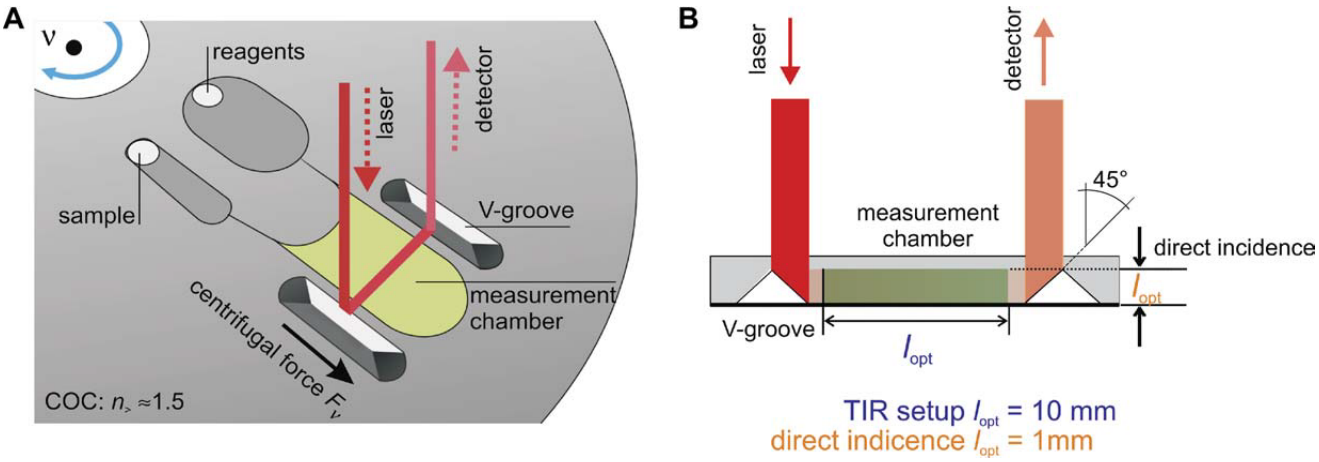

Figure 1.15: The system developed by Steigert *et al.* features two V-grooves on either side of the detection chamber. After the sample and the reagents are sent to the detection chamber by spinning the disc, a laser beam is pointed at one of the V-grooves for detection (A). The laser beam is directed through the sample along a path parallel to the surface of the disc, utilizing a longer optical path length and increasing the detection sensitivity. (Reproduced from Reference [133], ©2005, SAGE Pub.)

Amperometric detection has been successfully integrated onto the LoD platform using either a slip ring-and-brush setup [45] or a low-noise slip ring with liquid mercury for moving electrical contact [139]. In this detection scheme, three electrodes are typically used: a working electrode, a reference electrode, and an auxiliary electrode. An electrical potential is applied between the working electrode and a reference electrode. At the appropriate potential, a redox reaction occurs, and a current is generated. This current, measured between the working and auxiliary electrode, is directly proportional to the concentration of analyte being measured, while the voltage potential, measured between the working and reference electrodes, can be used for inferring the presence of a specific analyte in the system [140].

One application of this method is the detection of proteins or antigens in bodily fluids based on the redox reaction of a substrate bound to the target proteins or antigens. Kim *et al.* recently used this method to detect C-reactive protein (CRP) [138]. This electrochemical method can be used to replace the optical component of standard ELISAs, reducing the footprint of the system.

Another application of an electrochemical measurement is on-disc flow monitoring. Abi-Samra *et al.* determined the average volumetric flow rate by measuring the current of a ferrocyanide solution flowing over an embedded electrode array (See Figure 1.16). This method is called "flow velocimetry". Ferrocyanide was flowed from the loading chamber, across the electrode array, and into a collection chamber using centrifugal force. Since the flow of the solution enhanced the mass transfer of the electroactive species to the surface of the electrode, an increase in current could be detected as the flow rate increased. The current measured across the electrodes was determined to be proportional to the flow rate across the electrodes [141]. This powerful electrochemical technique uses no bulky hardware or expensive setups, making it ideal for portable applications.

Nwankire *et al.* developed an electrochemical LoD platform that performed whole blood fractionation and label-free detection of SKOV3 cells from whole blood [143]. They achieved a detection limit of 214±5 captured cells/mm^2 and a capture efficiency of 87%.

1.7.3 Future Outlook for Analyte Detection Strategies

While colorimetric detection for molecular diagnostics has not yet been implemented on a centrifugal microfluidic platform, several techniques developed by molecular biology groups can be integrated on a disc in the near future [144–147]. These colorimetric detection schemes can reduce hardware complexity where thermocycling is required and cut the cost of reagents compared to fluorescent detection schemes. However, streamlining and automation of multiple steps to achieve colorimetric detection will be required.

Other future work in analyte detection on a CD may involve integration of more compact and user-friendly optical methods and enhancing their lower limit of detection in applications such as early disease diagnosis and measurement of minute concentrations of biological toxins in waste water. The move towards the use of inexpensive and modular CD and DVD drives

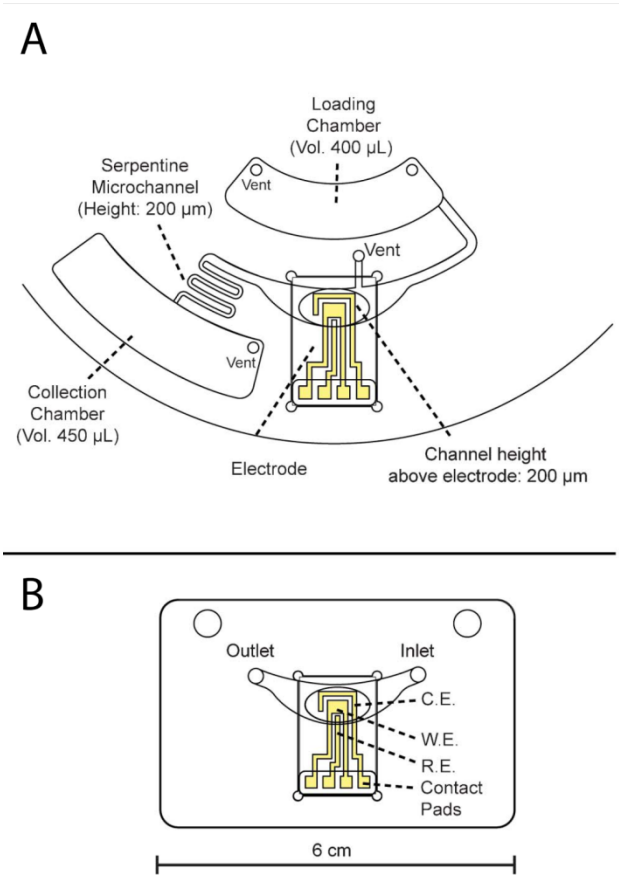

Figure 1.16: Abi-Samra *et al.* developed an electrochemical flow velocimetry device by integrating an electrode array onto a centrifugal microfluidic platform. (A) The solution is loaded into the loading chamber, passes over a bubble-free loading chamber with the electrode array integrated, and empties into the collection chamber. The serpentine microchannel parameters, including channel length and width, control the liquid velocity. The bubble-free loading chamber was based on the design by Siegrist *et al* [142]. (B) The gold electrode array was deposited onto a glass substrate insert and mounted onto the CD platform for flow velocimetry. (Adapted from Reference [141] with permission of The Royal Society of Chemistry.)

for optical detection is another future goal [148]. However, despite advancements in optical hardware, the move toward electrochemical detection, which is less costly and more compact, may be inevitable. In addition, optical detection requires complicated image analysis, which is generally difficult to automate and can be slow. With advances in microelectrode arrays, electrochemical detection can be easily integrated into microfluidic discs and provides fast analysis.

The future integration of electrochemical detection on a CD, which has already been successfully achieved via an electrical slip ring (see slip ring in Figure 7d) or induction, provides several advantages. Replacement of optical detection schemes allows for cheaper, biocompatible materials to be used instead of the expensive, optically clear substrates required for imaging. Smaller electrodes can be produced for a smaller footprint on the disc, leaving space for other features.

Furthermore, electrochemical DNA biosensors pose an attractive alternative to DNA microarrays and other optical DNA detection methods [149–151]. The most common electrochemical biosensors detect DNA hybridization by labeling the target DNA with a tag such as ferrocene, a redox active enzyme [152] [153] [154], or redox active silver or gold nanoparticles [155, 156]. Azek *et al.* demonstrated the sensitivity of this technique with their enzyme label-based biosensor [157]. The group used a peroxidase enzyme label and a screen printed carbon electrode to detect DNA sequences in *Human cytomegalovirus*. The limit of detection was 0.6 amol/mL of target, making the technique 83 times more sensitive than standard hybridization techniques detected using colorimetric methods.

Due to the redox active nature of certain DNA nucleotides, label-free electrochemical detection methods have also been successfully developed [158, 159]. Paleček *et al.* showed that both DNA and RNA produce reduction and oxidation signals following hybridization [160]. Since guanine is the most redox active DNA nucleotide, successful label-free electrochemical DNA hybridization sensors have immobilized guanine-free DNA probes for target detection.

Chen *et al.* created an ultrasensitive label-free electrochemical DNA biosensor by using self-assembled DNA nanostructures for signal amplification [161]. The limit of detection was measured as 2 amol/mL of target, making this sensor more sensitive than any optical technique.

While these electrochemical DNA biosensors have not yet been integrated in CD microfluidics, they present a cost effective yet highly sensitive alternative to optical detection methods, particularly in the burgeoning field of molecular diagnostics.

1.8 Current and Emerging Commercial Systems on a CD

To date, the most successful commercial LoD systems developed have included the Abaxis Piccolo Xpress® blood chemistry analyzer [165], the WaterLink® Spin Lab optical water analyzer by LaMotte [166], the Samsung LABGEO^{IB10} immunoassay analyzer [167], the Gyrolab™xP immunoassay workstation [126,168]. Molecular diagnostics systems, due to the efficiency and precision required in any point-of-care diagnostic system, are more challenging to develop. While diagnostic system on a CD include the commercial 3M™Integrated Cycler by Focus Diagnostics [169] and the GenePOC molecular diagnostics system [97, 170], the former performs only very simple sample preparation, while the latter has not entered the market where such a system is in urgent need.

1.9 The Demand for True Sample-to-Answer Molecular Diagnostic Systems

A summary of many recently developed on-disc technologies can be found in Table 1.3. Despite rapid technological advancements, no true sample-to-answer LoD systems have been demonstrated by research groups and very few are on the commercial market. Point-of-care sample-to-answer commercial systems available on the market include the cobas® Liat system by Roche Molecular Systems Inc. [171], the GeneXpert System by Cepheid [172], the FilmArray® technology by Biofire Diagnostics [173], and the Alere™ i [174]. These systems boast impressive sample-to-answer turnaround times, with the cobas® Liat system returning a diagnosis in just 20 minutes and the Alere i returning one using isothermal amplification in just 10 minutes. However, these systems are expensive, test for as few as one biomarker at a time, and each test cartridge cannot process more than one sample at a time. The advantages of the centrifugal microfluidic platform, coupled with the capabilities of the latest developments in molecular diagnostics, makes it possible for novel technologies to compete with, or even surpass, the standards of existing technologies.

The complexity of molecular diagnostic assay systems demonstrates the evident need for the integration of modular hardware elements in point-of-care diagnostic systems. Such an approach would reduce the number of hardware components used in a fully-integrated system, reducing cost and complexity of operation. Lab-on-disc systems pose a solution to some of the challenges experienced by existing systems, including multiplexing, which is already an intrinsic feature of CDs, and modular hardware systems. One example of a multifunctional hardware component includes the use of Peltier elements for heating, cooling, as well as reversible valving [16]. Yet another example is the LabTube ® technology, which is not a microfluidic disc, but uses a traditional programmable centrifuge to execute fluidic opera-

tions within a specially designed centrifuge tube, reducing the cost of hardware development and production [175].

This thesis discusses such integration of several thermally controlled technologies, including the thermo-pneumatic pump (Section 2.1) and the multifunctional wax valves (Section 2.2) in a sample-to-answer molecular diagnostic microfluidic CD. Integration of the whole system with thermocycling to perform NA amplification (Section 3.1.1) is discussed in detail in Chapter 3. In addition, the characteristics and advantages of a diagnostic microarray are discussed in Section 3.1.3. Microarrays are biomarker detection tools that allow even further possibilities for multiplexing. Each microarray can hold probes of hundreds to thousands of biomarkers, which, combined with the centrifugal microfluidic system, can create new breakthroughs in clinical throughput. Furthermore, Chapter 3 discusses the development of a thermally-controlled, fully-integrated system. Hardware modularity, combined with strategic on-disc operations, will increase the portability and reduce the cost of the overall system, making it more amenable to commercial applications.

Table 1.3: Summary of fluidic operations and reagent storage techniques executed on centrifugal fluidic platforms.

Process	**Techniques for implementation on LoD platforms**	**Advantages when used on LoD platforms**	**Applications**
Fluid-handling processes			
Volume definition	Centrifugation in combination with design of geometric features [6, 64, 65]	Bubble-free aliquots of samples lead to accurate volume definition.	Defining liquid volumes for optimal sample-reagent ratios; blood-plasma separation [64, 68–72]; real-time PCR (aliquoting) [75]; nanoparticle synthesis [66, 67]
Mixing	Magnet-aided [90]; droplet-based [162]; serpentine channels [81, 163]; flow reciprocation [34, 84]	Two types of mixing: diffusion-based and convection-based (via disc oscillation or flow reciprocation)	Most biological or chemical assays
Reagent storage			
Liquid reagent storage	Glass capsules [96]; metallized pouches [95]	Can be opened by centrifugal force or external actuation	Long term storage and on-demand reagent release in assays
Dry reagent storage	Wax-passivated [94]	Easy to control liquid flow during resuspension	Long term storage and on-demand reagent release in assays
Sample preparation			
Particle sorting	Magnet-aided particle sorting [103, 104]; size exclusion rail [105]; V-cup array [47–49]	Unique force gradients and pseudo forces allow development of novel separation techniques	Sedimentation-based sorting of functionalized beads [106, 107]; sorting of biological cells [104]
Sedimentation and filtration	Centrifugation in combination with reservoir geometry [64, 68–70, 101, 112, 116, 117]; integration of filtering structures [118, 119]	Spinning the CD induces rapid density-based separation and liquid flow through filters	Blood-plasma separation, and separation of other sample precipitates and supernatants; filtration of rare cells [101]
Sample purification and concentration	Fully automated laboratory protocol [111], solid phase extraction and elution [52, 108–110]	Fast extraction times and reduced volume of harmful organic solvents used	Purification and concentration of nucleic acids, environmental water pollutants, and proteins
Lysis	Mechanical lysis via bead-beating [11]	Mechanical lysis is easily implemented due to shear forces from glass beads	Nucleic acid retrieval
Analyte Detection Strategies			
Colorimetric detection	V-grooves for increasing light path length [64, 121, 132, 133]	Conformal, bubble-free filling increases sensitivity of measurement	Glucose, alcohol, and other assays measuring concentration of a substance
Fluorescent detection	Adoption of fluorescence-based assays for CD format [13, 110, 124, 125, 164]; magnetic biosensing [148]	Conformal, bubble-free filling increases sensitivity of measurement	Analyte detection, e.g. molecular diagnostics or immunoassay
Electrochemical detection	Integrated, miniaturized electrodes and slip ring setup allowing electrical contact during spinning [138]; mercury-based electrical slip ring [139]	Centrifugal force provides controlled flow to the electrodes, allowing continuous, rapid sampling.	Detection and quantification of a wide range of analytes [138, 139, 143]; flow velocimetry [141]; flow injection analysis

Chapter 2

Thermal Control Techniques for Fluid-Handling on a CD

In this chapter, two thermal control techniques are described: the thermo-pneumatic pump (TPP) and multifunctional wax valves.[1] The thermo-pneumatic pump uses a heat source to expand a pocket of air, pushing a liquid into another chamber. This technique can be used to transfer fluids to any position on the disc, but above all, to transfer fluids toward the center of the disc. This is advantageous since centrifugal force only pumps liquid outwards on a CD. The second technique, multifunctional wax valves, allows for liquid reagent storage, release, incubation, and downstream transfer. Besides paraffin wax loaded into the fluidic feature, this technique requires only a heat source for operation. Bother are active valving techniques and do not require any surface treatment during fabrication. The use of only a heat source for both techniques means that they can be combined into one platform to reduce the number of actuation hardware, thus reducing hardware cost and complexity. Integration of these two technologies into a fully-integrated platform is described in Section 3.2.1.

[1]Materials from this chapter used with kind permission from Springer Science+Business Media: Section 2.1 from Reference [44] ©Springer-Verlag 2011; Section 2.2 from Reference [92] ©Springer-Verlag Berlin Heidelberg 2014

2.1 Thermo-Pneumatic Pump

While the embedded fluidic pumping in a microfluidic CD by centrifugal force eliminates fluidic interconnects and enables multiplexing, motor-enabled fluidic operations generally only allow pumping of liquid toward the outer rim of the disc, a phenomenon termed "unidirectional liquid flow". The finite diameter of a centrifugal microfluidic device limits the number of fluidic steps that can be integrated into a sample-to-answer assay. To alleviate this problem, the thermo-pneumatic pump (TPP) was presented and was demonstrated to be capable of transferring a volume of liquid from any location of the disc toward the center of (or any other location on) the disc. The pumping mechanism involves heating a ventless chamber to expand the air inside, pushing the adjacent liquid into an existing channel. Using an infrared lamp, a non-contact heating method, vastly reduces complexity associated with fabrication or the integration of any hardware. The microfluidic disc has been fabricated with pristine polycarbonate material, meaning that surface treatment is not required, but can be modified in other ways to increase the efficacy of the pump. The ability to pump liquid toward the center of the disc opens the possibility for even more flexible fluidic operation and integration of longer assays on a disc.

2.1.1 Introduction

Although the centrifugal microfluidic platform has many advantages (see Table 1.1), the limited real estate from the finite disc diameter and the unidirectional liquid flow constraint pose a problem for long multi-step assays. Several techniques have been developed in the past to alleviate this problem, including pneumatic pumps by Gorkin *et al.* and Zehnle *et al.* [33, 36], capillary displacement by Garcia-Cordero *et al.* [176], the electrolysis pump by Noroozi *et al.* [45], and pumping using compressed air by Kong and Salin [177]. However, pneumatic pumps require high disc angular frequencies that can disrupt any fluidic steps

before the pneumatic pumping step and can limit the maximum angular frequency in the on-disc assay protocol. Capillary displacement is generally only sufficient for reciprocation and cannot transfer larger volumes to the center of the disc. The electrolysis pump requires direct electrical connection to the microfluidic CD chambers, raising the hardware and disc fabrication cost and placing a limited lifetime on certain hardware components such as slip ring setups (Figure 1.6). Lastly, pumping using compressed air requires a compressor or an external source and can introduce contaminants into the fluidic system.

To solve the problem of low real estate on a microfluidic CD, a technique termed "thermo-pneumatic pumping" was validated. Microfluidic reservoirs are usually designed to be near the center of the disc. The centrifugal force from spinning sends liquids toward the periphery, ending the fluidic path near the edge of the disc. For lengthier assays, the disc may not provide enough real estate. Increasing the diameter of the disc is possible but compromises its portability. The thermo-pneumatic pump (TPP) uses the principles of thermal expansion to control fluid flow, making flow toward the center of the disc possible.

The TPP uses a ventless chamber to pump a small amount of liquid toward the center of the disc. To operate the pump, it can be heated by a certain form of focused heating, such as radiation or contact heating. The air insides the pump expands and reaches the next chamber, pushing against the air-liquid interface of the liquid in the reservoir. The liquid is forced out of the exiting channel into a downstream chamber, which can be located anywhere on the disc, but gains more advantage when designed to be close to the center of the disc.

Two different designs, as shown in Figure 2.1, were used for analysis (Design A) and fluidic validation (Design B). Design A has a large microfluidic reservoir and a small collection reservoir and is not intended for complete liquid volume transfer. This design is used to model the pump after a large tank with a small leak, and more details will be given in the analysis section (Section 2.1.3). Design B is designed as a proof-of-concept experiment where a small volume of liquid can be completely transferred into the corresponding collection chamber. A

tapered geometry at the bottom of the microfluidic reservoir aids in the complete emptying of liquids.

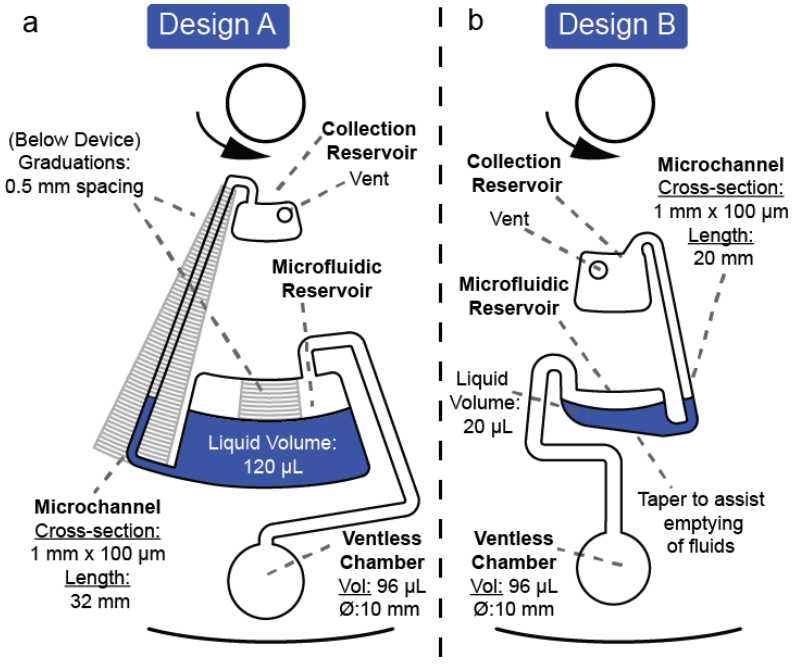

Figure 2.1: Two microfluidic TPP designs were implemented. Design A is used for analytical modeling. Graduation marks to track the change in fluidic level were positioned below the disc during experiments. This design is not intended for complete transfer (a). Design B is used to validate the fluidic design by completely transferring a volume of liquid toward the center of the disc.

2.1.2 Materials and Methods

The microfluidic disc was fabricated using the five-layer method illustrated in Figure 1.2. Clear polycarbonate sheets of 1 mm thickness were used for the plastic layers (McMaster-Carr, USA), which were machined using a CNC machine. Features were cut into two double-sided, pressure-sensitive adhesive layers (FLEXmount®DFM 200 CLEAR V-95 150 POLY H-9 V-95 400 POLY H-9, FLEXcon, USA) and channels were designed to be 100 μm in height.

The experimental setup for operating the TPP is shown in Figure 2.2. A halogen lamp served as the heat source (12 V 75 W, International Technologies MA) and an infrared temperature sensor (CSmicro, Optris, Berlin, Germany) was used to monitor the surface temperature, forming a feedback loop where the user can set temperature setpoints in a program made in LabVIEW software (National Instruments, TX, USA). The program received signals from the IR sensor and sent commands to a programmable power supply, which controlled the power of the lamp to reach the surface temperature setpoints. An imaging system that took one frame per revolution comprised a camera (Basler A311FC, 1/2in., C-Mount, 659 x 492, 73fps, color, CCD, 1394a, Germany), a strobe light (PerkinElmer MVS-4200, 6 μs duration), and a reflective trigger (D10DPFPQ, Banner D10 Expert Fiber-Optic Sensor, Minneapolis, MN, USA). All components were set up around a motor (Pacific Scientific Servo Motor, model PMB21B-00114-00) which was configured to spin a CD using the ToolPAC™ 4.1 software from Pacific Scientific (Pacific Scientific, Rockfield, IL).

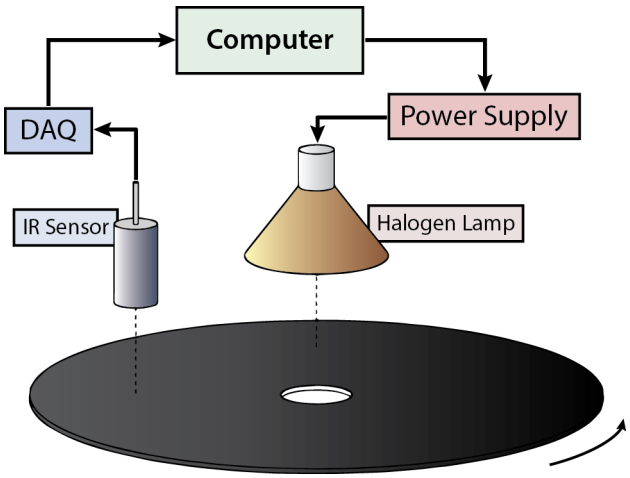

Figure 2.2: This flowchart illustrates communication between parts of the system's hardware– the computer controls input information and relays and displays output information. A signal is sent to the power supply, which turns on the lamp. The infrared temperature sensor points at the same radius of the disc as the lamp, reading the temperature of the region being heated. The signal is sent through the DAQ and is read by the computer. All the components form a feedback loop controlled by a user-input value (temperature in °C). This setup is used for fluidic and valve testing.

All experiments were performed in triplicates. For the experiment performed with Design A, the microfluidic reservoir was loaded with 120 μL of colored water. Then, the reservoir was sealed with an adhesive while the collection chamber remains open to atmosphere. The microfluidic disc was spun at 600 RPM or 1,200 RPM while heat was applied to the TPP, or ventless chamber, with an IR lamp. The fluidic meniscus positions were recorded as a distance from the center of the disc before heating, and during heat application at 5°C incremental intervals. Heat application was stopped when the liquid meniscus in the microfluidic channel reached the collection chamber.

For the experiment performed with Design B, a smaller colored liquid volume of 20 μL was chosen to be loaded into the microfluidic reservoir. After sealing the loading hole to ensure that the TPP remains ventless, the disc was spun at 300 RPM, and heat was applied at the radial position of the TPP. Complete pumping was observed after the surface temperature reached roughly 57°C ($\pm$1°C). This test was performed in two different configurations—a clear disc stacked under the microfluidic disc and a black disc stacked under the microfluidic disc. Discussion and results of this test can be found in Results and Discussion (Section 2.1.4).

2.1.3 Analysis

Design A is mathematically modeled, as shown in in Figure 2.3.

The model describes two air volumes inside the ventless chamber and the microfluidic reservoir as isochoric processes [44]. Since the two spaces are connected by a channel, they are able to interact by the physical exchange of molecules. The lamp's radiation is always on one part of the disc (ventless chamber), heating one volume, while the connected volume (microfluidic reservoir) is unheated. The volume of the connecting channel is assumed to be negligible, while the liquid exiting the microfluidic reservoir is assumed to be small enough

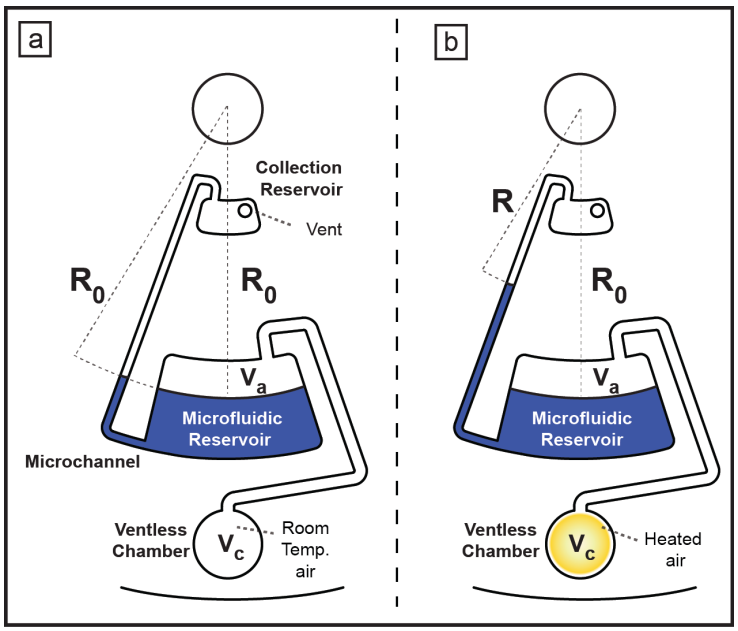

Figure 2.3: The thermo-pneumatic pump is modeled as labeled. A heated ventless chamber is treated as one volume while the space inside the microfluidic reservoir is treated as a second chamber. The model is developed to be similar to a large tank emptying through a small leak.

so that the liquid volume in the reservoir does not change. The system is modeled as a small leak from a large tank, and this is ensured by designing the cross section of the exiting channel to be small compared to the area of the air-liquid interface in the chamber—the former is 0.35% of the latter. The heated volume, V_h, and the unheated volume, V_R, are therefore always equal to the volume in the 2 spaces as shown in Figure 2.3. Also, to model the liquid in the microfluidic channel, the distance from the meniscus in the channel to the center of the disc before heating is represented by R_0. This assumption requires the contact angle to be approximately 90°, as it is for polycarbonate [178].

The following two equations use the ideal gas law to describe the initial conditions in the ventless chamber volumes:

$$P_0 V_h = n_1 R_c T_0 \tag{2.1}$$

$$P_0 V_R = n_2 R_c T_0 \tag{2.2}$$

where P_0 is the atmospheric pressure, n_1 and n_2 represent number of moles of molecules in volumes V_h and V_R, respectively, R_c is the ideal gas constant, and T_0 is the temperature of unheated air and can be assumed to be room temperature, or 25°C. The temperature for the ventless chamber is changed from T_0 to T as it is being heated by the IR radiation from the lamp.

$$PV_h = n_1' R_c T \tag{2.3}$$

$$PV_R = n_2' R_c T_0 \tag{2.4}$$

When heat is applied, the gas in V_h expands and the gas in V_R gets compressed. The number of moles of gas in each chamber is no longer the same, but the following equation holds true because the total number of moles of gas in the system can be assumed to remain the same before and after heating:

$$n_1 + n_2 = n_1' + n_2' \tag{2.5}$$

Substitute eqs. (2.1) to (2.4) into eq. (2.5):

$$\frac{P_0 V_h}{R_c T_0} + \frac{P_0 V_R}{R_c T_0} = \frac{PV_h}{R_c T} + \frac{PV_R}{R_c T_0} \tag{2.6}$$

Now isolate P:

$$P = P_0 \left(\frac{V_h + V_R}{V_h \frac{T_0}{T} + V_R} \right) \tag{2.7}$$

If P is subtracted from both sides of the equation, the change in total pressure in the system, ΔP, when heat is applied to V_h, can be found using the following expression:

$$\Delta P = P - P_0 = P_0 \left[\frac{V_h \left(1 + \frac{T_0}{T}\right)}{V_h \frac{T_0}{T} + V_R} \right] \tag{2.8}$$

With some rearranging, the equation for ΔP can be written as follows:

$$\Delta P = \frac{P_0 b \Delta T}{T_0 + (1-b)\Delta T} \tag{2.9}$$

while letting a volume fraction $b = V_h/(V_h + V_R) = V_h/V$ and temperature change $\Delta T = T - T_0$.

Even though the lamp heats the volume V_h only, it is necessary to point out that this volume increases over time and there are different possibility of temperature gradients. However, an approximation can be made to emphasize the relationship between the increasing temperature and volume. This relationship can be assumed to be proportional: $b = k\Delta T$. Substituting this into eq. (2.9), the next equation is obtained:

$$\Delta P = \frac{P_0 k \Delta T^2}{T_0 + \Delta T - k\Delta T^2} \tag{2.10}$$

The following equation relates the generated pressure to the height of liquid meniscus in the microchannel:

$$\Delta P = P(R) - P_0 = \frac{1}{2}\rho\omega^2(R_0^2 - R^2) \tag{2.11}$$

where ρ is the density of the liquid, ω is angular velocity of the spinning disc, and R is the distance from the channel liquid meniscus to the center of the disc after heat is applied. Solving for R^2/R_0^2 and substituting ΔP from eq. (2.10) gives:

$$\frac{R^2}{R_0^2} = 1 - \frac{2P_0}{\rho\omega^2 R_0^2}\frac{k\Delta T^2}{T_0 + \Delta T - k\Delta T^2} \tag{2.12}$$

In this equation, ρ is a constant and ω is a fixed value. R_0 is the position of liquid meniscus in the channel before heating, that is, when $\Delta T = 0$. For k, a relationship can be found

with ΔT_c, the temperature change for which $R = 0$, that is, when the liquid meniscus level inside the microchannel, R, is at the center of the disc.

Taking eq. (2.12) and substituting ε for $2P_0/\rho\omega^2 R_0^2$, the following equation results:

$$\Delta T_c = \frac{1 + \sqrt{1 + 4k(\varepsilon + 1)T_0}}{2k(\varepsilon + 1)} \tag{2.13}$$

where

$$k = \frac{T_0 + \Delta T_c}{\Delta T_c^2(\varepsilon + 1)} \tag{2.14}$$

It can be inferred that a change in volume ratio, V_h/V, can be easily induced, or caused by a smaller ΔT, when the constant k is larger. Tuning this relationship, specifically k, can improve the pump performance. Parameters that can be easily tuned include ω, the angular velocity of the disc, and R_0, the initial position of the microfluidic channel's liquid meniscus, although k is also affected by ρ, the density of the liquid being pumped, T_0, the initial temperate, and P_0, the atmospheric pressure,

In a specific circumstance where the liquid is pumped from R_0 to R_1, where $R_1 < R_0$, the pressure increase can be expressed as:

$$\begin{aligned} \Delta P &= P - P_0 - \frac{1}{2}\rho\omega^2(R_0^2 - R_1^2) \\ &= P_0\left(\left[\frac{T}{T_0}\right] - 1\right) - \frac{1}{2}\rho\omega^2(R_0^2 - R_1^2) \end{aligned} \tag{2.15}$$

The flow rate, Q of the liquid in the channel is then:

$$Q = \Delta P / R_{\text{hyd}} \tag{2.16}$$

where R_{hyd} is the hydrodynamic resistance of the channel and ΔP is the pressure change. The following equation is used to calculate R_{hyd} of a rectangular channel, where the cross section is denoted by $w \times h$, where $w > h$, the length is denoted by L, and the liquid has a viscosity of ν:

$$R_{\text{hyd}} \approx \frac{12\nu L}{1 - 0.63\frac{h}{w}} \frac{1}{h^3 w} \tag{2.17}$$

As the air in the ventless chamber is heated, it expands and flow rate slows down over time, and more pressure is needed for the liquid to continue flowing. To find the pressure change required over the entire pumping process, integrate from ΔT_{min} to ΔT_{max}:

$$\Delta P_{\text{avg}} = \frac{1}{\Delta T_{\text{max}} - \Delta T_{\text{min}}} \int_{\Delta T_{\text{min}}}^{\Delta T_{\text{max}}} \frac{P_0 k \zeta^2}{T_0 + \zeta - k\zeta^2} \, \mathrm{d}\zeta \tag{2.18}$$

where ΔT_{min} is the initial change of temperature needed to begin pumping the liquid, ΔT_{max} is the change of temperature needed to completely transfer the liquid, $\zeta = \Delta T$ is an integration variable.

ΔP_{avg} allows an average flow rate to be calculated from the model, so that total transfer time can be estimated. The constant k is related to the performance of the pump and how quickly heat is generated from the lamp and results in air expansion. Factors such as the material, color, and geometry of the pump can also play key roles in the liquid transfer process.

2.1.4 Results and Discussion

The relationship between R and ΔT can be shown in Figure 2.4, where normalized and squared distances of experimental liquid level values appear as points, and predicted values appear as lines. R_0, the initial meniscus position in the microchannel, is a constant. The

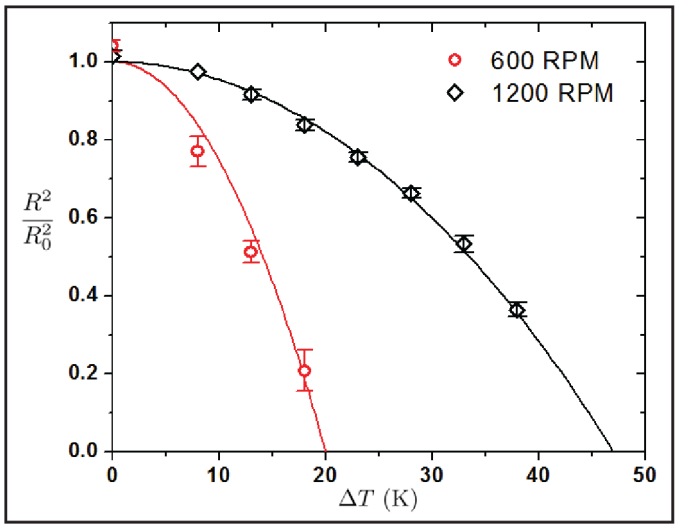

Figure 2.4: A graph of the normalized and squared distance of the liquid level in the microchannel versus the change in temperature as the IR lamp applies heat to the ventless chamber. The data shows the results from heating while spinning the disc at 600 RPM and 1200 RPM. Three trials were used for each condition.

relationship between $\frac{R^2}{R_0^2}$ and ΔT is given by Equation eq. (2.12). In general, a higher disc angular velocity requires a larger ΔT to achieve complete pumping.

From the experiments performed using microfluidic disc Design B, the pumping time was recorded and an average flow rate was calculated. Table 2.1 shows these flow rates and their corresponding calculated k constants. The data shows that for devices enhanced with a more IR-absorptive surface or color, the pump is more efficient (achieving a higher V_h/V ratio for the same ΔT value) than when the devices was simply stacked with clear polycarbonate as a negative control.

The TPP operates in a non-contact manner and multiplexes with ease. The ventless chamber can be adjusted in a variety of ways, such as increasing the depth or footprint size to improve pump performance or reducing these parameters when pumping a smaller volume of liquid in order to minimize the use of materials and on-disc real estate. Another factor to consider is the pump geometry. The pump used in the model was a circle, but the pump can be elongated and positioned along a single radius on the disc maximize its size and contact

Configuration type	**Below Disc**	**Rotational Speed (RPM)**	**Flow Rate (μL/min)**	**Calculated Model Constant** $k(\times 10^{-4}\ \mathbf{C}^{-1})$
Low IR absorption	Clear, colorless polycarbonate disc	300	8.26 ± 0.46	3.73 ± 0.78
High IR absorption	Opaque, Black polycarbonate disc	300	17.6 ± 1.5	5.74 ± 0.91

Table 2.1: Table of configurations below each disc for performing thermo-pneumatic pumping and the corresponding experimental and calculated parameters.

time with the heat source. Furthermore, if heating of the liquid to be pumped is not desired, the ventless chamber should be designed to be on a different radius than the fluidic reservoir.

The TPPs are chambers designed into the disc so that fabrication is simplified, and no extra step is necessary. The lack of moving parts within the device makes the technology more robust and reliable. The TPP is compatible with a variety of material surfaces and liquids. In addition, the TPP is suitable for the CD platform because the the spinning of the disc is necessary for the efficacy of the pump; the centrifugal force pushes the fluid outward, organizing the liquid so that there is an even air-liquid interface for the expanding air to push on. These features make the TPP inexpensive to integrate with disposable devices and simple to operate .

2.2 Multifunctional Wax Valves

Recently, a number of biological assays have become available on the centrifugal microfluidic platform. Despite many innovative solutions developed for on-disc fluid handling for these assays, certain challenges, including liquid incubation and simplification of a multi-step assay on a plastic device, still need to be further addressed. Incubating liquids that require downstream processing, which is termed "midstream incubation" here, can often be

difficult on the microfluidic disc platform due to surface tension changes induced by varying temperatures, thus causing operating instability. This chapter describes strategies for liquid reagent storage, release, incubation, and transfer, all of which utilize a single combination of actuation methods—wax valving and heat actuation by halogen lamp—on a centrifugal microfluidic device made using pristine materials. The strategies used to perform these steps, termed multifunctional wax valves, enable manipulation of a microliter range liquid volume without the need for complex fabrication steps or hardware. This technology's reliability and ease of use will hopefully allow for more powerful clinical diagnostic tools to be created.

2.2.1 Introduction

The field of centrifugal microfluidics, also known as Lab-on-a-CD, has seen noteworthy gains in the last two decades due to interests from both academia and industry [179, 180]. The compact disc (CD) platform has been used in a variety of applications, including biological and chemical assays and studies on living organism and physical phenomena. Researchers often choose the centrifugal microfluidic platform for a number of its advantages, such as an embedded fluid pump (centrifugal force generated by rotation of the motor), ease of multiplexing, and compatibility with many different types of liquids [3]. In addition, these devices embody the advantages of chip-based microfluidics, such as small reagent volume, smaller diffusion paths, portability, and programmability. Although the rotating platform is attractive, new strategies are constantly sought for more robust fluid control.

While the operation of microfluidic CDs seems straightforward, microfluidic assays with increasing numbers of steps have become more complex and unreliable to operate using passive valves [3]. Meanwhile, active valves, or valves controlled by external sources, have been developed and made available. Nevertheless, research has not yielded simple-to-implement techniques that can be easily integrated into a platform for fluidic control of processes

including liquid storage [96], release [41, 59, 71, 95, 98], incubation [13, 16], and transfer [3, 10, 31, 33, 44, 45]. Such a process is crucial for certain nucleic acid amplification processes. Therefore, the multifunctional wax valves technology aims to expand the toolbox of fluid handling strategies by using paraffin wax-based non-contact heating to performing these fluid handling steps.

A defining feature of rotating microfluidic platforms is that fluids are manipulated in a non-contact fashion by spinning the disc to generate centrifugal forces [2, 3, 6]. In this case, non-contact control refers to the use of operating equipment, besides the motor, that does not need to be in physical contact with the disc's surface during actuation; typically, non-contact control is achieved by spinning of the motor at various angular frequencies. The main advantage of non-contact control on the centrifugal microfluidic platform is that minimal alignment of external equipment to disc is necessary. Thermal energy is one strategy that has progressively gained more attention and can be potentially implemented in a non-contact fashion on a rotating platform. Previously, heat has been used in several cases to achieve on-disc valving and pumping [41, 44]. High sensitivity assays, such as polymerase chain reaction (PCR), require heat and have been executed on a rotating disc by research groups as well as by commercial groups [13, 16, 124], but heat also has the potential to be paired with microfluidic discs to perform other biological and chemical assays such as immunoassay, protein characterization, and glucose concentration measurement [181–184]. Although there has been some concerns regarding the loss of sample volume by evaporation during high-temperature incubation processes [185], this problem has been addressed by Amasia *et al.* using ice valves on a temporarily stationary disc and by others by simply spinning to recollect evaporated and condensed sample at the end of a fluidic path [16, 75]. However, no group has yet utilized the CD platform to perform "midstream incubation", which is defined here as incubation as an intermediate step in a multi-step assay, without depending on contact valving. This is due to the unpredictability and lack of reliability of current passive valving techniques for liquid-handling when heat is applied. Meanwhile,

midstream incubation is important because sample preparation steps that precede incubation and pre-detection steps that follow incubation can often complicate the implementation of the incubation step. This section presents multifunctional wax valves, a technique that performs fluid-handling using paraffin wax and non-contact heating while leveraging the rotation of the device to, for example, recollecting condensate during thermo-cycling and pumping using non-contact control. This technique can be used to address the challenges encountered when implementing high-temperature midstream incubation. Multifunctional wax valves integrate a liquid storage solution that uses normally closed ("normally closed" refers to a valve that is closed until opened and is often single-use) paraffin wax valves in the incubation chamber where other fluid handling steps are performed. In the past, only a few storage techniques on a disc have been explored [51, 95, 96]. The storage solution to be described here is implemented by forming layers of wax surrounding the liquid to be stored while the disc is spinning. Furthermore, the release of the stored liquid is integrated with a technique that enables liquid incubation and transfer into a downstream chamber, all of which use only one heat source for actuation, reducing the complexity of implementation.

2.2.2 Materials and Methods

Microfluidic Disc Fabrication

Typically, microfluidic discs are fabricated by pressing layers of plastic and double-sided pressure-sensitive adhesives together (see Figure 1.2). Since the microfluidic devices in this experiment were heated for long periods of time during experiments, adhesives initially disintegrated after 10-15 min, resulting in air and liquid leaks; therefore, more heat-resistant materials were sought and the materials and fabrication method were reconsidered so that fewer layers were directly in contact with the liquid and the possibility of heat-induced delamination was diminished (see Figure 2.5). New discs were fabricated using a 3-D CNC

machine, Roland MDX-40A (Roland DGA Co., Irvine, CA), which was used to mill 1.2-mm-deep chambers into clear polycarbonate plastic sheets (McMaster-Carr, USA). Chambers and channels were cut into a single-sided, PCR-compatible adhesive (9793R, 3M, St. Paul, MN), which was topped by another layer of the same type of single-sided pressure-sensitive adhesive with only loading holes. The layers so far ensure that the fluidic features inside the disc would not detach during the heating process. In addition, since heat-generated pressure was needed for this experiment, a rigid polycarbonate layer was attached to the top of the disc using a double-sided pressure-sensitive adhesive (Flexmount®DFM 100 Clear V-326 150 Poly H-9, FLEXcon, USA). Loading holes accessing the experimental chamber allowed manual loading of solid paraffin wax obtained from Calwax (Irwindale, CA) and sample liquid loading via manual pipetting. Note that no surface treatments were done—all devices were made with pristine materials.

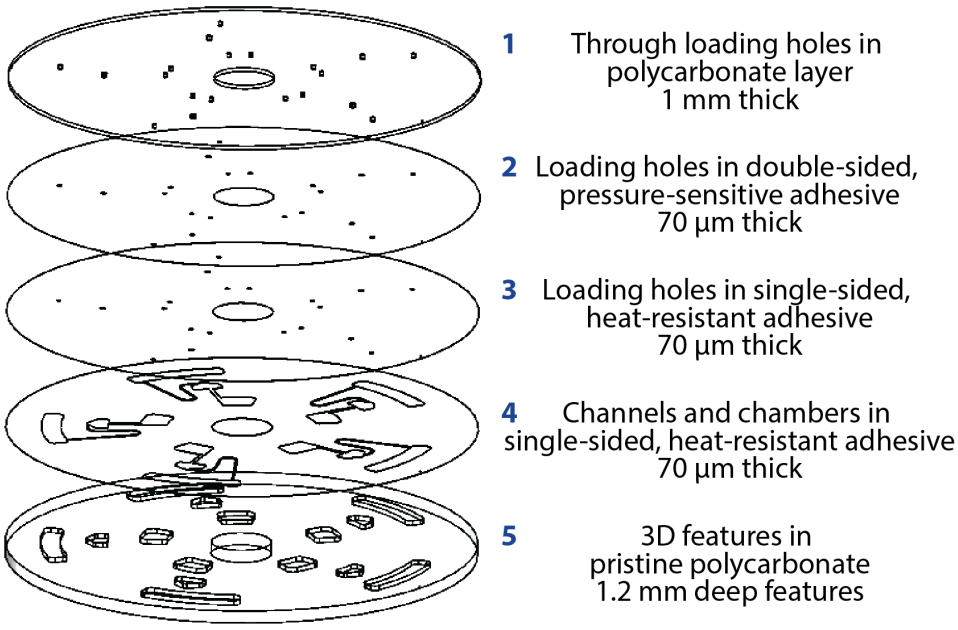

Figure 2.5: Layers in the microfluidic disc, used in implementing multifunctional wax valves, are shown. All features, besides loading holes, are in either layer 5 (deep 3-D chambers) or layer 4 (chamber and channels cut into an adhesive layer whose thickness defines the feature depth). Layers 3 and 4 are heat-resistant adhesives, chosen to prevent delamination of disc layers during heating. Layer 1 is used to ensure that microfluidic chambers have rigid walls for the implementation of built-in thermo-pneumatic pumping and is held on to layers 3, 4, and 5 using layer 2. All layers are clear and colorless and free of any surface treatments

Experimental Setup

Microfluidic discs were mounted onto a spin stand, which comprised a programmable spinning motor (Pacific Scientific Servo Motor), which allows for the full control of spin speeds, and a strobe-triggered camera (Basler A301bc, 640 480 pixels, 80 fps), which allows for visualization and acquisition of one image frame per revolution. More details of the set-up was given by Noroozi *et al* [34]. Focused thermal energy was delivered to the rotating microfluidic disc in a non-contact fashion by an infrared heating setup mounted above the disc. This setup, which consisted of a halogen lamp (12 V 75 W, International Technologies, MA, USA) and an infrared sensor for surface temperature monitoring (CSmicro, Optris, Berlin, Germany), is described in Section 2.1.2 and shown in Figure 2.2. All reported experimental temperatures are of the disc surface.

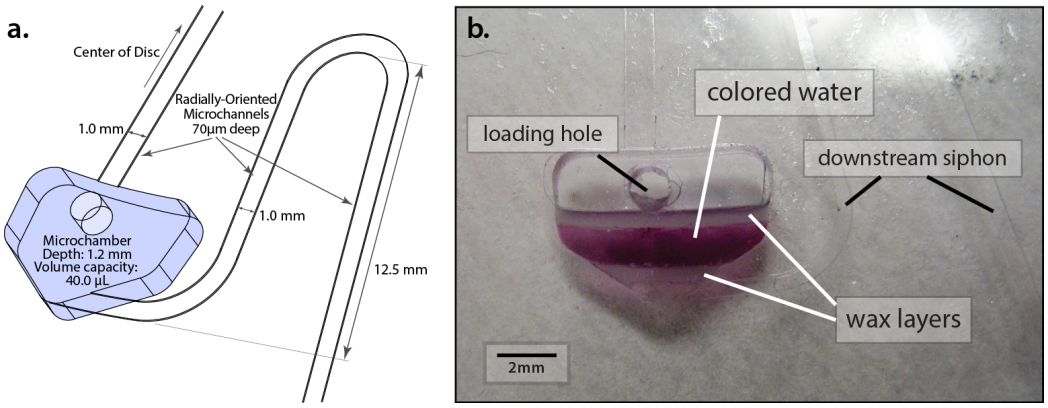

Figure 2.6: **a.** Schematic of the chamber and connecting channels used for liquid storage, incubation, and transfer. The top edge of the chamber is located 3.5 cm from the center of the disc and the infrared radiation was applied directly to the center of the chamber. **b.** A liquid volume iss stored between layers of wax in this chamber.

Methods: *In situ* storage of liquids using paraffin wax

To store liquid reagents on a microfluidic disc, paraffin wax was melted directly inside the liquid-holding chamber (shown in Figure 2.6a) to encapsulate the liquid between wax layers, as shown in Figure 2.6b. Wax layers were formed at the top and bottom of the liquid in

order to form a vapor-tight seal that encloses the fluid. Because molten wax is less dense than aqueous solutions and always floats closer to the center of the chamber, forming this seal is a two-step process. First, about 2 mg of wax (T_m = 65.6-73.9°C) was loaded into the chamber. The loading hole of the chamber was then sealed with and adhesive and the disc was spun at 2,000 RPM. The chamber was heated to 80°C to ensure complete melting and collection of the wax at the bottom of the chamber. Then, the disc was passively cooled to 30°C. Melting of the wax blocked fluid access to the downstream channel of the chamber, preventing any liquid or vapor from entering the downstream chamber. Next, 25 μL of liquid and 4 mg of wax (T_m = 57.2-62.7°C) were loaded into the chamber. The disc was again spun at 2,000 RPM while heating to 60°C to only melt the low-melt wax. Once a uniform layer of wax was formed over the liquid, the disc was cooled to 30°C before spinning was stopped.

Note that under stationary conditions and low spin speeds, low surface tension causes molten wax to preferentially adhere to the disc's polycarbonate surfaces. The adhesive forces between the molten wax and the polycarbonate dominate, causing the wax to rise along the chamber walls. Although this does not prevent sealing of the liquid by the wax altogether, a thinner and more fragile layer of solid wax results as more wax is lost to the chamber walls. A relatively small amount of paraffin wax was used in order to preserve chamber space for effective thermo-pneumatic pumping (described in the next section). Consequently, spinning the disc at a sufficiently high angular velocity, which, in this case, is 2,000 RPM, is required to generate a centrifugal force large enough to maintain the uniformity of the molten wax layer. With a different liquid-transfer method where the amount of wax use in a chamber is not limited, a smaller centrifugal force and more wax could then be used to encapsulate liquids.

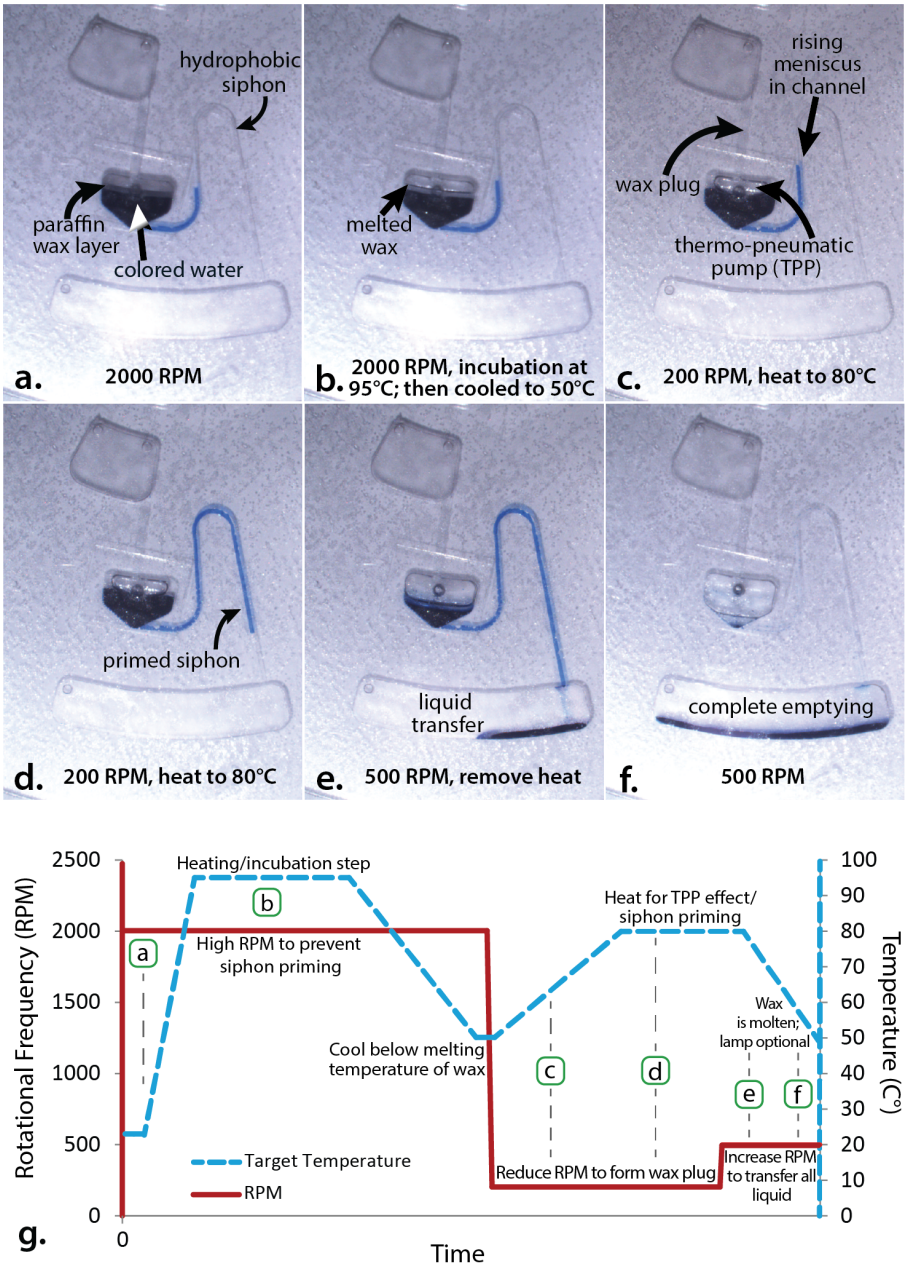

Figure 2.7: a-f Time-lapse sequence of fluidic control mechanism. A solid paraffin wax layer above the liquid is shown in (a). Heat is applied to attain a steady temperature of, for example, 95°C, while the disc is spun at 2,000 RPM, enabling the melting of wax as shown in (b). The chamber is then cooled to 50°C. In (c), the disc is slowed down to 200 RPM. When heat is applied, the low centrifugal force allows the wax to wick into the upstream channel, forming a thermo-pneumatic pump (TPP). In (d), the liquid in the siphon is pushed towards the downstream chamber. Liquid is being transferred in (e) before the liquid has cooled down and the transfer is complete in (f). g The spin and heat profile for the process. The slopes for the temperature changes are estimations of actual ramping rates, and the alphabetical labels in the green boxes refer to time points at which the corresponding events in a-f occur.

Methods: A technique for non-contact, midstream sample incubation and transfer

The fluidic chamber and channels shown in Figure 2.6, in which liquid is stored using paraffin wax valves, was also used to perform release and incubation of the stored liquid before the liquid was transferred into a downstream chamber. The steps for the transfer of the liquid are illustrated in Figure 2.7a through 2.7f. First, 25 μL of water and 4 mg of low-melt paraffin wax were loaded directly into the incubation chamber. The liquid storage set-up described in the previous section can also be used (Figure 2.7a).

After the loading hole of the incubation chamber was sealed, the incubation chamber had no direct connection to ambient air. The upstream and downstream chambers were each vented to ambient air to prevent pressure build-up and facilitate liquid transfer, while the incubation chamber accessed the upstream chamber via a simple hydrophobic channel and the downstream chamber via a hydrophobic siphon. The disc was spun at 2,000 RPM during incubation so that the centrifugal force constantly overcame any capillary force that could prematurely wet (prime) the downstream siphon and lead to liquid transfer; as a result, the liquid remained in the incubation chamber during this step. The incubation chamber should be heated to a sufficiently high temperature to ensure complete melting of any paraffin wax. In this particular case, IR energy was applied at the radius of the spinning disc where the incubation chamber was located for the chamber to reach 95°C in order to simulate high-temperature incubation (Figure 2.7b).

In preparation for the liquid transfer step, the disc was passively cooled to 50°C before its angular frequency was slowed down to 200 RPM. Heat was once again applied so that the disc reached no more than 80°C. Because of low centrifugal force, capillary forces pull the molten wax towards the center of the disc into the upstream channel, creating a ventless chamber and a thermo-pneumatic pump effect (Figure 2.7c). The expansion of air inside

a ventless volume (TPP) pushed the liquid over the crest of the downstream hydrophobic siphon, which is the energy barrier before reaching the next chamber (Figure 2.7d). Because the molten wax plug is temporary, the thermo-pneumatic pump acts as a light-duty pump and only sufficiently powerful to prime the downstream siphon. Although the pump pushes the molten wax plug up at the same time as it pushes the liquid down, the capillary forces in the upstream channel are sufficient to retain the molten wax in the channel for the operation of the TPP. The liquid meniscus in the channel must pass over the crest of the hydrophobic siphon and reach below (closer to the outer perimeter of the disc) the liquid meniscus level in the chamber in order for a hydrostatic pressure difference to be present. Due to this hydrostatic pressure difference, the liquid transfer began when the rotational frequency of the disc was increased to 500 RPM (Figure 2.7d).

Finally, continuous spinning at 500 RPM completed the transfer while the wax is still molten (Figure 2.7e-f). The lamp can be controlled accordingly. In this case, because the temperature for the previous step was much higher than the melting temperature of the wax, the lamp was turned off during transfer. At the end of the transfer, most of the wax remains in the incubation chamber. The target temperatures for the disc and the spin profile used are shown in Figure 2.7g.

2.2.3 Results and Discussion

Multifunctional wax valves can be used anywhere in a complex multi-step assay. If no reagent needs to be stored, the wax plug does not need to be formed beforehand, and paraffin wax can be loaded directly into the incubation chamber; however, if necessary, the wax can also facilitate storage of liquid reagents. On the other hand, additional liquids that need to mix with the stored liquid volume can be introduced just before the incubation step. Due to the heating and spinning protocols required to actuate downstream transfer, any required

mixing of liquids can be easily implemented using gentle oscillations of the disc without risk of premature transfer. Multifunctional wax valves use a combination of non-contact actuation techniques—paraffin wax and focused IR heating—to implement seamless release, incubation, and transfer of a stored liquid volume. The simplicity of implementation of these methods enables non-contact sample incubation and valve actuation on a platform where, previously, fluid handling under heat application had been difficult and unreliable to implement. Non-contact heating is advantageous because it does not require alignment of the device to stationary components and allows for effortless multiplexing [44]. Uniform heating is achieved simply by spinning the disc, and the lamp can be positioned at any radius where elements need to be heated. Contact valves, such as ice valves and pinch valves, which are more difficult to implement due to the need to align external elements with the microfluidic device, are no longer required when the rotation of the platform is leveraged for the multiplexed heating of fluids. While continuous spinning is required for uniform heating, it also performs other functions, including collection of condensate from more centrally located fluidic features to reduce liquid volume loss by evaporation, as well as elimination of unwanted bubble formation during heating by density-based separation [3,75].

The multifunctional wax valves technique transfers liquid downstream using only wax and heat. During heating, capillary forces pull the wax into the upstream channel, creating a ventless chamber, and thus, a thermo-pneumatic pumping effect. The behavior of the thermo-pneumatic pump has been previously characterized experimentally and analytically (See Section 2.1) [44]. The force generated from the expansion of the ventless volume enables sufficient priming of the downstream siphon, forming a hydrostatic pressure difference between the liquid level in the incubation chamber and the meniscus in the siphon. With the pressure difference present, complete transfer of liquid to the downstream chamber was achieved simply by increasing the centrifugal force. Because both heat and the required RPM must be present in order for the valve to function, the feature is categorized as an active valve, implying increased reliability. In addition, the delivery of focused IR energy ensures

rapid heating of the polycarbonate disc and hence, quick on-demand valve actuation. Since heat must be applied to actuate the pump for transferring liquid downstream, the incubated liquid must be heat insensitive, limiting the number of applications. However, considering that heat decreases the surface tension of a fluid, which can affect passive valves' burst frequencies, incubations that require heat may find this technique to be advantageous. Note that although heat and wax are used for valving purposes, this technology has a different utility and operating protocol than simple wax valves [41] in that while heat is applied to the incubation chamber, liquid will not move to the next chamber at a high disc angular frequency even if wax is molten. In addition, a regular wax valve would open at any angular velocity when heated, while the multifunctional valve will not allow exit of liquid if the angular frequency of the disc is high (*i.e.* 2,000 RPM or higher).

To explore the versatility of the technology, experiments were performed to test the range of working volumes of colored water that can be handled during downstream transfer from the incubation chamber (Table 2.2). Each incubation chamber is 40 μL in volume but is never filled to capacity so that space is left for the ventless volume to form before pumping. In the design used for these tests, all channels are 1 mm wide and 70 μm deep. Each trial was tested on an new and pristine microfluidic unit. "Successful trials" refer to trials that completely pumped after performing the protocol once, while "re-attempted trials" refer to trials that did not pump on the first try. In the latter case, a high angular frequency (2,000 RPM or higher) was applied to the disc, and the heat was turned off to "reset" the contents of the microfluidic chamber to their starting state before the protocol is repeated. From the table, it can be concluded that the pumping process works the best when the volume being pumped is close to half of the capacity of the chamber. However, the pumping technology is versatile given that it is still able to pump a wide range of volumes.

The current work is a proof-of-concept of a technology that is easy to fabricate and can reliably perform several crucial fluidic steps with minimal external hardware. Thus

A. Liquid volume (μL)	B. Total number of trials	C. Successful trials	D. Successful re-attempted trials
10	4	3	1
15	4	4	N/A
25	3	3	N/A
35	4	2	2

Table 2.2: Number of trials testing downstream transfer out of the incubation chamber for a range of liquid volumes (column A), where liquid refers to colored water. The protocol in Section 2.2.2 was implemented on a number of fluidic units (B), and the number of successful trials was recorded (C). For trials that were not successful, the fluidic unit was "reset" by cooling and spinning the unit at high spin frequency before the protocol was attempted again. The number of successful re-attempted trials was recorded (D).

far, paraffin wax has shown to have high permeability on a spectrum of different classes of materials [135], which is not optimized for liquid storage. Nevertheless, future work will involve further optimization of the technique and its applications. To implement paraffin wax valves for longer period storage, wax can be placed directly in the channels and tested in conjunction with liquid incubation and transfer. One application discussed in Chapter 3 is amplification of nucleic acid biomarkers (e.g. DNA) using polymerase chain reaction (PCR). In traditional tube-based PCR methods, evaporation during thermo-cycling was reduced by keeping the tube closed or adding a layer of oil or paraffin wax [186, 187]. The latter method did not have a negative side effect, justifying the use of the multifunctional wax valves technique for PCR applications. Direct integration of this technology into a full molecular diagnostics assay is expected in the near future.

For the first time, multifunctional wax valves utilize heat wax to perform seamless storage, incubation, and transfer of liquids. The compatibility of paraffin wax with biological samples allows for this technique to be used in many assays, especially when a heated mid-stream incubation step is necessary. The user can store a liquid reagent in the incubation chamber before releasing it and using existing hardware, required for heating, and paraffin wax for pumping. Moreover, the pump utility was shown to be not only reliable because it is an active valve that depends on both the heating and the spin frequency sequence, but also versatile in the amount of liquid it can transfer. Multiplexing is effortless, and the need for

aligning the disc to control any valve in a contact manner is eliminated. These characteristics of the multifunctional wax valves technique on the centrifugal microfluidic platform enable more possibilities for versatile and robust fluid handling in future assays.

Chapter 3

A Fully-Integrated Detection Platform Using PCR and Microarray

One of the popular and heavily explored applications of the centrifugal platform is the amplification of genomic material (nucleic acid) through a high-sensitivity assay termed polymerase chain reaction (PCR). Error-free automation of an assay and DNA amplification will vastly reduce the time involved in manual work and lead to rapid and sensitive diagnoses at the point of care. However, very few truly complete sample-to-answer disease diagnosis systems have been developed due to the complexity involved in automating all the steps from sample preparation to detection. This chapter discusses the integration of the thermo-pneumatic pump (Section 2.1) and the multifunctional wax valves (Section 2.2) into a microfluidic disc-based system that performs sample-to-answer processing. In addition, a custom-built hardware system is capable of all fluidic operations. The system serves as a platform for biological assays that perform nucleic acid amplification using polymerase chain reaction (PCR) and DNA microarrays. Besides the integration of the modular fluidic technologies onto a microfluidic platform, this chapter will discuss the relevant molecular biology

background, the hardware for the system, and results from PCR experiments performed on microfluidic discs.

3.1 Molecular Diagnostics and Centrifugal Microfluidics

Molecular diagnostics techniques have been a crucial component in point-of-care diagnostics, boasting high specificity and low limit of detection. Nevertheless, while nucleic acid amplification has been the focus of scientists and industry for several decades [188], typical tests are still associated with cumbersome laboratory bench preparatory steps, long experimental durations, and low throughput. Improvements to these tests can embody full automation and the comprehensive integration of sample preparation steps as well as post processing steps. Researchers in the field of centrifugal microfluidics have contributed to this goal by developing microfluidic devices and hardware systems that are capable of rapid PCR, although improvements are still crucial. This chapter describes a fully-integrated system with reduced hardware complexity and higher multiplexing capabilities that will hopefully attribute to further developments in point-of-care technologies.

3.1.1 Nucleic Acid Amplification

Nucleic Acid (NA) amplification is an integral part of genetic analysis, allowing for the detection of a low starting quantity of biomarkers, which is especially valuable when attempting to diagnose a disease in its early stage. One of the most commonly used techniques for NA amplification is polymerase chain reaction (PCR), an enzyme-driven reaction that amplifies a sequence of target DNA by cycling between specific temperatures. For certain other cases, where the sample consists of RNA strands, reverse-transcriptase PCR (RT-PCR) is required.

In RT-PCR, strands of RNA are transcribed into their complementary DNA (cDNA) before the cDNA strands are amplified with PCR.

PCR generally cycles between three target temperatures to perform three steps—a denaturation step to separate the single strands in double stranded DNA, an annealing step for PCR primers to adhere to the DNA templates, and an elongation step for the polymerase enzyme to synthesize the complementary strand to the template. Denaturation generally occurs at 95°C. The annealing temperature depends on the primer used and is generally a few degrees below its melting point; the temperature control for this step must be very precise for high specificity. The elongation step is generally performed around 72°C [189]. The number of cycles for the assay depends on the required limit of detection; generally, up to 40 cycles are performed [190]. The exact temperature protocol must be optimized for each sample and each set of reagents and equipment used. In general, the main time-limiting step is the long ramping times between the target temperatures, especially with large liquid volumes. Furthermore, large temperature changes lead to substantial power consumption and generally require bulky hardware.

3.1.2 Current Centrifugal Microfluidic PCR Technologies

To address the challenges of slow temperature cycling times and high power consumption, PCR thermocycling has been incorporated on miniaturized centrifugal microfluidic platforms. By increasing the sample's surface area to volume ratio, a larger area of the sample is exposed to temperature gradients, yielding faster thermocycling times. Moreover, utilizing smaller components decreases power consumption.

One of the first uses of PCR on a centrifugal microfluidic system was by Kellogg *et al.* who amplified E. coli DNA. A Peltier element, embedded in a spinning PCB, is in direct contact with the thermocycling chamber on the microfluidic disc, and an integrated thermistor was

used for temperature feedback control to achieve a ramping rate of 2 C°/s for a 25 μL reaction volume [191]. The disc was spun to minimize loss of sample volume so that liquid that condensed upstream returned to the PCR chamber. Contact heating has since been used for effective and fast PCR thermocycling by Amasia *et al.*, who used a stationary disc and ice valves for vapor-tight sealing of the PCR chamber during thermocycling [16, 192]. The design by Amasia *et al.* used Peltier elements for heating, cooling, and valving (shown in Figure 3.1).

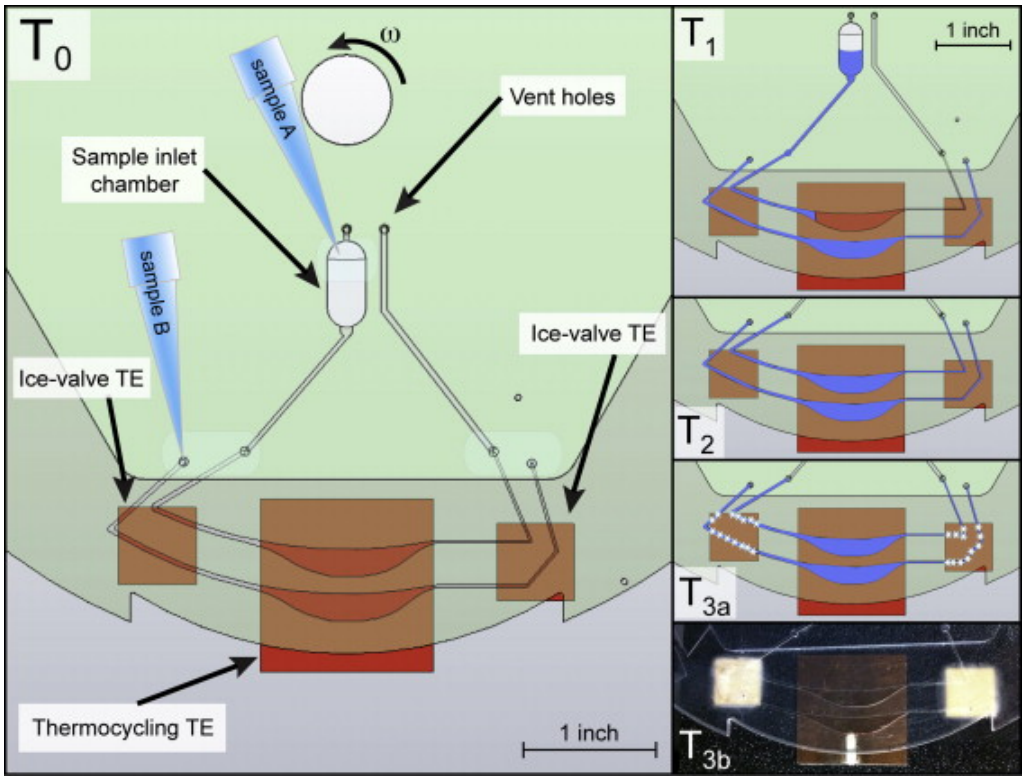

Figure 3.1: Schematics showing Amasia *et al.*'s integrated CD setup for PCR thermocycling. A sample, "sample A", is pipetted into the inlet chamber and the disc is spun, transferring the sample into the inner PCR chamber. A negative control, "sample B", can be directly pipetted into the loading hole, filling the outer PCR chamber. Two small Peltier elements act as ice valves for channel sealing, and one large Peltier element acts as a heater for thermocycling. Once the samples properly fill the PCR chambers, the disc is stopped and the ice valves are turned on, sealing off the chambers. Thermocycling can be performed with minimal loss by evaporation. (Reprinted from Reference [16], ©2012, with permission from Elsevier.)

Non-contact heating was first used by Mårtensson *et al.*, who utilized an IR lamp positioned directly above the PCR chamber on a rotating disc to actively heat liquids to desired temperatures [193]. While spinning the disc, both centrifugal and Coriolis forces contributed to the increased circulation and temperature homogenization of the sample. Passive cooling was implemented by fast spinning of the disc. A single cycle time of 20.5 seconds was achieved for a 100 μL sample, with 45 cycles of PCR finished within 15 minutes. The method of using pseudo forces on a disc for temperature homogenization of a sample, called Super-Convection, was patented by AlphaHelix Molecular Diagnostics AB. Burger *et al.* used an IR thermocycler with an integrated on-disc wireless temperature system to improve non-contact heating [194]. The group obtained a heating rate of 5°C/s with a PID controller by optimizing disc materials and depth of the sample-holding cavity.

Another technique for NA amplification, reported by Sundberg *et al.*, is digital PCR, a method used to quantify genomic material in a sample [124]. In digital PCR, a sample is diluted and distributed into small chambers so that each vessel has either one or zero copies of DNA strands present. After distribution, PCR is performed, and dyes that bind to double-stranded DNA are added. A reader then determines whether each reaction chamber is positive or negative, so that the number of genomic templates from the original sample can be inferred. Sundberg *et al.* used a disc with 1,000 nano-liter-sized wells into which the sample was aliquoted by centrifugal force (shown in Figure 3.2). The small volumes allowed for 45 thermocycles to be performed in just 25 minutes.

PCR thermocycling times can be further optimized by using droplets on a CD, which significantly increases the surface area-to-volume ratio [162]. Wang *et al.* used density difference pumping to move a 3 μL droplet between two thermo-electric elements held at 95°C and 60°C for performing real-time PCR [195]. A single cycle time of 60 seconds was reported. However, despite the rapid thermocycling methods innovated by various research groups, it should be noted that there is a tradeoff between amplification efficacy, which is

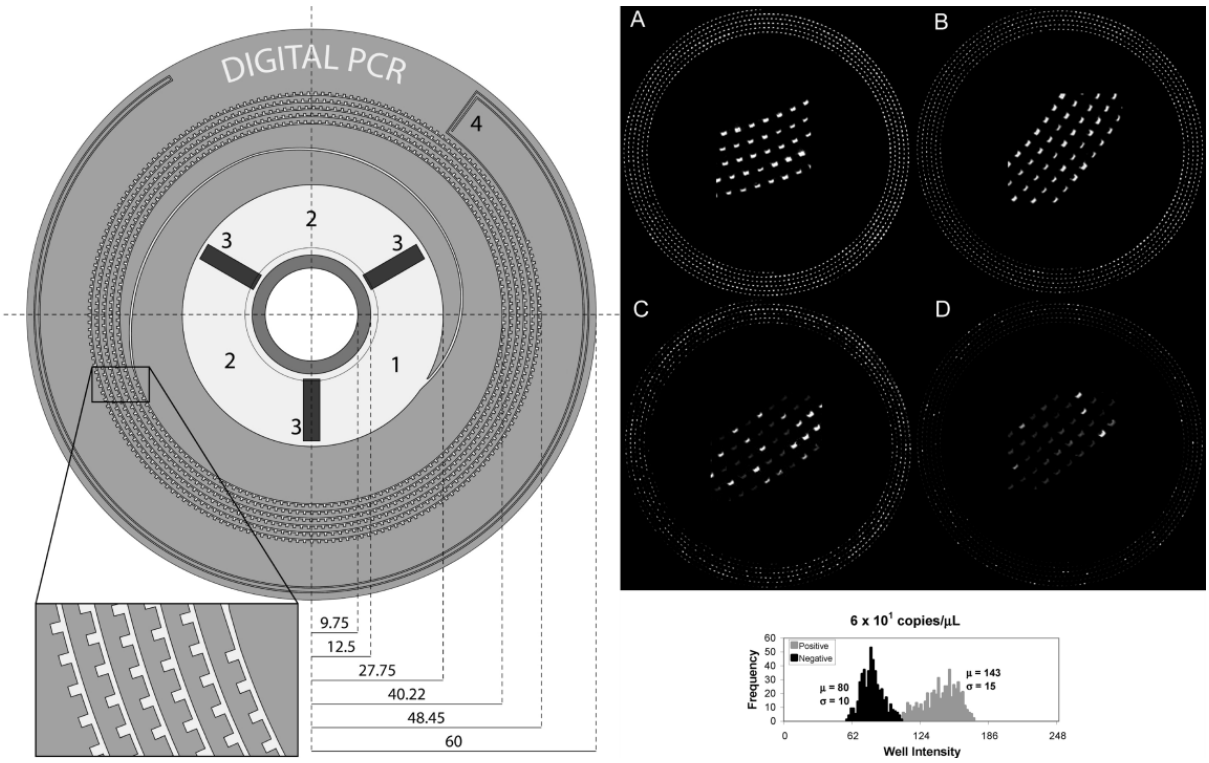

Figure 3.2: Sundberg *et al.* designed a microfluidic disc containing 1,000 nanoliter-sized wells to perform digital PCR (left). The DNA sample was diluted so that each well contained one or zero copies of DNA. The end results were imaged with a CCD camera, and ImageJ was used to analyze the wells (right). (Reprinted (adapted) with permission from Reference [124], ©2010, American Chemical Society.)

usually better with more accurate temperatures and therefore slower run times, and fast thermocycling due to the risk of temperature overshoot.

3.1.3 Microarrays used for Detection of Nucleic Acid Targets

DNA microarrays are used for high-throughput visualization of genetic markers, are quantitative, and can obtain hundreds to thousands of quantitative results in one test. While DNA microarrays are commonly known to be capable of evaluating gene expression, it can also be used for disease diagnosis. Microarray-based nucleic acid detection techniques allow the detection and quantification of a large array of biomarkers and do not require aliquoting or splitting of sample volumes in tests such as digital PCR, which could be problematic if

a minimum sample volume is required for analyte detection. While microarray technologies are advantageous, traditional laboratory bench methods incorporate long manual protocols that can be tedious and time-consuming. In addition, analysis of results requiring trained technicians is not cost-effective. The use a centrifugal microfluidic system can potentially alleviate this problem as these systems can be easily automated from beginning to end.

Some common applications of nucleic acid microarrays include gene expression analysis and the detection of pathogenic microorganisms. For these tests, genetic probes of known sequences are either adsorbed or covalently bonded to a non-porous material, such as glass, silicon, or nylon [149]. These probes are commonly double-stranded DNA sequences or single-stranded oligonucleotides. The probes are bound to target sequences by hybridization. In cases where the target concentration is very low, especially for disease detection, the hybridization step may be preceded by nucleic acid amplification.

With the potential for automation of the laboratory bench steps, multiplexing of target biomarker detection, and automated image analysis of the microarray spots, the microarray method has powerful relevance to the detection of multiple diseases. Diseases with NA sequences with shared primer regions are especially compatible with this method. For example, a test for fungal sequences took advantage of common regions of multiple fungal strains by designing primer sequences to be from these regions, making it possible to amplify an large array of disease biomarkers and providing many diagnoses for these diseases within the duration of a single test [196]. Another test also demonstrated partially multiplexed amplification of Influenza A and Influenza B strains by designing primers to correspond to conserved areas of the genetic sequences in several sample species [197]. The platform discussed in this chapter provides a basis for processing such sample types for high-throughput disease screening and can be customized for each specific assay. Automation of the once-completed platform means that no operator involvement is required besides sample input and pushing a "start" button.

3.2 Design of Diagnostic Device and Platform

This section describes original work consisting of the design of a sample-to-answer microfluidic disc in detail and corresponds each step to its biological function, if any. It also describes the actuation steps required external to the spinning of the disc itself. The hardware components will be described in detail in Section 3.2.2.

3.2.1 The Sample-to-Answer Disc Design

As described in Section 1.6, a number of steps are required to prepare a biological sample before the nucleic acid content can be effectively amplified (Figure 1.13). The assay steps designed to be executed using the microfluidic device are modified to achieve the required specificity and sensitivity while conserving adequate fluidic simplicity and on-disc real estate and maintaining a standard 120 mm disc diameter. The sample-to-answer fluidic disc design incorporates steps from sample lysis to analyte detection.

Fluidic Steps in the Assay

The steps for an example assay are shown in Table 3.1. The disc is designed to accept and process a raw sample. Such a sample can be sputum or mucus taken using a swab and suspended in Tris-EDTA (TE), a buffer that aids in NA extraction. While this platform has been not been tested with actual samples, reagents, such as TE buffer, have been used whenever possible. The cells in the raw sample first need to be lysed and the sample homogenized using the bead beating process [11] to extract the genomic material from the cells in the sample (Step 1). This step was not yet integrated, but another technique that performs the same function will be explained later in this section. Next, the sample is clarified by centrifugal force while the disc is spinning at 1,500 RPM in order to separate the nucleic acid

in the supernatant from unwanted components in the precipitate, such as cell membranes and connective tissue (Step 2).

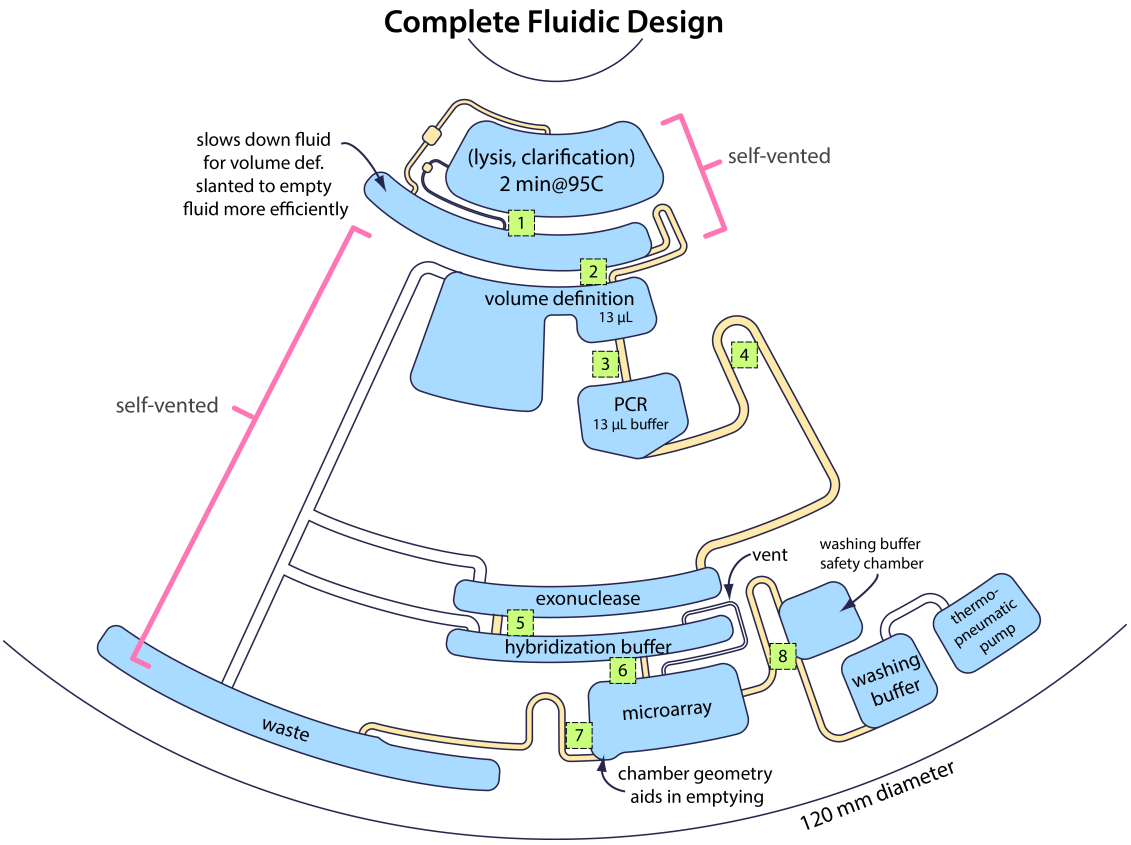

Figure 3.3: The complete design for the sample-to-answer microfluidic disc. Yellow channels are fluidic channels, while white channels are venting channels. Valves are labeled with numbered green boxes — 1) burst, 2) hydrophobic siphon actuated by TPP, 3) burst (multifunctional wax valves, upstream), 4) hydrophobic siphon (multifunctional wax valves, downstream), 5) burst, 6) burst, 7) hydrophobic siphon actuated by overflow, 8) TPP.

At this point, the lysed sample containing the nucleic acid cannot yet be effectively amplified. According to Aldous *et al.*, incubation of a lysed sample at 95°C composes an adequate measure to ensure effective nucleic acid amplification. Here, this step is termed inactivation of PCR inhibitors (Step 3) [100]. Heating a sample at 95°C for two or more minutes kills mycobacteria and inactivate proteins, and ensures that the polymerase will function properly later on. Elution or dilution, alternative methods of purifying DNA, is not necessary when this heating step is performed. When incorporated into the fluidic assay on a CD, these alternative methods may result in increased fluidic complexity and heavy use of

Step no.	Fluidic Step	Method/Description	Spin rate	Temp (°C)
1	Cell Lysis	Retrieve DNA from cells by physically crushing sample	650	N/A
2	Clarification	Spin down cells to isolate suspension of DNA solution	1,500	N/A
3	Inactivation of PCR Inhibitors	Heat at 95°C for 2 minutes	700	95
3a	Catchment	Extra chamber prevents fluid from leaking when killing PCR inhibitors	1,500	50
3b	Transfer to VD	Use TPP to transfer fluids to volume definition	700	80
4	Volume Definition	Fluidically determine volume of sample entering the PCR chamber	4,000	N/A
5	PCR Thermocycling	Cycling through specific temperatures for DNA amplification	2,000	various
5a	Prime PCR Siphon	Fluidically prepare the siphon for transfer of sample downstream	200	80
6	Exonuclease	Sending fluid to resuspend dry exonuclease	400, 800	N/A
7	Hybridization Buffer	Sending fluid to resuspend dry hybridization buffer	1,000	50
8	Sample to Microarray	Flow through sample through microarray for hybridization	1,500	N/A
9	Sample to Waste	Empty microarray to waste chamber; automatic after filling of microarray	1,500	N/A
10	Washing Buffer	Pump washing buffer to completely cover microarray using TPP	300	80
11	Empty Washing Buffer	(Optional) Send washing buffer to waste channel	1,500	N/A

Table 3.1: Fluidic steps for the sample-to-answer microfluidic disc. The working spin rates and temperatures have been obtained and displayed in the last two columns.

valuable on-disc real estate. Inactivation of PCR inhibitors can be executed at 700 RPM, which provides sufficient centrifugal force to keep the sample volume in place and maintain a uniform meniscus, yet is low enough to reduce convective cooling and promote rapid heating.

The lysis chamber has an outgoing burst channel located near the bottom, but not at the absolute bottom, of the chamber, which segregates the sedimented portion from the clarified portion. The chamber immediately downstream from the lysis chamber is an intermediate chamber designed to prevent small amounts of liquid from prematurely entering the volume definition (Step 3a) before PCR inhibitor inactivation at 700 RPM (Step 3) is completed. A vent channel connects the top of the lysis chamber to the top of this intermediate chamber to relieve the pneumatic pressure generated during the PCR inhibitor inactivation step. Both the vent channel and the intermediate chamber are necessary to ensure adequate heat treatment of the entire sample volume.

After heating, the disc is continually spun at 700 RPM to passively cool the heated part of the disc to roughly 50°C. This is because the step for transferring the sample to the volume definition uses the thermo-pneumatic pump, which requires a larger increase in temperature (ΔT) to effectively transfer a larger liquid volume (Section 2.1). The disc is then spun at 1,500 RPM to transfer the entire clarified portion of the liquid sample (supernatant) to the intermediate chamber. The lysis and catchment units are designed as a built-in thermo-pneumatic pump, as previously mentioned, which enables easy transfer of the supernatant to the volume definition unit by heating to 80°C, where a desired volume, designed to be 13 μL here, is aliquoted and the rest overflows into a waste chamber (Step 3b).

At 4,000 RPM, the aliquoted volume is forced to enter the PCR chamber by high centrifugal force (Step 4). The PCR chamber integrates multifunctional wax valves to perform midstream incubation and downstream transfer without any physically blocking valves. As an option, it can also store and release liquid reagents. The high disc angular frequency of 4,000 RPM is required to perform this step because the PCR chamber is not internally

vented to any fluidic features preceding it in the assay; once a small portion of liquid is transferred from the volume definition unit to the PCR chamber, or if there are pre-stored liquid reagents inside the PCR chamber (the liquid reagents can be stored between wax chambers; see Section 2.2), the outlet of the PCR chamber is blocked and the air pressure in the chamber counters the flow of the upstream liquid. High centrifugal force pushes the remaining liquid volume to overcome the air pressure and enter the PCR chamber.

The PCR chamber is pre-loaded with paraffin wax, which has not been shown prevent or reduce liquid evaporation during PCR (see Appendix A), but aids in downstream transfer of liquid after PCR. Paraffin wax had been previously shown to have no negative effects on PCR efficacy [186, 187]. The paraffin wax in the PCR chamber can be standalone (ball) or encapsulates liquid reagents (layers). Reagents required for PCR (primers, dNTPs, Taq polymerase, reverse transcriptase, and magnesium ions and components required to be in solution) can either be encapsulated in a wax ball or stored between wax layers in solution. One of the two primers to be used for this assay is attached to a fluorescent marker, which would provide the signal for the microarray later on.

To prepare for PCR, the angular frequency of the disc is set to 2,000 RPM to collect any condensate from sample evaporation, and the sample is heated for 95°C for 2 minutes, a processed called "hot start". This process separates oligonucleotides, such as primers, and proteins that are nonspecifically bound to the nucleic acids to be amplified and ensures that the amplification process is accurate and efficient. The thermocycling process begins immediately after hot start, and consists of the typical denaturation, annealing, and elongation steps (Step 5). For fluidic testing, 1-2 cycles is performed to simulate the thermal conditions, and actual PCR experiments are performed separately (see Section 3.2.2). After thermocycling, spinning of the disc at 2,000 RPM continues until the sample is cooled to 50°C to prepare for transfer to the exonuclease chamber.

Steps of operation for the multifunctional wax valves technique (Section 2.2) are used to transfer the sample volume into the exonuclease chamber. The angular frequency of the disc is set to 200 RPM, and heat is applied to the PCR chamber to melt the wax, which wicks into the channel upstream from the PCR chamber at low disc angular frequencies, forming a temporary ventless chamber inside the PCR chamber. As the temperature continues to increase, the air inside the PCR chamber expands, pushing the liquid sample into the outlet siphon (5a). Sufficient heating expands the air to push the liquid sample over the crest of the siphon and below the hydrostatic level of the liquid in the PCR chamber (Step 5a). While the disc is in this fluid state, spinning at 400 RPM empties the entire liquid sample into the exonuclease chamber, where an enzymatic solution was dried prior to disc assembly (Step 6). The function of exonuclease is to reduce competitive binding of the complementary strand to the target strand during sample hybridization with the microarray. Exonuclease digests nucleic acid from 5' to 3' and highly prefers phosphorylated 5' ends. The microarray requires the target strand to be separated from the complementary strand, so five minutes of incubation of the sample with exonuclease would ensure that the complementary strand is digested before the sample reaches the microarray. The target strands could then effectively hybridize with the oligonucleotides spotted or immobilized on a substrate. The target strands would not be digested, most likely due to the presence of the fluorescent marker attached to the 5' end [198].

Although paraffin wax is not experimentally observed to transfer downstream, the fluidic design must ensure that no paraffin wax reaches the DNA microarray, since this will damage the microarray. To prevent any paraffin wax from traveling further downstream, the sample in the exonuclease chamber is passively cooled to around 50°C. Spinning the disc at 800 RPM allows the liquid to spread out throughout the chamber and resuspend the exonuclease.

To transfer the liquid sample to the hybridization chamber, where another solution was dried prior to disc assembly, the disc is spun at 1,000 RPM (Step 7). Components of the hy-

bridization buffer include 6X saline-sodium phosphate-EDTA, 0.03% polyvinyl-pyrrolydone, and 30% formamide, which would enhance the signal of the microarray. Spinning at 1,500 RPM feeds the sample into the microarray chamber, where hybridization occurs (Step 8). When the microarray chamber is almost full, the meniscus's hydrostatic level overcomes the downstream siphon crest's hydrostatic position, priming the siphon and emptying the microarray chamber (Step 9). After the microarray chamber is completely empty of the sample liquid, a washing buffer is pumped into the microarray chamber by heating a TPP while spinning at 300 RPM (Step 10). Step 10 can be replaced by the breakage of a thin-walled glass capsule, which makes for a more vapor-tight liquid reagent storage solution (see Appendix B). The emptying of the washing buffer at 1,500 RPM is an optional step due to the ability of a CCD camera to image the microarray weather it is filled or empty (Step 11).

The system includes a total of seven valves, each experimentally characterized to operate at the burst frequencies shown in Table 3.1. A schematic of the design is shown in Figure 3.3. Chambers are labeled by basic function in the assay, and the valves are numbered in green boxes. Valves 1, 3, 5, and 6 are hydrophobic valves, valve 7 is a passive volume-defined valve, and valves 2, 4, and 8 required heat to be actuated. With 3 out 8 valves being active, the design significantly increases in reliability. For future work, in order to completely automate the process, the duration of heating and spinning processes must be also be experimentally determined.

Figure 3.4 shows photo sequences for a successful manually operated trial. A clear microfluidic disc was used and black polycarbonate material was placed underneath the disc to aid in the absorption of radiation energy.

Finally, the microfluidic disc assay requires a world-to-chip (WTC) interface in order to promote its ease of use. A world-to-chip interface is a built-in mechanism that aids in the sample introduction by the user so that complexity and the number of manual steps are minimized. In order to implement this system in the most user-friendly manner, Soroori

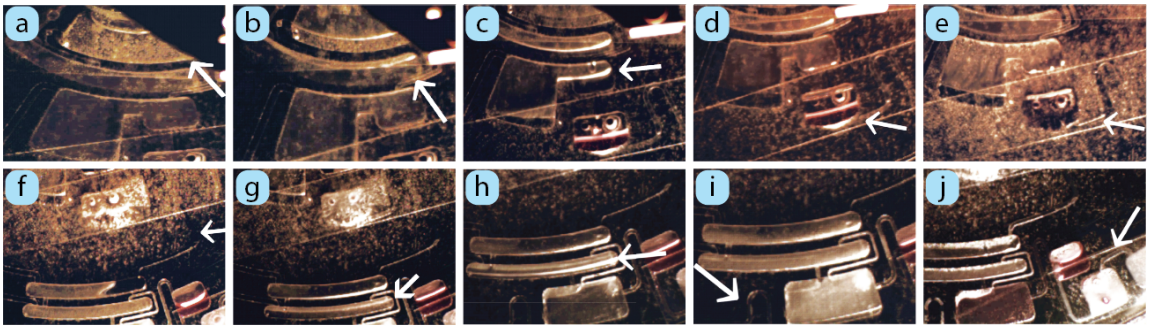

Figure 3.4: The image sequence for a fluidic trial. A clear disc was used with black material underneath. a) Inactivation of PCR inhibitors at 95°C. b) Clarification, then transfer into intermediate chamber. c) Volume definition. d) Transfer into PCR chamber. e) Simulated PCR. f) Transfer to exonuclease chamber. g) Transfer to hybridization buffer chamber. h) Flow through PCR microarray. i) Empty sample to waste. j) Send washing buffer into microarray chamber.

described the implementation a world-to-chip interface that involves obtaining patient sample using a cotton swab and accommodates the fluidic assay described in this chapter. The cotton swab is inserted into an apparatus mounted in the center hole of the microfluidic CD, and an impinging blade cuts the neck of the cotton swab when the handle of the swab is removed. Closing a plastic cap on the WTC interface pushes a pouch onto a blade, releasing a resuspension buffer which picks up the biological tissue from the cotton swab head. The bottom portion of the WTC interface consists of an upside-down conical shaped chamber, which holds ceramic beads. By oscillating the spin frequency of the disc, the ceramic beads move up and down the slant wall of the cone to perform lysis on the biological tissue sample. At a high, unidirectional spin frequency, the resuspended sample flows outwards, up the conical chamber wall, and into the on-disc lysis and clarification chambers, which, due to the lysis step in the WTF interface, can be redesigned for clarification only. As most of these steps are operated by either simple manual steps or automated spinning of the microfluidic disc, the WTC interface is suitable for an extremely user-friendly system. Due to the conical shape of the apparatus, the combination of the microfluidic disc and the WTC interface require a special mount to be attached to the spinning motor. Further details and illustrations can be found in the dissertation by Soroori [199].

Experimental Setup and Multiplexing

For fluidic testing, the test platform includes a halogen lamp as the heat source (12 V 75 W, International Technologies MA), an infrared surface temperature sensor (CSmicro, Optris, Berlin, Germany), and an imaging system around a motor (Pacific Scientific Servo Motor, model PMB21B-00114-00) with a custom-made and mounted spin chuck. The heating lamp is controlled by a programmable power supply, which together with the temperature sensor, are interfaced with a program written in LabVIEW software (National Instruments, TX, USA) that controls the power of the lamp to achieve a set sensor temperature value. For visualization, a stroboscopic setup enables the camera's capture frequency to be synced to the spin frequency, providing a live view of the on-disc events to the user in real time. The setup consists of a camera (Basler A311FC, 1/2in., C-Mount, 659 x 492, 73fps, color, CCD, 1394a, Germany), a strobe light (PerkinElmer MVS-4200, 6 μs duration), and a reflective trigger (D10DPFPQ, Banner D10 Expert Fiber-Optic Sensor, Minneapolis, MN, USA) that takes one image per revolution. The motor is controlled using the ToolPAC™ 4.1 software obtained from Pacific Scientific (Pacific Scientific, Rockfield, IL). This setup is summarized in Figure 2.2.

While multiplexing of fluidic operations is already intrinsic and convenient on a spinning microfluidic CD, the use of a heating lamp contributes even more to this ease of multiplexing. As the disc spins, heating any point on the disc means that a radial ring containing the heated position is also heated. It is important to note that heat is a modular component used in multiple valving and pumping operations, since the reduction of the number of external actuation methods in the system minimizes the hardware complexity, and therefore, cost and space requirement for the entire system. Spinning of the disc is required to keep the liquid volumes organized and maintain uniform menisci. Since heating by radiation can be very rapid, spinning the disc also ensures that overheating and melting of the disc does not

occur. During the thermocycling process, spinning collects any evaporated and condensed sample to reduce loss of liquid at high temperatures.

Multiplexing can also be integrated into the assay in a biological manner. As explained in Section 3.1.3, an appropriately chosen array markers can be detected in a high throughput manner using just one PCR reaction and one microarray. The designed microfluidic disc contains four identical quadrants and therefore can process four sets of such samples, for example, either four different sets of disease biomarkers for one patient or the same set of biomarkers for four different patients.

Fabrication

Due to extensive exposure of the microfluidic disc to heat and the complex structures on the disc, the common method used for CD fabrication (Section 1.3) was deemed inadequate. The pressure-sensitive, double-sided adhesive that is generally used in bonding discs (FLEXmount®DFM 200 CLEAR V-95 150 POLY H-9 V-95 400 POLY H-9, or FLEXmount®DFM 100 Clear V-326 150 Poly H-9, FLEXcon, USA) begin disintegrating above 60°C, hence providing inadequate structural integrity required with the applied heat and causing leakage of fluids through what should be barriers. Additionally, these adhesives inhibit PCR and cannot be designed to be in contact with the sample. A more inert material or surface must be used for the inner chamber walls.

Shown in Figure 3.5 is an improved method of CD fabrication. All the features, except for the loading holes, were milled into a clear polycarbonate sheet of 1/8 inch thickness (McMaster-Carr, USA) with 3-axes CNC machine (MDX-40a, Roland DGA Corporation, Irvine, CA). The machine is capable of a critical dimension down to roughly 110 μm and has a tolerance of about 10 μm. A single-sided PCR compatible adhesive (9793R, 3M, St. Paul, MN) was applied directly to the bottom layer, enclosing all fluidic features. In order to

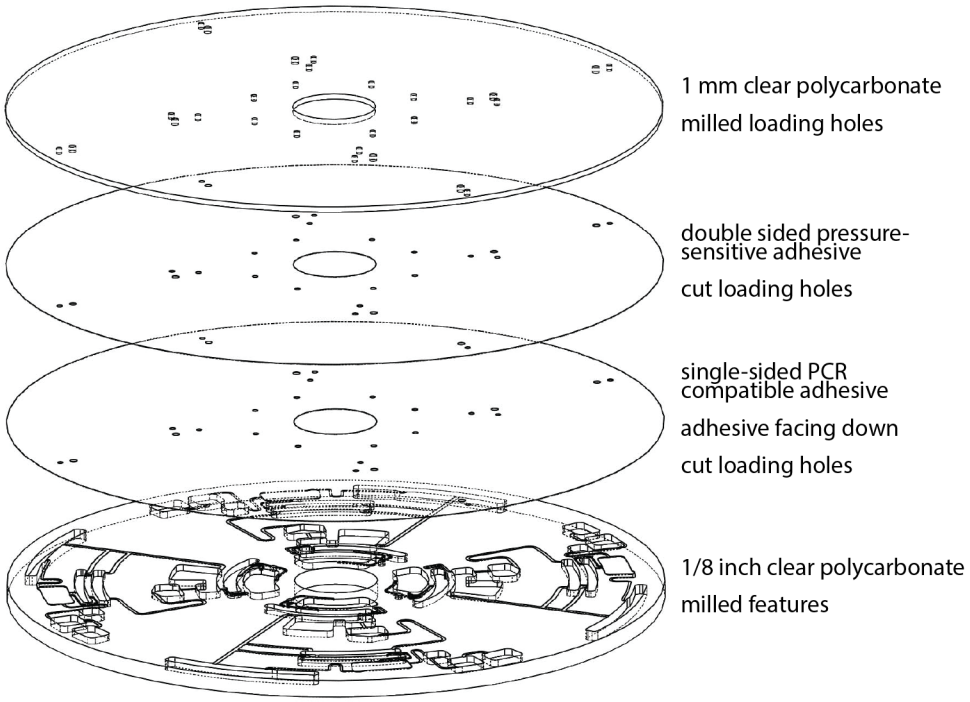

Figure 3.5: Features, including all channels and chambers, are milled into the bottom polycarbonate layer, while loading holes are cut into the three top layers. The top three layers include, from top to bottom: 1 mm thick polycarbonate, double-sided, pressure-sensitive adhesive, and 3M 9793R single sided adhesive.

generate pressure for the thermo-pneumatic pumping, a stiff top layer was needed. This was milled into a 1 mm clear polycarbonate layer (McMaster-Carr, USA), which was attached to the single-sided adhesive with a double-sided adhesive (Flexmount®DFM 100 Clear V-326 150 Poly H-9, FLEXcon, USA).

Furthermore, in order to optimize the disc, a few measures were taken to maximize heat absorption and reduce the overall heat capacity of the disc. The top layer of the disc was replaced with 0.020 inch thick clear polycarbonate sheet (McMaster-Carr, USA) and the bottom layer was replaced with 3 millimeter thick black polycarbonate sheet (Makrolon, Bayer, USA) which was further machined down to roughly 2 millimeters in thickness. To assemble the disc together, the layers were manually aligned and pressed together with a roller press.

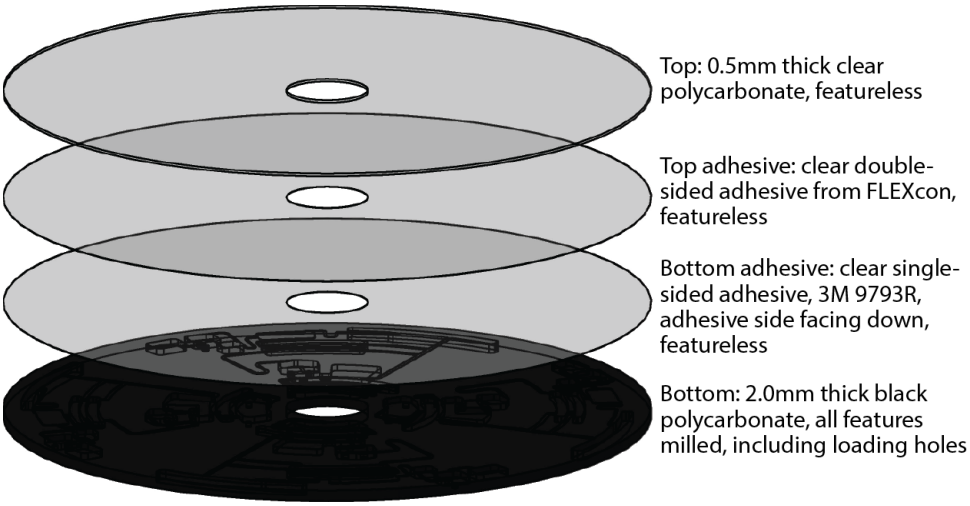

Figure 3.6: The improved fabrication technique uses black polycarbonate sheet, modified to have a thickness of 2 mm, for a bottom layer that includes all features and loading holes. The remaining layers are featureless and are in the original order.

The vent holes were originally cut into the top layers—single-sided adhesive, double sided adhesive, and 1 mm thick polycarbonate. In order to segregate the sample from the double-sided adhesive, which can inhibit PCR, the vent holes were removed from the top polycarbonate and adhesive layers and drilled into the bottom layer instead. Doing this eliminates complexity and imperfection from sealing of the chambers and reduces the possibility of leakage and contamination. The new configuration of the disc layers is shown in Figure 3.6.

The single-sided adhesive was found to delaminate after long period of exposure to high temperature ($> 80°C$) or rigorous temperature cycling. Later, another single-sided adhesive from 3M (9795R, 3M, St. Paul, MN) was tested instead of the 9793R adhesive and was found to remain intact at 95°C for longer periods of time with adequate bonding pressure.

However, the bonding is still not perfect and delamination can occur during 45 rigorous cycles of heating and cooling. The ideal solution is to fabricate parts in polycarbonate only and bond the parts to each other using either laser or ultrasonic bonding to obtain complete microfluidic discs. Laser bonding requires that one of the parts be black to absorb the laser

power, heating the plastic and melting the plastic part slightly for bonding. Fittingly, the black plastic would also contribute to faster heating rates during infrared heating, making laser bonding an appropriate solution. However, heating of the plastic parts can possibly damage heat-sensitive reagents, so the laser bonding solution must be carefully evaluated before it can be chosen as a mass manufacturing solution. Ultrasonic bonding may not be an appropriate solution for a similar reason; the transfer of energy into the plastic parts may cause extreme heating of plastic parts, which can damage any heat-sensitive reagents that need to be dried or stored on-disc before bonding. Solvent bonding is yet another option but was not considered due to the very small geometric features, the presence of reagents already on the disc, and the complications involved with the bonding process.

Laser bonding and ultrasonic bonding are proposed solutions for mass production only and cannot be implemented in-house. For an immediate solution, another method involving thermoplastic elastomer (TPE) was tried. This material, a clear, elastomeric polymer, easily bonds with cyclic olefin polymer (COP; or, commercially available as Zeonor®), a hard plastic, without requiring extreme temperatures or application of chemicals. These two materials bond permanently, and the bonding process is faster when incubated at a temperature higher than room temperature. Both materials are compatible with injection molding processes, and the assembly will not delaminate during PCR thermocycling. Bonding between TPE and polycarbonate is also a viable option, with the only requirement for good bonding being a higher incubation temperature. A potential problem with the use of TPE is due to its oleophobic behavior. Both polycarbonate and COP are oleophilic, which is essential in the operation of the multifunctional wax valves, so when the fluidic reservoirs and channels are fabricated into TPE instead, multifunctional wax valves do not behave consistently. If TPE were to be used in the disc construction, the fluidic features must be fabricated into an oleophilic material to provide more surface area to support the wicking of molten paraffin wax.

3.2.2 Hardware System and Performance

In order to perform a multi-step assay rapidly and accurately, the entire assay must be automated. This calls for the development of a custom hardware system to automate and perform the assays. This section first discusses the goal and current progress for the instrumentation development (Section 3.2.2). Some results on heating and cooling rates, presented in Section 3.2.2, can be used to infer the pros and cons of different heating and cooling elements, including halogen heating lamp, heating resistors, Peltier elements, and air blowers. Integrating the hardware with a thermistor and a feedback mechanism allows precise temperature cycling during PCR, for which data was obtained (Section 3.2.2).

Integration of Hardware

The control system is custom-built in the form of a spin stand box. A diagram of the hardware components in the spin stand is shown in Figure 3.7. Photos of the system are shown in Figure 3.8. The system has been designed to perform the following functions with the listed hardware components:

1. Full control of the CD's spin rate is required, including an angular velocity range that accommodates the disc operation. In this case, the range is 0 to 7,000 RPM.

    - A **servo motor** provides ample power for reliably spinning the disc at up to roughly 8,500 RPM. The CD is mounted onto the motor through either a custom-made chuck or a slip ring and the motor is controlled through user input in a computer user interface or by an automated spin protocol.

2. At least one heat source is required for the heating steps during PCR thermocycling and actuation of thermo-pneumatic pumps.

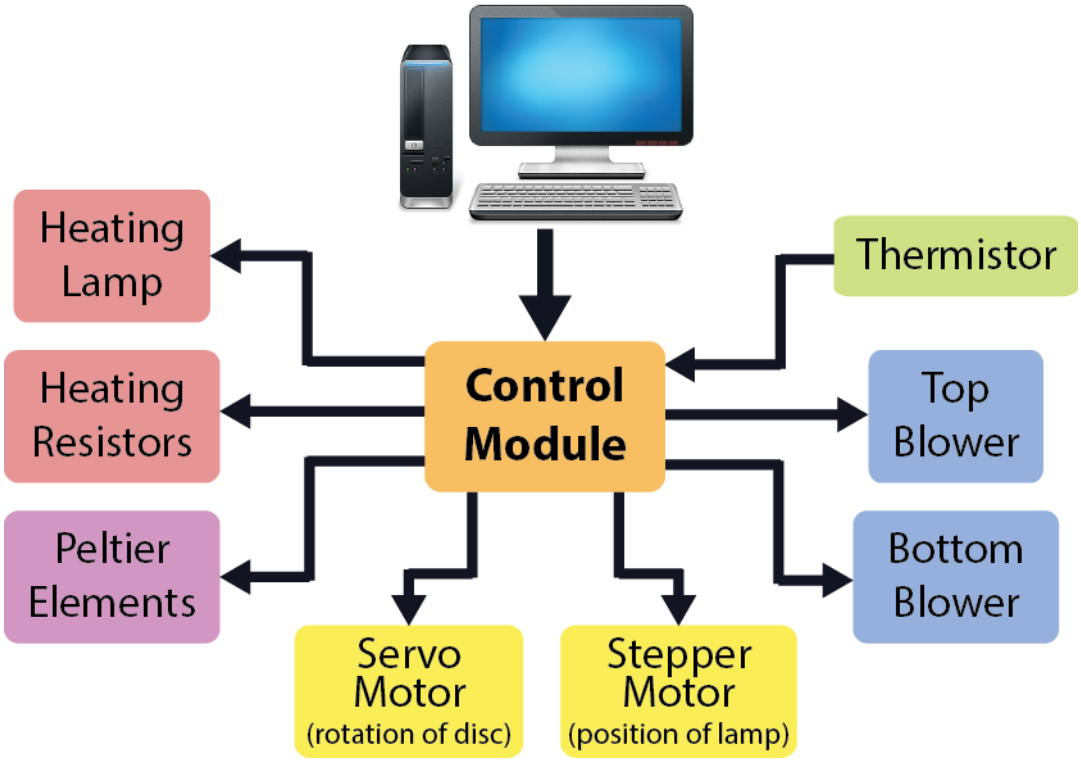

Figure 3.7: Schematic illustrating the control and communication of the components of the custom-built spin stand hardware system. This spin stand is mainly used to automate thermocycling but can be further developed to operate the entire assay in the future.

- A **heat lamp** can be positioned at an optimal distance to heat a specific radius on the disc. During spinning of the disc, the lamp heats one radius of the entire disc, making multiplexing of heating operations easy. This lamp is mounted on a **linear actuator** and **stepper motor** ensemble which can be programmed to position the lamp between the center and the perimeter of the disc, making it possible to automate heating at any desired radius on the disc. Two small blowers pointing to the lamp body prevents overheating of the lamp whenever it is on.
- **Heating resistors** can heat up rapidly and are chosen as a candidate for implementing rapid thermocycling. **Peltier elements** are capable of actively heating and cooling and can also potentially achieve fast ramping rates. These components must be in contact with the disc to be effective, so the heating method is

termed "contact heating". The two types of contact heating elements are not used with each other but each type can be combined with the heat lamp.

- In order to use contact heating elements, electricity must be provided to these elements which must spin with the disc. A **slip ring and brush setup** can be integrated with a **CD-shaped printed circuit board (PCB)** to deliver heat to the microfluidic disc via contact heating. A slip ring and brush setup can be seen in Figure 1.6d. If made into a commercial product, the PCB would be a part of the permanent hardware (as opposed to a disposable) and spins together with the disc. As such, the heating elements cannot be moved during the assay and must be placed strategically. For brief heating operations such as thermo-pneumatic pumping, the heating lamp can be used, saving the contact heating elements for the rigorous PCR thermocycling process.

3. Cooling is generally necessary after a heat-dependent operation, and rapid, efficient cooling is essential for PCR thermocycling.

    - Passive cooling by **spinning of the disc** is an option but not the most efficient method.
    - Two powerful **air blowers** are mounted above and below the disc at the radius where the PCR chamber is located to perform active cooling. These blowers are programmed to turn on during the appropriate steps in thermocycling to cool the disc and to precisely control temperature through a feedback mechanism.
    - If utilized, **Peltier elements** are capable of active cooling.

4. Precise temperature sensing is required for effective DNA amplification. The temperature reading of the liquid sample cannot be more than 0.5°C away from the actual temperature due to the sensitive nature of the PCR protocol.

- An electronic temperature sensing element—a **thermistor** in this case, is placed directly in one of the liquid samples. This is the most accurate way to measure the temperature and no calibration other than for the thermistor is required.
- The ideal system would consist of permanent hardware and plastic disposable discs as separate, modular elements. For this purpose, a thermistor may be avoided and the use of a non-contact **infrared temperature sensor** can be substituted. However, due to the different temperature ramping patterns of the internal and superficial parts of the microfluidic CD, extensive calibration must be performed and this task is set for future work.

5. In order to control as well as automate all the hardware components described, an electronic central control system must be designed to send commands to the different components and relay feedback between them.
   - A custom-made **control module** is an electronic hardware component that controls all the hardware components described. It consists of a microcontroller with embedded software and peripherals. The control module can be connected to PC via RS232 interface, with which requests can be obtained from the user and corresponding commands are relayed to operate the spin stand. The control module can also be preprogrammed from a PC to perform sequences of tasks autonomously, making manual user operation unnecessary.
6. An enclosure for the system would integrate and protect the hardware components.
   - An **aluminum frame** forms the frame for the overall system. Once completed, panels can be added to the side to for a complete box. This step ensures that the hardware components, as well as the users, are protected and makes it easy to transport the system.

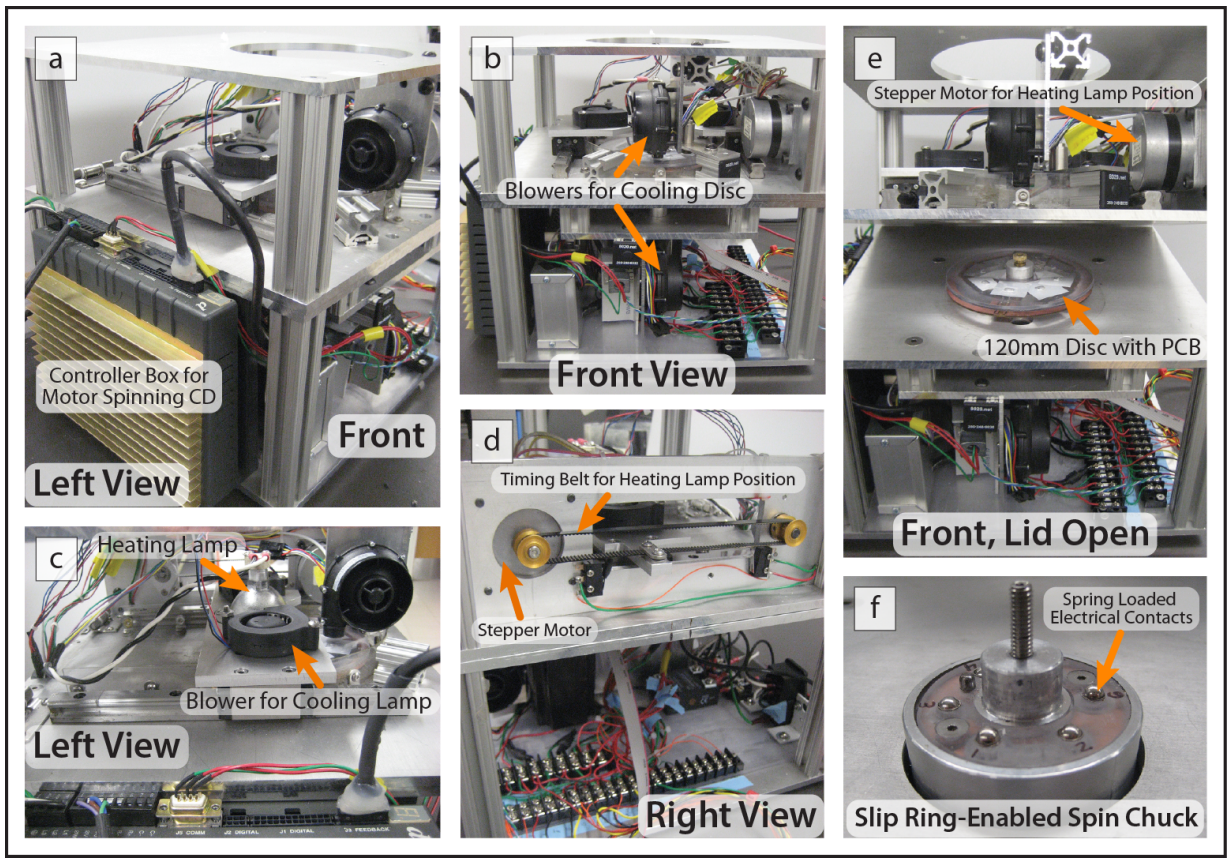

Figure 3.8: Photos and overview of the custom-built spin stand, including the front view (a,b,e), the left view (a, c), and the right view (d). Components shown include the controller box for the spinning motor responsible for the angular velocity of the microfluidic disc (a), heating lamp (c), small blowers for cooling the lamp (c), blowers for cooling the disc (b), stepper motor and timing belt for positioning the heating lamp (d, e), PCB and disc mounted on the spin stand (e), and spring loaded contacts on the slip ring-enabled spin chuck (f). The spin stand is about $0.35m \times 0.31m \times 0.30m$ in overall dimensions

Temperature Ramping Tests

In this section, methods of heating and cooling that aid in thermocycling for polymerase chain reaction (PCR) are compared and analyzed. These methods include heating by radiation from a halogen lamp, contact heating using special heating resistors, and active cooling using high-pressure blowers. In addition, components were operated in parallel for even higher ramping rates. Since short PCR assay durations require efficient heating and cooling, the methods to be described will contribute to minimal time in the transition temperature

ranges. The system achieved heating rates of up to 9.5 C°/s from contact heating, up to 7.5 C°/s for non-contact heating, and up to 11 C°/s for a combination of contact and non-contact heating.

With PCR applications in mind, various heating and cooling options were explored in-depth. Rapid heating was performed in a non-contact manner using radiation from a halogen lamp and in a contact manner using heating resistors. The latter method requires a slip ring-and-brush setup, as described by Noroozi *et al* [45]. Each method is uniquely advantageous in specific applications. Non-contact heating using the lamp is useful in situations where heat may be used to open valves at different locations on the microfluidic disc. The lamp can be positioned using a linear actuator and software control. Once the lamp is positioned at where the heating needs of take place, the lamp will heat all microfluidic features in that radius while the disc is spinning, making any required multiplexing easy. Moreover, turning off the lamp will instantly cut off the heat source while passive cooling takes place. Radiative heating is the most effective when the disc is fabricated from a black bottom layer and a clear top layer, as this configuration facilitates the absorption of light.

On the other hand, the resistive heating method requires the use of a custom printed circuit board (PCB) to create an electrical connection to a power source for heating during spinning (Figure 3.9a,c). These PCBs were fabricated using IsoPro Software and a QuickCircuit 5000 CNC machine (T-Tech, Inc., Norcross, Georgia, USA). All heating elements must be designed into the PCB according to the positions of the fluidic features to be heated, meaning that there is no flexibility for heating various radial positions of the disc and the PCB must be redesigned with every fluidic disc design change affecting the heated regions. Alignment of resistive heating elements can be minimized by designing shallow recesses into the bottom side of the disc where the heating elements can sit and make contact with a foil seal (Figure 3.9b). The foil seal is immediately adjacent to the sample volume, facilitating heat conduction during thermocycling. This design prevents potential sliding of components

during spinning. Since the resistors are always in contact with the features to be heated, heat transfer is a lot more efficient in this case compared to radiative heating, whereas each fluidic feature is exposed to the lamp emission for a brief moment per revolution. Because of the direct contact in resistive heating, it may seem that spinning is not required. However, spinning is advantageous in that if the fluidic reservoir being heated is connected to other fluidic structures on the disc, the centrifugal force will keep the liquids organized within the reservoir and prevent any unwanted transfer of liquid to other chambers.

Meanwhile, cooling is an equally important contributor to efficient thermocycling. While spinning of the disc results in passive cooling, two blowers dominate the task of cooling the disc. To measure temperature of the liquid in the disc, a small thermistor is inserted into the liquid-holding chamber. Monitoring liquid temperature in real time or implementing automated feedback requires that the thermistor be connected to a PCB and that the spin stand incorporates the slip ring and brush components. These heating and cooling methods were used to achieve competitive ramping rates. Later, PCR tests were conducted using biological samples on discs with chambers that each hold 30 μL of liquid sample.

Microfluidic discs of different configurations were fabricated to be compatible with each heating method for ramping rate experiments. For microfluidic discs containing the full design, features were milled into a 3 mm thick piece of polycarbonate (McMaster-Carr, USA) using a 3D milling machine (Roland DGA Co, Irvine, CA). This plastic layer was sealed with a PCR-compatible adhesive (9793R, 3M, St. Paul, MN). A layer made of a stiff material is needed to perform any variation of thermo-pneumatic pumping, so a 0.5 mm thick piece of polycarbonate sheet (McMaster-Carr, USA) was held onto the 9793R layer using a double-sided adhesive (Flexmount DFM 100 Clear V-326 150 Poly H-9, FLEXcon, USA). This configuration is shown in Figure 3.9d and modified for each heating setup. A clear polycarbonate disc with several PCR chambers milled into the same radius was used for heating using IR lamp. The 3 mm thick clear stock polycarbonate sheets were milled to

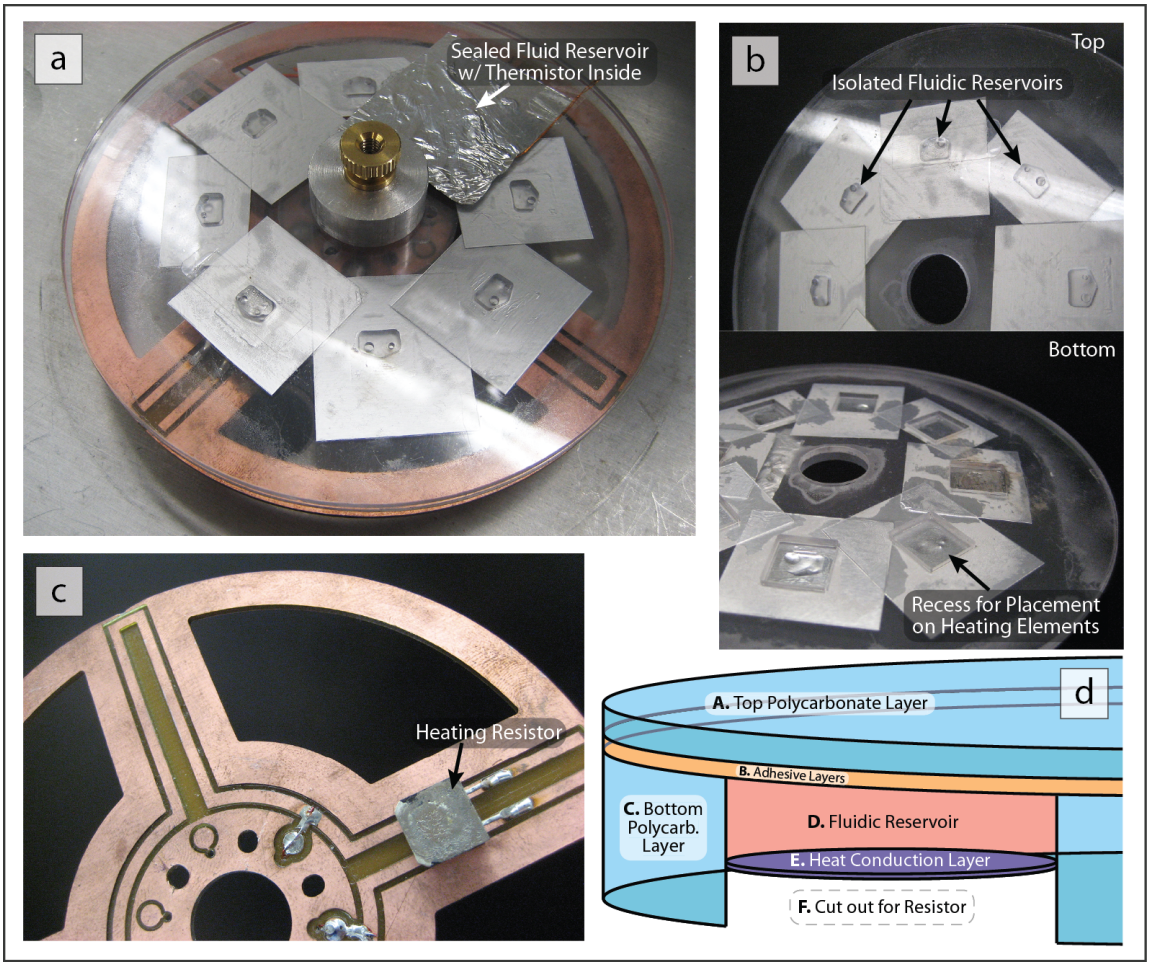

Figure 3.9: Setup for contact heating on-disc using a custom-made printed circuit board (PCB). A PCB, a plastic spacer (not visible), and a CD with fluidic reservoirs are set up on the custom-built spin stand; Reservoirs are sealed with PCR-compatible foil prior to thermocycling (a). A disc with isolated fluidic reservoirs has loading holes on top and cut-out recesses on the bottom for alignment with heating resistors (b). A copper PCB with a soldered heating resistor; the bottom side of the PCB (not shown) has electrical contacts for the slip ring and correspond to the contacts on the top side of the PCB (c). Schematic of the fluidic disc configuration (d). The heat conduction layer (E) is usually a PCR-compatible foil. The cut out (F) is not necessary if only heating lamp is used for heating.

a thickness of 2 mm in order to reduce the overall mass, and therefore, heat capacity, of disc materials surrounding the PCR chamber. Black polycarbonate was also used to increase absorption of lamp emission, and hence, heating rate. Stock sheets of 3 mm thick black polycarbonate (McMaster-Carr, USA) were machined down to 2 mm in thickness, and the

fluidic features were enclosed with adhesive and clear polycarbonate similar to the clear polycarbonate disc.

For discs to be used for contact heating, an area of polycarbonate material that forms the bottom wall of the PCR chamber was cut out and replaced with a piece of 60 μm thick PCR foil in order to increase efficiency of heat conduction. This configuration also prevents misalignment of heating elements, which could be caused by the heating resistors sliding across the plastic disc during spinning. The PCR chambers for all devices were 1.2 mm deep, and each chamber has a 40 μL capacity, while only 30 μL of sample was used. The center of each PCR chamber was located roughly 30 mm from the center of the disc.

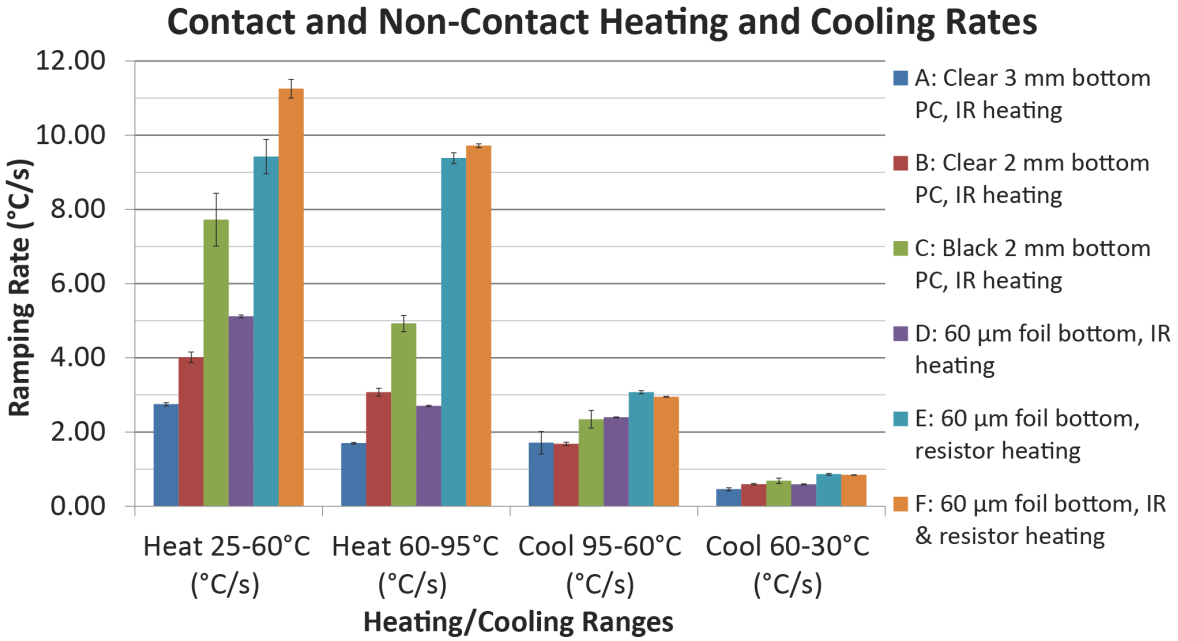

Figure 3.10: Bar graph indicates average heating and cooling rates for different heating modes and disc configurations. Active cooling was performed using blowers above and below the disc. Two temperature ranges are explored to reduce the spread of the approximation. Configurations are described in the legend. Error bars show standard deviation. The number of trials is 3 for A, 10 for B, 8 for C, 3 for D, 3 for E, and 2 for F. (Adapted from [179] ©2013 The Royal Society of Chemistry.)

Results of the ramping tests are shown in Figure 3.10. Tests were performed with six different configuration and setup combinations in order to explore the most feasible methods for use with DNA samples. From the results, it was observed that contact heating was the

fastest, with a heating rate of up to 9.4 C/s; contact heating also had the fastest cooling rates. Of the different thicknesses of discs tested with IR heating, discs with less material surrounding the chamber being heated generally had higher heating rates as well as cooling rates. Discs with a cutout and foil region (optimized for contact heating) were also heated using the heating lamp, and this setup was discovered to have only a slight increase in heating rates and as slight decrease in cooling rates from discs made using 2 mm thick polycarbonate sheets. Additionally, a combination of contact and radiative heating were used on the discs configured for contact heating, which proved to be even faster than contact heating alone. However, the amount of power supplied to the hardware should be taken into account for later versions of the testing platform design. The black polycarbonate discs experienced much higher heating rates by radiation than clear discs; however, they were later discovered to be incompatible with PCR samples due to observed PCR inhibition, possibly due to the pigment in the plastic. Feasible commercial solutions can be found if black plastics are to be used. An alternative solution is to adhere a black film to the outer side of a clear polycarbonate disc to increase lamp emission absorption.

Optimized Thermocycling Tests

Due to the complexity of the fluidic network on the complete microfluidic disc, the PCR chamber is isolated from the rest of the fluidic features; a disc containing only multiplexed PCR chambers is fabricated for these experiments. This will allow testing of only the PCR reaction in the microfluidic device, making it easier to analyze the efficacy of the hardware setup or material choice. PCR thermocycling was conducted using gDNA from *B. subtilis* CCRI-20762 at 1 x 10^4 copies/μL. A 157 μL tube of master mix was combined with 1.3 μL of Taq promega and 17.6 μL gDNA of *B. subtilis* CCRI-20762. Due to the high surface to volume ratio of the microfluidic PCR chamber, surface treatment of the PCR chamber is necessary to prevent interaction between the reservoir surface and PCR biomolecules. This

was achieved via dynamic passivation of the PCR sample with various concentrations of Bovine Serum Albumin (BSA) [185, 200]. 30 μL of the combined solution was loaded into the PCR chamber, the disc was spun at 2,000 rpm, and the following PCR parameters were followed:

1. Heat to 95°C for 180 seconds (hot start)
2. Heat to 95°C for 1 second
3. Cool to 59°C for 20 seconds
4. Heat to 72°C for 20 seconds
5. Repeat 2 through 4 for 45 cycles

The temperature of the liquid was monitored via a thermistor placed directly inside one of the PCR chambers. Thermocycling using the heating lamp was conducted with the biological sample and reagents described above and for several disc configurations: 3 mm clear bottom disc with 0.5 mm clear top, 3 mm black bottom disc with 0.5 mm clear top, 2.3 mm clear bottom disc with 0.5 mm clear top. Thermocycling with sample and reagents was also conducted using resistive contact heating for the following disc configurations: 2.3 mm clear bottom disc with cut out and foil bottom for PCR chamber, 3 mm clear bottom disc with foil bottom for PCR chamber. The thermocycling was automated and operated by a custom-made LabVIEW (National Instruments Co, Austin, TX) program which uses an electronic proportional-integral-derivative (PID) controller to reach temperature setpoints and reduce heating and cooling overshoots.

To test for the effectiveness of on-disc amplification, the PCR products were processed in an Agilent Bioanalyzer (Agilent 2100 Bioanalyzer, Santa Clara, CA, United States) which provides results upon a gel electrophoresis assay. The gel electrophoresis assay separates strands of DNA by size, so that sequences of same lengths travel through the gel to the same

Table 3.2: Table of PCR amplification results from isolated chambers in clear discs.

Trial No.	**No. of Samples**	**% BSA**	**Actual Annealing Temp. (°C)**	**Cycle Time (m:ss)**	**Total Time (min)**	**Results**
1	4	1.33	59	1:52	88	3 amplifications; thermistor marker smeared
2	4	1.33	59	1:52	82	1 amplification; thermistor and other markers smeared
3	2	0.166	59	1:44	81	1 amplification
4	2	0.166	59	1:44	81	1 amplification
5	2	0.101	58.5	1:45	82	no amplification

position, while sequences of shorter lengths travel farther. Each assay performed using the Agilent Bioanalyzer includes a positive control, which consists of the same sample amplified in a commercial amplifier (MJ Research PTC-225, Waltham, MA, United States; now a part of Bio-Rad Laboratories, Inc.). When gel electrophoresis is performed on the positive control and sample, the positive control generally reliably indicates the position that the sample should that reflects the position that the amplified sample should should. The sample target is a 348-base pairs(bp)-sequence, so the thermocycling parameters, particularly the annealing temperature, were adjusted to obtain a bar at the 348-bp ladder position. Temperature sensing was implemented inside one fluid sample in each experiment by placing a thermistor inside a PCR chamber in a multiplexed PCR experiment, which was adequate for precise temperature control in all chambers due to the multiplexing.

As shown in Table 3.2, results were obtained from PCR runs with several samples in a clear disc. These PCR amplification trials performed on-disc using the heating lamp and blowers for cooling. All discs are clear in color. Due to PCR-inhibiting dyes in the black polycarbonate used, positive results were not obtained with black polycarbonate discs. Due to the use of a thermal paste to ensure that thermistor chambers are sealed properly, PCR is usually inhibited in the samples with thermistor inside. A number of successful trials with a marker showing at 348 bp have been obtained and several markers, which line up with the positive control marker indicated, are shown in Figure 3.11. From the

table, it is concluded that 59°C is the ideal target annealing temperature for use with the current hardware and program setup. The entire protocol was also consistently performed under 90 minutes when heated using the heating lamp and cooled using the blowers. The protocol can be performed in under 70 minutes, or about 1 minute and 30 seconds per cycle, when black polycarbonate is used to fabricate the microfluidic disc. While a darker colored material increases absorption of emission by the heat lamp, the black polycarbonate material used for current experiments inhibits PCR, so materials with PCR-compatible pigments must be researched for this purpose. Heating using heating resistors was incorporated into PCR experiments so far. However, programming and electronic errors may have caused uncontrolled current flow of heating resistors, evaporating samples completely even while the chambers are sealed with strong PCR foil.

Analysis and Further Work

Due to the unreliable nature of programs created with the LabVIEW software, crashes sometimes occur during thermocycling when the program handles too much information. This can be fixed by an improved version of the software which has been coded in the C# programming language. The new program is capable of streamlining the code for thermocycling, reducing hangs and crashes. Additional fine tuning of the PID can result in overall decrease in thermocyling time. The most recent work on the platform includes a microcontroller that customizes the operation of the different heating and cooling components. This implementation, with a dedicated controller for the temperature control elements, can fix the overheating problem with the heating resistor

Future work will involve incorporation of thermoelectric heating and cooling using Peltier elements. Peltier elements are solid state devices that employ the Peltier effect, converting a potential difference across thermocouples into a temperature difference. While one side acts as a heat sink, the other cools down to well below ambient temperature within seconds, and

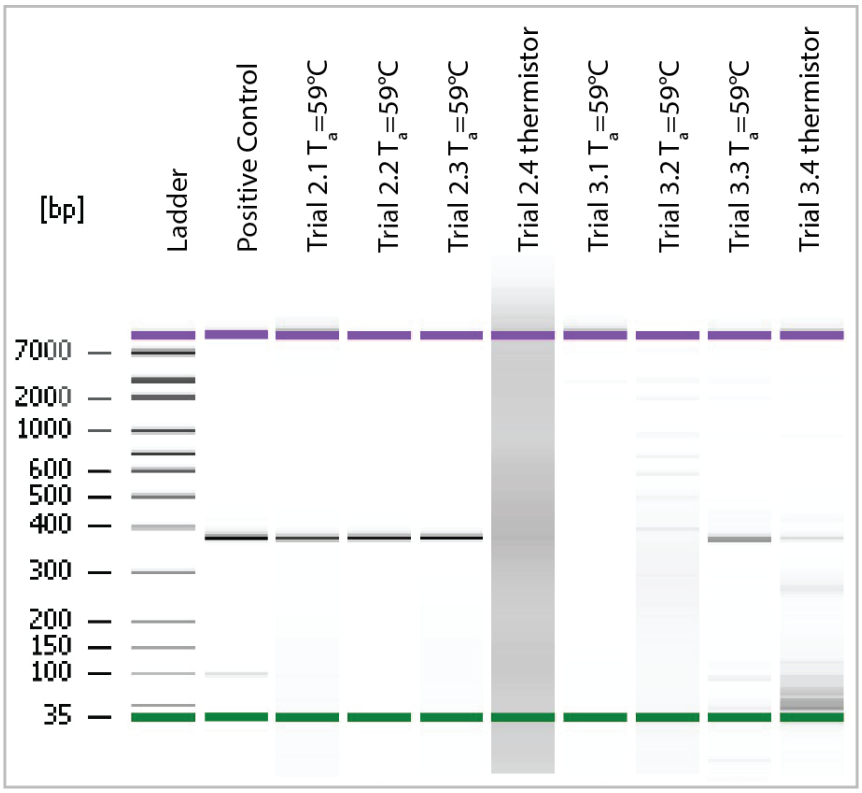

Figure 3.11: Results from two on-disc trials (trials 2 and 3 in Table 3.2) of PCR are shown here. The target marker should appear around 349 bp, which can be seen in several lanes. Thermal conductive paste has been applied to the thermistor chambers, so contamination may have caused smearing in the corresponding lanes. Due to multiplexing of several samples in each trial, errors in implementing the tests in parallel may have cause improper amplification in Trials 3.1 and 3.2.

this could switched by reversing the polarity of the voltage source. Above all, the advantage of utilizing a Peltier element on a spinning device is that a heat sink may not be necessary due to the removal of the excess thermal energy by convective heat transfer. This concept simplifies the setup by eliminating one bulky component. This idea would not only allow localized contact heating, similar to the resistive heating explored in the current work, but also contact cooling in the same manner.

Lastly, the black polycarbonate material currently used inhibits PCR. A commercial, chemically inert, injection molding-compatible black material will required for faster operation of heating lamp-enabled thermocycling and fluidic operations. Alternatively, a layer

of black material can be placed or bonded beneath a clear polycarbonate layer containing fluidic features to increase heating rates with the heating lamp while maintaining PCR compatibility. Prospectively, the black color will not interfere with optical detection due to its low autofluorescence and ability to absorb unwanted wavelengths.

3.3 Conclusion and Future Outlook

The original sample-to-answer microfluidic disc design was proven to be feasible for sample processing after incorporating heat- and wax-based microfluidic technologies such as the thermo-pneumatic pump and the multifunctional wax valves. A platform capable of molecular diagnostic tests or other heat-based tests has been developed and can accommodate various specialized assays in the future. While enormous progress has been made on the microfluidic device and the surrounding system, the current platform still requires further improvement before becoming a candidate for a clinical point-of-care diagnostic system. Future work will include the following tasks:

1. Streamlining the hardware and software to promote consistency from trial to trial and reduce technical errors.
2. Fine tuning the feedback mechanism to reduce runtime.
3. Running the entire assay with biological reagents to finalize assay protocol and scaling down the limit of detection.
4. Evaluating final material and bonding optionals for mass manufacturing of device.

At the moment, nucleic acid amplification is the rate-limiting step in biomarker detection assays on centrifugal platforms, requiring complex thermocycling hardware, specialized

sample preparation steps, and solutions to reduce sample evaporation and CD delamination. There are two main future directions for NA amplification on a CD:

1. Hardware optimization: Although both contact and non-contact heating methods (summarized in Section 3.1.2) have been demonstrated for PCR thermocycling, further improvements in heating and cooling ramping rates still need to be made. Techniques implemented while the platform is spinning are preferred, because sample evaporation is reduced as condensate is collected back into the reservoir [92]. More concentrated efforts to improve temperature control and to decrease the complexity and power requirements of hardware used in contact and non-contact heating methods on CDs must be made.

   A good example along these lines, although not specifically used for NA amplification, is by Chen *et al.* who wirelessly heated localized areas on a spinning disc using micropatterned resonant heaters by controlling the frequency of the external radiofrequency (RF) field [201]. This team used inductive heating to achieve temperatures up to 93°C. These heaters are low-cost, can be selectively activated, and the target heater temperature can be easily adjusted by varying the RF power output, making it an ideal technology for PCR applications.

2. Advanced isothermal amplification techniques: Although PCR has been historically favored for nucleic acid amplification due to its potency for achieving the highest sensitivity and accuracy, isothermal amplification methods, which eliminate the need for temperature cycling, have been developed since year 2000 and have improved over time [202]. The sensitivity levels of isothermal amplification methods have been refined to come close to those of PCR [203–205].

   Examples of isothermal DNA amplification methods include Recombinase Polymerase Amplification (RPA) [13, 206, 207], Loop Mediated Isothermal Amplification (LAMP), and Nucleic Acid Sequence Based Amplification (NASBA). These techniques utilize

simpler and less expensive hardware, making them ideal for use on LoD platforms. An example of isothermal PCR on a CD is the recent use of RPA in a lab-on-a-foil disc system by Lutz *et al.*, who achieved amplification at room temperature in less than 20 minutes with a 10 μL sample volume [13]. This is a good starting point for future NA amplification assays that are both fast and effective.

The current work serves as a platform where future developments in fluidics, hardware, and biology can contribute to even more revolutionary systems. With the unique advantages of centrifugal microfluidic platforms such as high multiplexing power and isolated fluidic systems, the development of novel and competitive point-of-care diagnostic systems will be highly anticipated.

References

[1] G. Jia, *Fast and Automated DNA Assays on a Compact Disc (CD)-Based Microfluidic Platform.* doctorate, University of California, Irvine, 2006.

[2] R. Gorkin, J. Park, J. Siegrist, M. Amasia, B. S. Lee, J.-M. Park, J. Kim, H. Kim, M. Madou, and Y.-K. Cho, "Centrifugal microfluidics for biomedical applications.," *Lab on a chip*, vol. 10, pp. 1758–73, July 2010.

[3] M. Madou, J. Zoval, G. Jia, H. Kido, J. Kim, and N. Kim, "Lab on a CD.," *Annual review of biomedical engineering*, vol. 8, pp. 601–28, Jan. 2006.

[4] R. Burger and J. Ducrée, "Handling and analysis of cells and bioparticles on centrifugal microfluidic platforms.," *Expert review of molecular diagnostics*, vol. 12, pp. 407–21, May 2012.

[5] R. Burger, D. Kirby, M. Glynn, C. Nwankire, M. O'Sullivan, J. Siegrist, D. Kinahan, G. Aguirre, G. Kijanka, R. a. Gorkin, and J. Ducrée, "Centrifugal microfluidics for cell analysis.," *Current opinion in chemical biology*, vol. 16, pp. 409–14, Aug. 2012.

[6] J. Ducrée, S. Haeberle, S. Lutz, S. Pausch, F. V. Stetten, and R. Zengerle, "The centrifugal microfluidic Bio-Disk platform," *Journal of Micromechanics and Microengineering*, vol. 17, pp. S103–S115, July 2007.

[7] J. Kim, H. Kido, R. H. Rangel, and M. J. Madou, "Passive flow switching valves on a centrifugal microfluidic platform," *Sensors and Actuators B: Chemical*, vol. 128, pp. 613–621, Jan. 2008.

[8] M. J. Madou and G. J. Kellogg, "The LabCD: a centrifuge-based microfluidic platform for diagnostics," vol. V, pp. 80–93, Feb. 1998.

[9] D. C. Duffy, H. L. Gillis, J. Lin, N. F. Sheppard, and G. J. Kellogg, "Microfabricated Centrifugal Microfluidic Systems: Characterization and Multiple Enzymatic Assays," *Analytical Chemistry*, vol. 71, pp. 4669–4678, Oct. 1999.

[10] J. Siegrist, R. Gorkin, L. Clime, E. Roy, R. Peytavi, H. Kido, M. Bergeron, T. Veres, and M. Madou, "Serial siphon valving for centrifugal microfluidic platforms," *Microfluidics and Nanofluidics*, vol. 9, pp. 55–63, Nov. 2010.

[11] H. Kido, M. Micic, D. Smith, J. Zoval, J. Norton, and M. Madou, "A novel, compact disk-like centrifugal microfluidics system for cell lysis and sample homogenization.," *Colloids and surfaces. B, Biointerfaces*, vol. 58, pp. 44–51, July 2007.

[12] M. J. Madou, L. J. Lee, K. W. Koelling, S. Daunert, S. Lai, C. G. Koh, Y.-j. Juang, L. Yu, and Y. Lu, "Design and fabrication of polymer microfluidic platforms for biomedical applications," in *ANTEC-SPE 59th*, vol. 71, pp. 2534–2538, 2001.

[13] S. Lutz, P. Weber, M. Focke, B. Faltin, J. Hoffmann, C. Müller, D. Mark, G. Roth, P. Munday, N. Armes, O. Piepenburg, R. Zengerle, and F. von Stetten, "Microfluidic lab-on-a-foil for nucleic acid analysis based on isothermal recombinase polymerase amplification (RPA).," *Lab on a chip*, vol. 10, pp. 887–93, Apr. 2010.

[14] J. Kim and X. Xu, "Excimer laser fabrication of polymer microfluidic devices," *Journal of Laser Applications*, vol. 15, no. 4, p. 255, 2003.

[15] D. Chen, M. Mauk, X. Qiu, C. Liu, J. Kim, S. Ramprasad, S. Ongagna, W. R. Abrams, D. Malamud, P. L. a. M. Corstjens, and H. H. Bau, "An integrated, self-contained microfluidic cassette for isolation, amplification, and detection of nucleic acids.," *Biomedical microdevices*, vol. 12, pp. 705–19, Aug. 2010.

[16] M. Amasia, M. Cozzens, and M. J. Madou, "Centrifugal microfluidic platform for rapid PCR amplification using integrated thermoelectric heating and ice-valving," *Sensors and Actuators B: Chemical*, vol. 161, pp. 1191–1197, Jan. 2012.

[17] R. Truckenmüller, Y. Cheng, R. Ahrens, H. Bahrs, G. Fischer, and J. Lehmann, "Micro ultrasonic welding: joining of chemically inert polymer microparts for single material fluidic components and systems," *Microsystem Technologies*, vol. 12, pp. 1027–1029, Apr. 2006.

[18] Y. I. Yun, K. S. Kim, S.-J. Uhm, B. B. Khatua, K. Cho, J. K. Kim, and C. E. Park, "Aging behavior of oxygen plasma-treated polypropylene with different crystallinities," *Journal of Adhesion Science and Technology*, vol. 18, pp. 1279–1291, Jan. 2004.

[19] R. Chen, Y. Bayon, and J. a. Hunt, "Preliminary study on the effects of ageing cold oxygen plasma treated PET/PP with respect to protein adsorption.," *Colloids and surfaces. B, Biointerfaces*, vol. 96, pp. 62–8, Aug. 2012.

[20] A. Vesel and M. Mozetic, "Surface modification and ageing of PMMA polymer by oxygen plasma treatment," *Vacuum*, vol. 86, pp. 634–637, Jan. 2012.

[21] C. Canal, R. Molina, E. Bertran, and P. Erra, "Wettability, ageing and recovery process of plasma-treated polyamide 6," *Journal of Adhesion Science and Technology*, vol. 18, pp. 1077–1089, Jan. 2004.

[22] M. Kitsara, C. E. Nwankire, L. Walsh, G. Hughes, M. Somers, D. Kurzbuch, X. Zhang, G. G. Donohoe, R. OKennedy, and J. Ducrée, "Spin coating of hydrophilic polymeric films for enhanced centrifugal flow control by serial siphoning," *Microfluidics and Nanofluidics*, vol. 16, pp. 691–699, Sept. 2013.

[23] J. L. Moore, A. McCuiston, I. Mittendorf, R. Ottway, and R. D. Johnson, "Behavior of capillary valves in centrifugal microfluidic devices prepared by three-dimensional printing," *Microfluidics and Nanofluidics*, vol. 10, pp. 877–888, Nov. 2010.

[24] "Desktop Integrated Manufacturing Platforms (DIMPs).," 2014.

[25] S. Lai, S. Wang, J. Luo, L. J. Lee, S.-T. Yang, and M. J. Madou, "Design of a compact disk-like microfluidic platform for enzyme-linked immunosorbent assay," *Analytical chemistry*, vol. 76, pp. 1832–1837, Apr. 2004.

[26] T. H. G. Thio, S. Soroori, F. Ibrahim, W. Al-Faqheri, N. Soin, L. Kulinsky, and M. Madou, "Theoretical development and critical analysis of burst frequency equations for passive valves on centrifugal microfluidic platforms.," *Medical & biological engineering & computing*, vol. 51, pp. 525–35, May 2013.

[27] D. Chakraborty, R. Gorkin, M. Madou, L. Kulinsky, and S. Chakraborty, "Capillary filling in centrifugally actuated microfluidic devices with dynamically evolving contact line motion," *Journal of Applied Physics*, vol. 105, no. 8, p. 084904, 2009.

[28] J. M. Chen, P.-C. Huang, and M.-G. Lin, "Analysis and experiment of capillary valves for microfluidics on a rotating disk," *Microfluidics and Nanofluidics*, vol. 4, pp. 427–437, July 2007.

[29] F. Ibrahim and A. Nozari, "Analysis and experiment of centrifugal force for microfluidic ELISA CD platform," *... IECBES), 2010 IEEE ...*, no. December, pp. 466–470, 2010.

[30] A. Kazemzadeh, P. Ganesan, F. Ibrahim, S. He, and M. J. Madou, "The effect of contact angles and capillary dimensions on the burst frequency of super hydrophilic and hydrophilic centrifugal microfluidic platforms, a CFD study.," *PloS one*, vol. 8, p. e73002, Jan. 2013.

[31] R. Gorkin, S. Soroori, W. Southard, L. Clime, T. Veres, H. Kido, L. Kulinsky, and M. Madou, "Suction-enhanced siphon valves for centrifugal microfluidic platforms," *Microfluidics and Nanofluidics*, vol. 12, pp. 345–354, Sept. 2011.

[32] S. Soroori, L. Kulinsky, H. Kido, and M. Madou, "Design and implementation of fluidic micro-pulleys for flow control on centrifugal microfluidic platforms," *Microfluidics and Nanofluidics*, Oct. 2013.

[33] R. Gorkin, L. Clime, M. Madou, and H. Kido, "Pneumatic pumping in centrifugal microfluidic platforms," *Microfluidics and Nanofluidics*, vol. 9, pp. 541–549, Feb. 2010.

[34] Z. Noroozi, H. Kido, R. Peytavi, R. Nakajima-Sasaki, A. Jasinskas, M. Micic, P. L. Felgner, and M. J. Madou, "A multiplexed immunoassay system based upon reciprocating centrifugal microfluidics.," *The Review of scientific instruments*, vol. 82, p. 064303, June 2011.

[35] M. M. Aeinehvand, F. Ibrahim, S. W. Harun, W. Al-Faqheri, T. H. G. Thio, A. Kazemzadeh, and M. Madou, "Latex micro-balloon pumping in centrifugal microfluidic platforms.," *Lab on a chip*, vol. 14, pp. 988–97, Mar. 2014.

[36] S. Zehnle, F. Schwemmer, G. Roth, F. von Stetten, R. Zengerle, and N. Paust, "Centrifugo-dynamic inward pumping of liquids on a centrifugal microfluidic platform.," *Lab on a chip*, vol. 12, pp. 5142–5, Dec. 2012.

[37] F. Schwemmer, S. Zehnle, D. Mark, F. von Stetten, R. Zengerle, and N. Paust, "A microfluidic timer for timed valving and pumping in centrifugal microfluidics," *Lab Chip*, vol. 15, pp. 1545–1553, 2015.

[38] G. Czilwik, I. Schwarz, M. Keller, S. Wadle, S. Zehnle, F. von Stetten, D. Mark, R. Zengerle, and N. Paust, "Microfluidic vapor-diffusion barrier for pressure reduction in fully closed PCR modules," *Lab Chip*, vol. 15, pp. 1084–1091, 2015.

[39] K. W. Oh and C. H. Ahn, "A review of microvalves," *Journal of Micromechanics and Microengineering*, vol. 16, pp. R13–R39, May 2006.

[40] C. Zhang, D. Xing, and Y. Li, "Micropumps, microvalves, and micromixers within PCR microfluidic chips: Advances and trends.," *Biotechnology advances*, vol. 25, no. 5, pp. 483–514, 2007.

[41] K. Abi-Samra, R. Hanson, M. Madou, and R. A. Gorkin, "Infrared controlled waxes for liquid handling and storage on a CD-microfluidic platform.," *Lab on a chip*, vol. 11, pp. 723–6, Feb. 2011.

[42] W. Al-Faqheri, F. Ibrahim, T. H. G. Thio, J. Moebius, K. Joseph, H. Arof, and M. Madou, "Vacuum/compression valving (VCV) using parrafin-wax on a centrifugal microfluidic CD platform.," *PloS one*, vol. 8, p. e58523, Jan. 2013.

[43] J.-M. Park, Y.-K. Cho, B.-S. Lee, J.-G. Lee, and C. Ko, "Multifunctional microvalves control by optical illumination on nanoheaters and its application in centrifugal microfluidic devices.," *Lab on a chip*, vol. 7, pp. 557–64, May 2007.

[44] K. Abi-Samra, L. Clime, L. Kong, R. Gorkin, T.-H. Kim, Y.-K. Cho, and M. Madou, "Thermo-pneumatic pumping in centrifugal microfluidic platforms," *Microfluidics and Nanofluidics*, vol. 11, pp. 643–652, June 2011.

[45] Z. Noroozi, H. Kido, and M. J. Madou, "Electrolysis-Induced Pneumatic Pressure for Control of Liquids in a Centrifugal System," *Journal of The Electrochemical Society*, vol. 158, no. 11, p. P130, 2011.

[46] J. L. Garcia-Cordero, D. Kurzbuch, F. Benito-Lopez, D. Diamond, L. P. Lee, and A. J. Ricco, "Optically addressable single-use microfluidic valves by laser printer lithography.," *Lab on a chip*, vol. 10, pp. 2680–7, Oct. 2010.

[47] R. Burger, P. Reith, V. Akujobi, and J. Ducrée, "Rotationally controlled magneto-hydrodynamic particle handling for bead-based microfluidic assays," *Microfluidics and Nanofluidics*, vol. 13, pp. 675–681, May 2012.

[48] R. Burger, P. Reith, G. Kijanka, V. Akujobi, P. Abgrall, and J. Ducrée, "Array-based capture, distribution, counting and multiplexed assaying of beads on a centrifugal microfluidic platform.," *Lab on a chip*, vol. 12, pp. 1289–95, Apr. 2012.

[49] R. Burger, D. Kurzbuch, R. Gorkin, G. Kijanka, M. Glynn, C. McDonagh, and J. Ducrée, "An integrated centrifugo-opto-microfluidic platform for arraying, analysis, identification and manipulation of individual cells," *Lab Chip*, vol. 15, pp. 378–381, 2015.

[50] S. Haeberle, N. Schmitt, R. Zengerle, and J. Ducrée, "Centrifugo-magnetic pump for gas-to-liquid sampling," *Sensors and Actuators A: Physical*, vol. 135, pp. 28–33, Mar. 2007.

[51] R. Gorkin, C. E. Nwankire, J. Gaughran, X. Zhang, G. G. Donohoe, M. Rook, R. O'Kennedy, and J. Ducrée, "Centrifugo-pneumatic valving utilizing dissolvable films.," *Lab on a chip*, vol. 12, pp. 2894–902, Aug. 2012.

[52] N. Dimov, E. Clancy, J. Gaughran, D. Boyle, D. Mc Auley, M. T. Glynn, R. M. Dwyer, H. Coughlan, T. Barry, L. M. Barrett, T. J. Smith, and J. Ducrée, "Solvent-selective routing for centrifugally automated solid-phase purification of RNA," *Microfluidics and Nanofluidics*, Sept. 2014.

[53] R. Mishra, R. Alam, D. J. Kinahan, K. Anderson, and J. Ducrée, "Lipophilic-membrane based routing for centrifugal automation of heterogeneous immunoassays," *Proceedings of the 28th International Conference on Micro Electro Mechanical Systems*, pp. 3–6, 2015.

[54] D. J. Kinahan, M. T. Glynn, N. A. Kilcawley, S. M. Kearney, and J. Ducrée, "Laboratory unit operations on centrifugal lab-on-a-disc cartridges using dissolvable-film enabled flow control," *Proceedings of the 4th European Conference on Microfluidics*, pp. 1–12, 2014.

[55] N. A. Kilcawley, D. J. Kinahan, D. P. Kernan, and J. Ducrée, "Reciprocating, buoyancy-driven radial pumping on centrifugal microfluidic platforms," *Proceedings of the 4th European Conference on Microfluidics*, 2014.

[56] D. J. Kinahan, R. Burger, A. Vembadi, N. A. Kilcawley, D. Lawlor, M. T. Glynn, and J. Ducrée, "Baking-powder driven centripetal pumping controlled by event-triggering of functional liquids," *Proceedings of the 28th International Conference on Micro Electro Mechanical Systems*, pp. 504–507, 2015.

[57] D. Kinahan, S. Kearney, M. Glynn, and J. Ducrée, "Imbibition-modulated event-triggering of centrifugo-pneumatic cascading for multi-stage dilution series," *17th International Conference on Miniaturized Systems for Chemistry and Life Sciences*, no. October, pp. 317–319, 2013.

[58] C. E. Nwankire, M. Czugala, R. Burger, K. J. Fraser, T. M. O'Connell, T. Glennon, B. E. Onwuliri, I. E. Nduaguibe, D. Diamond, and J. Ducrée, "A portable centrifugal analyser for liver function screening.," *Biosensors & bioelectronics*, vol. 56, pp. 352–8, June 2014.

[59] C. E. Nwankire, D.-S. S. Chan, J. Gaughran, R. Burger, R. Gorkin, and J. Ducrée, "Fluidic automation of nitrate and nitrite bioassays in whole blood by dissolvable-film based centrifugo-pneumatic actuation.," *Sensors (Basel, Switzerland)*, vol. 13, pp. 11336–49, Jan. 2013.

[60] N. Godino, E. Vereshchagina, R. Gorkin, and J. Ducrée, "Centrifugal automation of a triglyceride bioassay on a low-cost hybrid paper-polymer device," *Microfluidics and Nanofluidics*, Nov. 2013.

[61] J. Gaughran, D. Boyle, J. Murphy, and J. Ducrée, "Graphene Oxide membranes for phase-selective microfluidic flow control," *2015 28th IEEE International Conference on Micro Electro Mechanical Systems (MEMS)*, pp. 2–5, 2015.

[62] W. Al-Faqheri, F. Ibrahim, T. H. G. Thio, M. M. Aeinehvand, H. Arof, and M. Madou, "Development of novel passive check valves for the microfluidic CD platform," *Sensors and Actuators A: Physical*, vol. 222, pp. 245–254, Feb. 2015.

[63] D. Carpentras, L. Kulinsky, and M. Madou, "A Novel Magnetic Active Valve for Lab-on-CD Technology," *Journal of Microelectromechanical Systems*, vol. PP, no. 99, pp. 1–1, 2015.

[64] J. Steigert, T. Brenner, M. Grumann, L. Riegger, S. Lutz, R. Zengerle, and J. Ducrée, "Integrated siphon-based metering and sedimentation of whole blood on a hydrophilic lab-on-a-disk.," *Biomedical microdevices*, vol. 9, pp. 675–9, Oct. 2007.

[65] P. Andersson and G. Ekstrand, "Retaining microfluidic microcavity and other microfluidic structures," 2005.

[66] B. H. Park, D. Kim, J. H. Jung, S. J. Oh, G. Choi, D. C. Lee, and T. S. Seo, "An advanced centrifugal microsystem toward high-throughput multiplex colloidal nanocrystal synthesis," *Sensors and Actuators B: Chemical*, vol. 209, pp. 927–933, 2015.

[67] B. H. Park, J. H. Lee, J. H. Jung, S. J. Oh, D. C. Lee, and T. S. Seo, "A centrifuge-based stepwise chemical loading disc for the production of multiplex anisotropic metallic nanoparticles," *RSC Adv.*, vol. 5, pp. 1846–1851, 2015.

[68] C.-H. Shih, C.-H. Lu, W.-L. Yuan, W.-L. Chiang, and C.-H. Lin, "Supernatant decanting on a centrifugal platform.," *Biomicrofluidics*, vol. 5, p. 13414, Jan. 2011.

[69] M. Amasia and M. Madou, "Large-volume centrifugal microfluidic device for blood plasma separation.," *Bioanalysis*, vol. 2, pp. 1701–10, Oct. 2010.

[70] S. Haeberle, T. Brenner, R. Zengerle, and J. Ducrée, "Centrifugal extraction of plasma from whole blood on a rotating disk.," *Lab on a chip*, vol. 6, pp. 776–81, June 2006.

[71] Y.-K. Cho, J.-G. Lee, J.-M. Park, B.-S. Lee, Y. Lee, and C. Ko, "One-step pathogen specific DNA extraction from whole blood on a centrifugal microfluidic device.," *Lab on a chip*, vol. 7, pp. 565–73, May 2007.

[72] C. Nwankire, M. Czugala, and R. Burger, "Single-step, multi-parameter monitoring of liver function on a portable centrifugal analyzer," *17th International Conference on Miniaturized Systems for Chemistry and Life Sciences*, no. October, pp. 1147–1149, 2013.

[73] D. Mark, T. Metz, S. Haeberle, S. Lutz, J. Ducrée, R. Zengerle, and F. von Stetten, "Centrifugo-pneumatic valve for metering of highly wetting liquids on centrifugal microfluidic platforms.," *Lab on a chip*, vol. 9, pp. 3599–603, Dec. 2009.

[74] D. Mark, P. Weber, S. Lutz, M. Focke, R. Zengerle, and F. Stetten, "Aliquoting on the centrifugal microfluidic platform based on centrifugo-pneumatic valves," *Microfluidics and Nanofluidics*, vol. 10, pp. 1279–1288, Jan. 2011.

[75] M. Focke, F. Stumpf, G. Roth, R. Zengerle, and F. von Stetten, "Centrifugal microfluidic system for primary amplification and secondary real-time PCR.," *Lab on a chip*, vol. 10, pp. 3210–2, Dec. 2010.

[76] O. Strohmeier, S. Laßmann, B. Riedel, D. Mark, G. Roth, M. Werner, R. Zengerle, and F. Stetten, "Multiplex genotyping of KRAS point mutations in tumor cell DNA by allele-specific real-time PCR on a centrifugal microfluidic disk segment," *Microchimica Acta*, pp. 3–5, Oct. 2013.

[77] M. Keller, J. Naue, P. P. Vinayaka, O. Strohmeier, D. Mark, U. Schmidt, R. Zengerle, and F. V. Stetten, "Microfluidic App Featuring Nested PCR for Forensic Screening Assay on Off-the-Shelf Thermocycler," *17th International Conference on Miniaturized Systems for Chemistry and Life Sciences*, no. October, pp. 320–322, 2013.

[78] V. Hessel, H. Löwe, and F. Schönfeld, "Micromixersa review on passive and active mixing principles," *Chemical Engineering Science*, vol. 60, pp. 2479–2501, Apr. 2005.

[79] H. Chou, M. Unger, and S. Quake, "A microfabricated rotary pump," *Biomedical Microdevices*, vol. 3, no. 4, pp. 323–330, 2001.

[80] M. La, S. J. Park, H. W. Kim, J. J. Park, K. T. Ahn, S. M. Ryew, and D. S. Kim, "A centrifugal force-based serpentine micromixer (CSM) on a plastic lab-on-a-disk for biochemical assays," *Microfluidics and Nanofluidics*, vol. 15, pp. 87–98, Dec. 2012.

[81] J. Kuo and B. Li, "Lab-on-CD microfluidic platform for rapid separation and mixing of plasma from whole blood," *Biomedical microdevices*, Mar. 2014.

[82] G. R. Aguirre, V. Efremov, M. Kitsara, and J. Ducrée, "Integrated micromixer for incubation and separation of cancer cells on a centrifugal platform using inertial and dean forces," *Microfluidics and Nanofluidics*, July 2014.

[83] P. Garstecki, M. J Fuerstman, M. a. Fischbach, S. K. Sia, and G. M. Whitesides, "Mixing with bubbles: a practical technology for use with portable microfluidic devices.," *Lab on a chip*, vol. 6, pp. 207–12, Feb. 2006.

[84] Z. Noroozi, H. Kido, M. Micic, H. Pan, C. Bartolome, M. Princevac, J. Zoval, and M. Madou, "Reciprocating flow-based centrifugal microfluidics mixer.," *The Review of scientific instruments*, vol. 80, p. 075102, July 2009.

[85] M. M. Aeinehvand, F. Ibrahim, S. W. Harun, I. Djordjevic, S. Hosseini, H. A. Rothan, R. Yusof, and M. J. Madou, "Biosensing enhancement of dengue virus using microballoon mixers on centrifugal microfluidic platforms.," *Biosensors & bioelectronics*, Sept. 2014.

[86] I. Glasgow, J. Batton, and N. Aubry, "Electroosmotic mixing in microchannels.," *Lab on a chip*, vol. 4, pp. 558–62, Dec. 2004.

[87] Z. Yang, H. Goto, M. Matsumoto, and R. Maeda, "Active micromixer for microfluidic systems using lead-zirconate-titanate (PZT)-generated ultrasonic vibration," *Electrophoresis*, pp. 116–119, 2000.

[88] M. Grumann, A. Geipel, L. Riegger, R. Zengerle, and J. Ducrée, "Magneto-hydrodynamic Micromixing for Centrifugal Lab-on-a-Disk Platforms," in *Proceedings of the 8th international conference on micro total analysis systems*, pp. 593– 595, 2004.

[89] A. A. S. Watts, A. a. Urbas, E. Moschou, V. G. Gavalas, J. V. Zoval, M. Madou, and L. G. Bachas, "Centrifugal microfluidics with integrated sensing microdome optodes for multiion detection," *Analytical chemistry*, vol. 79, pp. 8046–54, Nov. 2007.

[90] M. Grumann, A. Geipel, L. Riegger, R. Zengerle, and J. Ducrée, "Batch-mode mixing on centrifugal microfluidic platforms.," *Lab on a chip*, vol. 5, pp. 560–5, May 2005.

[91] J. Siegrist, R. Gorkin, M. Bastien, G. Stewart, R. Peytavi, H. Kido, M. Bergeron, and M. Madou, "Validation of a centrifugal microfluidic sample lysis and homogenization platform for nucleic acid extraction with clinical samples.," *Lab on a chip*, vol. 10, pp. 363–71, Feb. 2010.

[92] L. X. Kong, K. Parate, K. Abi-Samra, and M. Madou, "Multifunctional wax valves for liquid handling and incubation on a microfluidic CD," *Microfluidics and Nanofluidics*, Oct. 2014.

[93] R. Seetharam, Y. Wada, S. Ramachandran, H. Hess, and P. Satir, "Long-term storage of bionanodevices by freezing and lyophilization.," *Lab on a chip*, vol. 6, pp. 1239–42, Sept. 2006.

[94] J. Kim, D. Byun, M. G. Mauk, and H. H. Bau, "A disposable, self-contained PCR chip.," *Lab on a chip*, vol. 9, pp. 606–12, Feb. 2009.

[95] T. van Oordt, Y. Barb, J. Smetana, R. Zengerle, and F. von Stetten, "Miniature stick-packaging–an industrial technology for pre-storage and release of reagents in lab-on-a-chip systems.," *Lab on a chip*, vol. 13, pp. 2888–92, Aug. 2013.

[96] J. Hoffmann, D. Mark, S. Lutz, R. Zengerle, and F. von Stetten, "Pre-storage of liquid reagents in glass ampoules for DNA extraction on a fully integrated lab-on-a-chip cartridge.," *Lab on a chip*, vol. 10, pp. 1480–4, June 2010.

[97] R. Peytavi and S. Chapdelaine, "Fluidic centripetal device," 2013.

[98] J. Garcia-Cordero, F. Benito-Lopez, D. Diamond, J. Ducrée, and A. Ricco, "Low-Cost Microfluidic Single-Use Valves and On-Board Reagent Storage using Laser-Printer Technology," in *2009 IEEE 22nd International Conference on Micro Electro Mechanical Systems*, pp. 439–442, IEEE, Jan. 2009.

[99] Y. Huang, E. L. Mather, J. L. Bell, and M. Madou, "MEMS-based sample preparation for molecular diagnostics.," *Analytical and bioanalytical chemistry*, vol. 372, pp. 49–65, Jan. 2002.

[100] W. K. Aldous, J. I. Pounder, J. L. Cloud, and G. L. Woods, "Comparison of six methods of extracting Mycobacterium tuberculosis DNA from processed sputum for testing by quantitative real-time PCR.," *Journal of clinical microbiology*, vol. 43, pp. 2471–3, May 2005.

[101] A. Lee, J. Park, M. Lim, V. Sunkara, S. Young, G. H. Kim, M.-h. Kim, and Y.-k. Cho, "All-in-One Centrifugal Microfluidic Device for Size- selective Circulating Tumor Cell Isolation with High Purity All-in-One Centrifugal Microfluidic Device for Size-selective Circulating Tumor Cell Isolation with High Purity," *Analytical chemistry*, vol. 86, no. 22, pp. 11349–56, 2014.

[102] T. Morijiri, S. Sunahiro, M. Senaha, M. Yamada, and M. Seki, "Sedimentation pinched-flow fractionation for size- and density-based particle sorting in microchannels," *Microfluidics and Nanofluidics*, vol. 11, pp. 105–110, Mar. 2011.

[103] D. Kirby, J. Siegrist, G. Kijanka, L. Zavattoni, O. Sheils, J. OLeary, R. Burger, and J. Ducrée, "Centrifugo-magnetophoretic particle separation," *Microfluidics and Nanofluidics*, vol. 13, pp. 899–908, July 2012.

[104] D. Kirby, M. Glynn, G. Kijanka, and J. Ducrée, "Rapid and cost-efficient enumeration of rare cancer cells from whole blood by low-loss centrifugo-magnetophoretic purification under stopped-flow conditions," *Cytometry Part A*, vol. 87, no. 6, pp. 74–80, 2015.

[105] M. Glynn, C. Nwankire, D. Kinahan, and J. Ducrée, "Cluster sizing of cancer cells by rail-based serial gap filtration in stopped-flow, continuous sedimentation mode," *2015 28th IEEE International Conference on Micro Electro Mechanical Systems (MEMS)*, pp. 192–195, 2015.

[106] U. Y. Schaff and G. J. Sommer, "Whole blood immunoassay based on centrifugal bead sedimentation.," *Clinical chemistry*, vol. 57, pp. 753–61, May 2011.

[107] C.-Y. Koh, U. Y. Schaff, M. E. Piccini, L. H. Stanker, L. W. Cheng, E. Ravichandran, B.-R. Singh, G. J. Sommer, and A. K. Singh, "Centrifugal Microfluidic Platform for Ultrasensitive Detection of Botulinum Toxin," *Analytical Chemistry*, vol. 87, pp. 922–928, 2015.

[108] E. A. Moschou, A. D. Nicholson, G. Jia, J. V. Zoval, M. J. Madou, L. G. Bachas, and S. Daunert, "Integration of microcolumns and microfluidic fractionators on multitasking centrifugal microfluidic platforms for the analysis of biomolecules.," *Analytical and bioanalytical chemistry*, vol. 385, pp. 596–605, June 2006.

[109] J. P. Lafleur and E. D. Salin, "Pre-concentration of trace metals on centrifugal microfluidic discs with direct determination by laser ablation inductively coupled plasma mass spectrometry," *Journal of Analytical Atomic Spectrometry*, vol. 24, no. 11, p. 1511, 2009.

[110] J. P. Lafleur, A. A. Rackov, S. McAuley, and E. D. Salin, "Miniaturised centrifugal solid phase extraction platforms for in-field sampling, pre-concentration and spectrometric detection of organic pollutants in aqueous samples.," *Talanta*, vol. 81, pp. 722–6, Apr. 2010.

[111] D. Mamaev, B. Shaskolskiy, E. Dementieva, D. Khodakov, D. Yurasov, R. Yurasov, D. Zimenkov, V. Mikhailovich, A. Zasedatelev, and D. Gryadunov, "Rotary-based platform with disposable fluidic modules for automated isolation of nucleic acids," *Biomedical Microdevices*, vol. 17, 2015.

[112] C. T. Schembri, T. L. Burd, A. R. Kopf-Sill, L. R. Shea, and B. Braynin, "Centrifugation and capillarity integrated into a multiple analyte whole blood analyser.," *The Journal of automatic chemistry*, vol. 17, pp. 99–104, Jan. 1995.

[113] J. Zhang, Q. Guo, M. Liu, and J. Yang, "A lab-on-CD prototype for high-speed blood separation," *Journal of Micromechanics and Microengineering*, vol. 18, p. 125025, Dec. 2008.

[114] A. E. Boycott, "Sedimentation of Blood Corpuscles," *Nature*, vol. 104, pp. 532–532, Jan. 1920.

[115] U. Schaflinger, "Centrifugal separation of a mixture," *Fluid Dynamics Research*, vol. 6, pp. 213–249, Dec. 1990.

[116] T.-H. Kim, H. Hwang, R. Gorkin, M. Madou, and Y.-K. Cho, "Geometry effects on blood separation rate on a rotating disc," *Sensors and Actuators B: Chemical*, vol. 178, pp. 648–655, Mar. 2013.

[117] D. J. Kinahan, S. M. Kearney, M. T. Glynn, and J. Ducrée, "Spira mirabilis enhanced whole blood processing in a lab-on-a-disk," *Sensors and Actuators A: Physical*, pp. 1–6, Nov. 2013.

[118] A. LaCroix-Fralish, E. J. Templeton, E. D. Salin, and C. D. Skinner, "A rapid prototyping technique for valves and filters in centrifugal microfluidic devices.," *Lab on a chip*, vol. 9, pp. 3151–4, Nov. 2009.

[119] E. J. Templeton and E. D. Salin, "A novel filtration method integrated on centrifugal microfluidic devices," *Microfluidics and Nanofluidics*, vol. 17, pp. 245–251, Nov. 2013.

[120] J. Kim, S. Hee Jang, G. Jia, J. V. Zoval, N. a. Da Silva, and M. J. Madou, "Cell lysis on a microfluidic CD (compact disc).," *Lab on a chip*, vol. 4, pp. 516–22, Oct. 2004.

[121] J. Steigert, M. Grumann, T. Brenner, L. Riegger, J. Harter, R. Zengerle, and J. Ducrée, "Fully integrated whole blood testing by real-time absorption measurement on a centrifugal platform.," *Lab on a chip*, vol. 6, pp. 1040–4, Aug. 2006.

[122] P. Sajeesh and A. K. Sen, "Particle separation and sorting in microfluidic devices: a review," *Microfluidics and Nanofluidics*, vol. 17, pp. 1–52, Nov. 2013.

[123] Y. Ukita, S. Kondo, T. Azeta, M. Ishizawa, C. Kataoka, M. Takeo, and Y. Utsumi, "Stacked centrifugal microfluidic device with three-dimensional microchannel networks and multifunctional capillary bundle structures for immunoassay," *Sensors and Actuators B: Chemical*, vol. 166-167, pp. 898–906, May 2012.

[124] S. O. Sundberg, C. T. Wittwer, C. Gao, and B. K. Gale, "Spinning disk platform for microfluidic digital polymerase chain reaction," *Analytical Chemistry*, vol. 82, pp. 1546–1550, Feb. 2010.

[125] L. Riegger, M. Grumann, T. Nann, J. Riegler, O. Ehlert, W. Bessler, K. Mittenbuehler, G. Urban, L. Pastewka, T. Brenner, R. Zengerle, and J. Ducrée, "Read-out concepts for multiplexed bead-based fluorescence immunoassays on centrifugal microfluidic platforms," *Sensors and Actuators A: Physical*, vol. 126, pp. 455–462, Feb. 2006.

[126] K. J. Fraley, L. Abberley, C. S. Hottenstein, J. J. Ulicne, D. R. Citerone, and M. E. Szapacs, "The Gyrolab immunoassay system: a platform for automated bioanalysis and rapid sample turnaround.," *Bioanalysis*, vol. 5, pp. 1765–74, 2013.

[127] R. Peytavi, F. R. Raymond, D. Gagné, F. J. Picard, G. Jia, J. Zoval, M. Madou, K. Boissinot, M. Boissinot, L. Bissonnette, M. Ouellette, and M. G. Bergeron, "Microfluidic device for rapid (<15 min) automated microarray hybridization.," *Clinical chemistry*, vol. 51, pp. 1836–44, Oct. 2005.

[128] Z. Zhao, R. Peytavi, G. a. Diaz-Quijada, F. J. Picard, A. Huletsky, E. Leblanc, J. Frenette, G. Boivin, T. Veres, M. M. Dumoulin, and M. G. Bergeron, "Plastic polymers for efficient DNA microarray hybridization: Application to microbiological diagnostics," *Journal of Clinical Microbiology*, vol. 46, no. 11, pp. 3752–3758, 2008.

[129] J. R. Epstein, I. Biran, and D. R. Walt, "Fluorescence-based nucleic acid detection and microarrays," *Analytica Chimica Acta*, vol. 469, no. 1, pp. 3–36, 2002.

[130] Y. Ukita and Y. Takamura, "A new stroboscopic technique for the observation of microscale fluorescent objects on a spinning platform in centrifugal microfluidics," *Microfluidics and Nanofluidics*, May 2014.

[131] J. Kuo, C.-h. Chiou, and W. Lee, "Design of PDMS microlenses bonded to a lab-CD chip for ELISA applications," *Journal of the Chinese Institute of ...*, vol. 35, no. 5, pp. 589–594, 2012.

[132] M. Grumann, J. Steigert, L. Riegger, I. Moser, B. Enderle, K. Riebeseel, G. Urban, R. Zengerle, and J. Ducrée, "Sensitivity enhancement for colorimetric glucose assays on whole blood by on-chip beam-guidance.," *Biomedical microdevices*, vol. 8, pp. 209–14, Sept. 2006.

[133] J. Steigert, M. Grumann, T. Brenner, K. Mittenbuhler, T. Nann, J. Ruhe, I. Moser, S. Haeberle, L. Riegger, and J. Riegler, "Integrated Sample Preparation, Reaction, and Detection on a High-frequency Centrifugal Microfluidic Platform," *Journal of the Association for Laboratory Automation*, vol. 10, pp. 331–341, Oct. 2005.

[134] H. Jiang, X. Weng, and D. Li, "Microfluidic whole-blood immunoassays," *Microfluidics and Nanofluidics*, vol. 10, pp. 941–964, Oct. 2010.

[135] M. J. Madou, *Fundamentals of Microfabrication: The Science of Miniaturization*. Boca Raton, FL: CRC Press, 2nd ed., 2002.

[136] J. Wang, "Electrochemical biosensors: towards point-of-care cancer diagnostics.," *Biosensors & bioelectronics*, vol. 21, pp. 1887–92, Apr. 2006.

[137] C. E. Nwankire, A. Venkatanarayanan, R. J. Forster, and J. Ducrée, "Electrochemical detection of cancer cells on a centrifugal microfluidic platform," in *MicroTAS*, pp. 1510–1512, 2012.

[138] T.-H. Kim, K. Abi-Samra, V. Sunkara, D.-K. Park, M. Amasia, N. Kim, J. Kim, H. Kim, M. Madou, and Y.-K. Cho, "Flow-enhanced electrochemical immunosensors on centrifugal microfluidic platforms.," *Lab on a chip*, vol. 13, pp. 3747–54, Sept. 2013.

[139] S. Z. Andreasen, D. Kwasny, L. Amato, A. L. Brø gger, F. G. Bosco, K. B. Andersen, W. E. Svendsen, and A. Boisen, "Integrating electrochemical detection with centrifugal microfluidics for real-time and fully automated sample testing," *RSC Adv.*, vol. 5, pp. 17187–17193, 2015.

[140] A. J. Bard and L. R. Faulkner, *Electrochemical methods: fundamentals and applications (Vol. 2)*. New York: Wiley Online Library, 1980.

[141] K. Abi-Samra, T.-H. Kim, D.-K. Park, N. Kim, J. Kim, H. Kim, Y.-K. Cho, and M. Madou, "Electrochemical velocimetry on centrifugal microfluidic platforms.," *Lab on a chip*, vol. 13, pp. 3253–60, Aug. 2013.

[142] J. Siegrist, M. Amasia, N. Singh, D. Banerjee, and M. Madou, "Numerical modeling and experimental validation of uniform microchamber filling in centrifugal microfluidics.," *Lab on a chip*, vol. 10, pp. 876–86, Apr. 2010.

[143] C. E. Nwankire, A. Venkatanarayanan, T. Glennon, T. E. Keyes, R. J. Forster, and J. Ducrée, "Label-free impedance detection of Cancer cells from whole blood on an integrated centrifugal microfluidic platform," *Biosensors and Bioelectronics*, vol. 68, pp. 382–389, Dec. 2014.

[144] L. Zhang, J. Zhu, T. Li, and E. Wang, "Bifunctional colorimetric oligonucleotide probe based on a G-quadruplex DNAzyme molecular beacon," *Analytical Chemistry*, vol. 83, pp. 8871–8876, 2011.

[145] R. Ke, A. Zorzet, J. Göransson, G. Lindegren, B. Sharifi-Mood, S. Chinikar, M. Mardani, A. Mirazimi, and M. Nilsson, "Colorimetric nucleic acid testing assay for RNA virus detection based on circle-to-circle amplification of padlock probes," *Journal of Clinical Microbiology*, vol. 49, no. 12, pp. 4279–4285, 2011.

[146] Z. Zheng, J. Han, W. Pang, and J. Hu, "G-quadruplex DNAzyme molecular beacon for amplified colorimetric biosensing of pseudostellaria heterophylla," *Sensors (Switzerland)*, vol. 13, pp. 1064–1075, 2013.

[147] F. Xia, X. Zuo, R. Yang, Y. Xiao, D. Kang, A. Vallée-Bélisle, X. Gong, J. D. Yuen, B. B. Y. Hsu, A. J. Heeger, and K. W. Plaxco, "Colorimetric detection of DNA, small molecules, proteins, and ions using unmodified gold nanoparticles and conjugated polyelectrolytes.," *Proceedings of the National Academy of Sciences of the United States of America*, vol. 107, no. 33, pp. 10837–10841, 2010.

[148] M. Donolato, P. Antunes, R. Burger, F. Bosco, M. Olsson, J. Yang, C.-h. Chen, Q. Lin, E. T. Hwu, A. Boisen, and M. F. Hansen, "Lab-on-Blu-ray: Low-cost analyte detection on a disk," in *Proceedings of the 18th International Conference on Miniaturized Systems for Chemistry and Life Sciences*, pp. 2044–2046, 2014.

[149] A. Sassolas, B. Leca-Bouvier, and L. Blum, "DNA Biosensors and Microarrays," *Chemical reviews*, 2008.

[150] T. G. Drummond, M. G. Hill, and J. K. Barton, "Electrochemical DNA sensors.," *Nature biotechnology*, vol. 21, pp. 1192–9, Oct. 2003.

[151] E. Paleček, "Fifty Years of Nucleic Acid Electrochemistry," *Electroanalysis*, vol. 21, pp. 239–251, Feb. 2009.

[152] S. Takenaka, K. Yamashita, and M. Takagi, "DNA sensing on a DNA probe-modified electrode using ferrocenylnaphthalene diimide as the electrochemically active ligand," *Analytical ...*, vol. 72, no. 6, pp. 1334–1341, 2000.

[153] Z. Wu, J. Jiang, G. Shen, and R. Yu, "Highly Sensitive DNA Detection and Point Mutation Identification : An Electrochemical Approach Based on the Combined Use of Ligase and Reverse Molecular Beacon," *Human mutation*, vol. 28, no. February, pp. 630–637, 2007.

[154] S. Suye, T. Matsuura, T. Kimura, H. Zheng, T. Hori, Y. Amano, and H. Katayama, "Amperometric DNA sensor using gold electrode modified with polymerized mediator by layer-by-layer adsorption," *Microelectronic Engineering*, vol. 81, pp. 441–447, Aug. 2005.

[155] E. Katz, I. Willner, and J. Wang, "Electroanalytical and Bioelectroanalytical Systems Based on Metal and Semiconductor Nanoparticles," *Electroanalysis*, vol. 16, pp. 19–44, Jan. 2004.

[156] M. Wang, C. Sun, L. Wang, X. Ji, Y. Bai, T. Li, and J. Li, "Electrochemical detection of DNA immobilized on gold colloid particles modified self-assembled monolayer electrode with silver nanoparticle label," *Journal of Pharmaceutical and Biomedical Analysis*, vol. 33, pp. 1117–1125, Dec. 2003.

[157] F. Azek, C. Grossiord, M. Joannes, B. Limoges, and P. Brossier, "Hybridization assay at a disposable electrochemical biosensor for the attomole detection of amplified human cytomegalovirus DNA.," *Analytical biochemistry*, vol. 284, pp. 107–13, Aug. 2000.

[158] J. Wang, A.-N. Kawde, and M. Musameh, "Carbon-nanotube-modified glassy carbon electrodes for amplified label-free electrochemical detection of DNA hybridization," *The Analyst*, vol. 128, no. 7, p. 912, 2003.

[159] C. Tlili, H. Korri-Youssoufi, L. Ponsonnet, C. Martelet, and N. J. Jaffrezic-Renault, "Electrochemical impedance probing of DNA hybridisation on oligonucleotide-functionalised polypyrrole.," *Talanta*, vol. 68, pp. 131–7, Nov. 2005.

[160] E. Paleček, "Oscillographic Polarography of Highly Polymerized Deoxyribonucleic Acid," *Nature*, vol. 188, pp. 656–657, Nov. 1960.

[161] X. Chen, C.-Y. Hong, Y.-H. Lin, J.-H. Chen, G.-N. Chen, and H.-H. Yang, "Enzyme-free and label-free ultrasensitive electrochemical detection of human immunodeficiency virus DNA in biological samples based on long-range self-assembled DNA nanostructures.," *Analytical chemistry*, vol. 84, pp. 8277–83, Oct. 2012.

[162] S. Haeberle, R. Zengerle, and J. Ducrée, "Centrifugal generation and manipulation of droplet emulsions," *Microfluidics and Nanofluidics*, vol. 3, pp. 65–75, July 2006.

[163] M. A. Ansari and K.-Y. Kim, "Shape optimization of a micromixer with staggered herringbone groove," *Chemical Engineering Science*, vol. 62, pp. 6687–6695, Dec. 2007.

[164] L. Wang and P. C. H. Li, "Optimization of a microfluidic microarray device for the fast discrimination of fungal pathogenic DNA.," *Analytical biochemistry*, vol. 400, pp. 282–8, May 2010.

[165] "Piccolo Xpress." `http://www.piccoloxpress.com/`, 2012.

[166] "WaterLink Spin Lab." `http://www.lamotte.com/en/pool-spa/labs/3576.html/`, 2014.

[167] "Samsung LABGEO IB10." `http://www.samsungmedison.com/ivd/labgeo_ib10.jsp/`, 2011.

[168] "Gyrolab xP workstation." `http://www.gyros.com/products/products-optimized/gyrolab-xp-workstation/`, 2014.

[169] "The 3M Integrated Cycler." `http://www.focusdx.com/3m-integrated-cycler/ic-us/`, 2012. [Online; accessed 2012].

[170] "GenePOC." `http://www.genepoc-diagnostics.com/`, 2012. [Online; accessed 2013].

[171] "cobas® Liat System." http://molecular.roche.com/instruments/Pages/cobasLIATsystem.aspx/, 2015. [Online; accessed 20th-May-2015].

[172] "Cepheid." http://www.cepheid.com/, 2012. [Online; accessed 15-November-2012].

[173] "BioFire Diagnostics, Inc. ." http://www.biofiredx.com/, 2012. [Online; accessed 15-November-2012].

[174] "Alere™ i." http://www.alere-i.com/alere-i-influenza-a-b/, 2015.

[175] A. Kloke, a. R. Fiebach, S. Zhang, L. Drechsel, S. Niekrawietz, M. M. Hoehl, R. Kneusel, K. Panthel, J. Steigert, F. von Stetten, R. Zengerle, and N. Paust, "The LabTube - a novel microfluidic platform for assay automation in laboratory centrifuges.," *Lab on a chip*, vol. 14, pp. 1527–37, May 2014.

[176] J. L. Garcia-Cordero, L. Basabe-Desmonts, J. Ducrée, and A. J. Ricco, "Liquid recirculation in microfluidic channels by the interplay of capillary and centrifugal forces," *Microfluidics and Nanofluidics*, vol. 9, pp. 695–703, Mar. 2010.

[177] M. C. R. Kong, A. P. Bouchard, and E. D. Salin, "Displacement Pumping of Liquids Radially Inward on Centrifugal Microfluidic Platforms in Motion," *Micromachines*, vol. 3, pp. 1–9, Dec. 2011.

[178] D. Subedi, R. Tyata, and D. Rimal, "Effect of uv-treatment on the wettability of polycarbonate," *... university journal of science, engineering and ...*, vol. 5, no. Ii, pp. 37–41, 2009.

[179] L. Kong, J. M. Rodriguez, A. Perebikovsky, J. Moebius, R. Mitchell, L. Kulinsky, and M. Madou, "Novel heating and cooling techniques on a centrifugal fluidic platform for polymerase chain reaction," in *Microtechnologies in Medicine and Biology*, p. 1, 2013.

[180] S. Soroori, L. Kulinsky, and M. Madou, "Centrifugal Microfluidics: Characteristics & Possibilities," in *Microfluidics and Microscale ...* (S. Chakraborty, ed.), ch. Centrifuga, pp. 149–186, CRC Press, 2013.

[181] N. Malmstadt, A. S. Hoffman, and P. S. Stayton, ""Smart" mobile affinity matrix for microfluidic immunoassays.," *Lab on a chip*, vol. 4, pp. 412–5, Aug. 2004.

[182] H.-H. Hou, Y.-N. Wang, C.-L. Chang, R.-J. Yang, and L.-M. Fu, "Rapid glucose concentration detection utilizing disposable integrated microfluidic chip," *Microfluidics and Nanofluidics*, vol. 11, pp. 479–487, May 2011.

[183] V. Miralles, A. Huerre, F. Malloggi, and M.-C. Jullien, "A Review of Heating and Temperature Control in Microfluidic Systems: Techniques and Applications," *Diagnostics*, vol. 3, pp. 33–67, Jan. 2013.

[184] D. M. Sagar, S. Aoudjane, M. Gaudet, G. Aeppli, and P. a. Dalby, "Optically Induced Thermal Gradients for Protein Characterization in Nanolitre-scale Samples in Microfluidic Devices," *Scientific Reports*, vol. 3, pp. 1–6, July 2013.

[185] C. Zhang and D. Xing, "Miniaturized PCR chips for nucleic acid amplification and analysis: latest advances and future trends.," *Nucleic acids research*, vol. 35, pp. 4223–37, Jan. 2007.

[186] L. A. Wainwright and H. S. Seifert, "Paraffin beads can replace mineral oil as an evaporation barrier in PCR.," *BioTechniques*, vol. 14, pp. 34–6, Jan. 1993.

[187] B. Hébert, J. Bergeron, E. F. Potworowski, and P. Tijssen, "Increased PCR sensitivity by using paraffin wax as a reaction mix overlay.," *Molecular and cellular probes*, vol. 7, pp. 249–52, June 1993.

[188] J. M. S. Bartlett and D. Stirling, "A short history of the polymerase chain reaction.," *Methods in molecular biology (Clifton, N.J.)*, vol. 226, pp. 3–6, Jan. 2003.

[189] M. Kubista, J. M. Andrade, M. Bengtsson, A. Forootan, J. Jonák, K. Lind, R. Sindelka, R. Sjöback, B. Sjögreen, L. Strömbom, A. Stå hlberg, and N. Zoric, "The real-time polymerase chain reaction," *Molecular Aspects of Medicine*, vol. 27, no. 2-3, pp. 95–125, 2006.

[190] W. Rychlik, W. J. Spencer, and R. E. Rhoads, "Optimization of the annealing temperature for DNA amplification in vitro," *Nucleic Acids Research*, vol. 19, no. 3, p. 698, 1991.

[191] G. J. Kellogg, T. E. Arnold, B. L. Carvalho, D. C. Duffy, and N. F. Sheppard, "Centrifugal Microfluidics: Applications," in *Proceedings of Micro Total Analysis Systems*, p. 239, 2000.

[192] M. Amasia, S.-W. Kang, D. Banerjee, and M. Madou, "Experimental validation of numerical study on thermoelectric-based heating in an integrated centrifugal microfluidic platform for polymerase chain reaction amplification.," *Biomicrofluidics*, vol. 7, p. 14106, Jan. 2013.

[193] G. Mårtensson, M. Skote, M. Malmqvist, M. Falk, A. Asp, N. Svanvik, and A. Johansson, "Rapid PCR amplification of DNA utilizing Coriolis effects.," *European biophysics journal : EBJ*, vol. 35, pp. 453–8, Aug. 2006.

[194] J. Burger, A. Gross, D. Mark, G. Roth, F. von Stetten, and R. Zengerle, "IR thermocycler for centrifugal microfluidic platform with direct on-disk wireless temperature measurement system," in *SPIE Microtechnologies* (U. Schmid, J. L. Sánchez-Rojas, and M. Leester-Schaedel, eds.), pp. 80661X–80661X–8, May 2011.

[195] G. Wang, H.-P. Ho, Q. Chen, A. K.-L. Yang, H.-C. Kwok, S.-Y. Wu, S.-K. Kong, Y.-W. Kwan, and X. Zhang, "A lab-in-a-droplet bioassay strategy for centrifugal microfluidics with density difference pumping, power to disc and bidirectional flow control.," *Lab on a chip*, vol. 13, pp. 3698–706, Sept. 2013.

[196] B. Spiess, W. Seifarth, M. Hummel, O. Frank, A. Fabarius, C. Zheng, H. Mörz, R. Hehlmann, and D. Buchheidt, "DNA microarray-based detection and identification of fungal pathogens in clinical samples from neutropenic patients," *Journal of Clinical Microbiology*, vol. 45, no. 11, pp. 3743–3753, 2007.

[197] J. He, M. E. Bose, E. T. Beck, J. Fan, S. Tiwari, J. Metallo, L. a. Jurgens, S. C. Kehl, N. Ledeboer, S. Kumar, W. Weisburg, and K. J. Henrickson, "Rapid multiplex reverse transcription-PCR typing of influenza A and B virus, and subtyping of influenza A virus into H1, 2, 3, 5, 7, 9, N1 (human), N1 (animal), N2, and N7, including typing of novel swine origin influenza A (H1N1) virus, during the 2009 O," *Journal of Clinical Microbiology*, vol. 47, no. 9, pp. 2772–2778, 2009.

[198] K. Boissinot, A. Huletsky, R. Peytavi, S. Turcotte, V. Veillette, M. Boissinot, F. J. Picard, E. A. Martel, and M. G. Bergeron, "Rapid exonuclease digestion of PCR-amplified targets for improved microarray hybridization," in *Clinical Chemistry*, vol. 53, pp. 2020–2023, 2007.

[199] S. Soroori, *Novel Flow Control Schemes Utilizing Intrinsic Forces on Centrifugal Microfluidic Platforms.* Dissertation, University of California, Irvine, 2013.

[200] C. Zhang, J. Xu, W. Ma, and W. Zheng, "PCR microfluidic devices for DNA amplification.," *Biotechnology advances*, vol. 24, no. 3, pp. 243–84, 2006.

[201] X. Chen, L. Song, B. Assadsangabi, J. Fang, M. S. Mohamed Ali, and K. Takahata, "Wirelessly addressable heater array for centrifugal microfluidics and escherichia coli sterilization.," *Conference proceedings : ... Annual International Conference of the IEEE Engineering in Medicine and Biology Society. IEEE Engineering in Medicine and Biology Society. Conference*, vol. 2013, pp. 5505–8, Jan. 2013.

[202] T. Notomi, H. Okayama, H. Masubuchi, T. Yonekawa, K. Watanabe, N. Amino, and T. Hase, "Loop-mediated isothermal amplification of DNA.," *Nucleic acids research*, vol. 28, no. 12, p. E63, 2000.

[203] P. Gill and A. Ghaemi, "Nucleic acid isothermal amplification technologies: a review.," *Nucleosides, nucleotides & nucleic acids*, vol. 27, pp. 224–43, Mar. 2008.

[204] P. J. Asiello and A. J. Baeumner, "Miniaturized isothermal nucleic acid amplification, a review.," *Lab on a chip*, vol. 11, pp. 1420–30, Apr. 2011.

[205] P. Craw and W. Balachandran, "Isothermal nucleic acid amplification technologies for point-of-care diagnostics: a critical review.," *Lab on a chip*, vol. 12, pp. 2469–86, July 2012.

[206] T.-H. Kim, J. Park, C.-J. Kim, and Y.-K. Cho, "Fully Integrated Lab-on-a-Disc for Nucleic Acid Analysis of Food-Borne Pathogens.," *Analytical chemistry*, Mar. 2014.

[207] C. Escadafal, O. Faye, A. A. Sall, O. Faye, M. Weidmann, O. Strohmeier, F. von Stetten, J. Drexler, M. Eberhard, M. Niedrig, and P. Patel, "Rapid molecular assays for the detection of yellow fever virus in low-resource settings.," *PLoS neglected tropical diseases*, vol. 8, p. e2730, Mar. 2014.

[208] V. Linder, S. K. Sia, and G. M. Whitesides, "Reagent-loaded cartridges for valveless and automated fluid delivery in microfluidic devices.," *Analytical chemistry*, vol. 77, pp. 64–71, Jan. 2005.

[209] M. J. Madou, *Fundamentals of Microfabrications and Nanotechnology: From MEMS to Bio-MEMS and Bio-NEMS*. Boca Raton, FL: CRC Press, 3rd ed., 2012.

[210] P. H.-D. Chen, J. B. Findlay, S. M. Atwood, and L. Bergmeyer, "Nucleic acid material amplification and detection without washing," 1995.

Appendix A

Effect of Paraffin Wax Layer on Sample Evaporation

Studies in the past have shown that paraffin wax can replace mineral oil, which acts to reduce sample evaporation, a role especially crucial when the sample volume is small (<500 μL). Paraffin wax was even found to increase the sensitivity of PCR assay outcomes [186, 187]. However, when utilizing the multifunctional wax valves (Section 2.2, [92]), whether the reduced evaporation was due to the presence of paraffin wax or spinning of the disc was not clear. This informal study was then performed to conclude if paraffin wax effectively reduces liquid sample evaporation. The outcome of the study will aid in the effective operation of PCR assays.

Twenty-two samples, consisting of 25μL colored water, were placed in a microfluidic unit identical to the ones being used for the multifunctional wax valves microfluidic unit (Figure 2.6). This microfluidic disc design ensures that the fluidic reservoir is open to atmosphere, enabling condition for evaporation. The disc containing each set of samples was spun at 2,000 RPM. Images were taken and quantitatively analyzed with SolidWorks software (Dassault Systèmes SOLIDWORKS Corp., Waltham, Massachusetts, USA). The remaining volume of each sample can be estimated with the software, and the percentage remaining is recorded.

The results were processed in a two-sample t-test, which evaluates two different sets of samples for their difference and determines that if it is likely for that difference to be present by chance. The result of the test is shown in Figure A.1. The obtained p-value was 0.82,

implying that it is extremely unlikely for the presence of wax to make a difference in reducing evaporation.

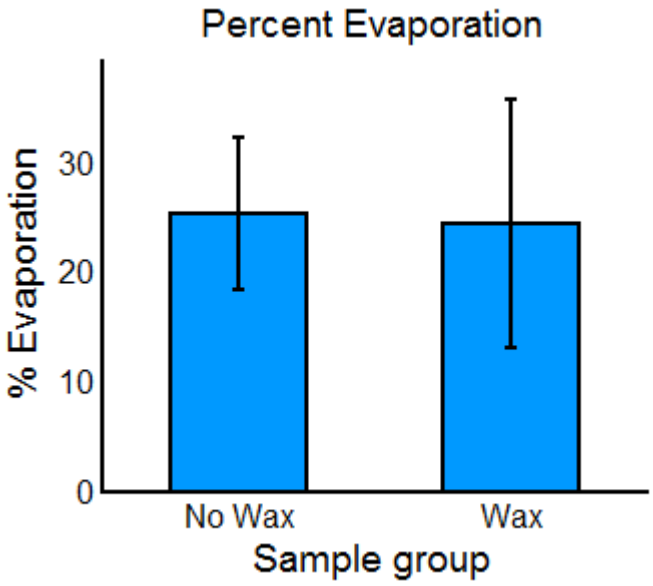

Figure A.1: The graph shows the loss by evaporation of water samples that have a wax layer or no wax layer above it. There were 12 samples with wax and 10 samples without wax. A two-sample t-test was performed on the data and a p-value of 0.82 was obtained, implying that wax is unlikely to reduce evaporation.

The efficacy of evaporation reduction thus comes from spinning of the disc. This phenomenon is effective at reducing evaporation because it maintains the organization of the liquid to reduce the area of the air-liquid interface. This allows less surface area for the aqueous phase to enter the gas phase. The reduction of evaporation is also due to the ability of centrifugation to re-collect condensate that settles closer to the center of the microfluidic disc. While paraffin wax is ineffective at preventing evaporation, it still plays an essential role in the multifunctional wax valves technology where it aids in transfer of liquid. However, in a situation where wax is unnecessary, eliminating it completely can reduce cost, complexity, and contamination.

Appendix B

Storage and Release of Liquid Reagents in Glass Capsules

Long term storage of liquid reagents, as discussed in Section 1.5, are not only crucial, but are significantly more difficult than storage of solid reagents, which can be may be dried, lyophilized or precipitated. When directly stored in a microfluidic device, the integrity of liquid reagents cannot remain for more than a few weeks and premature exchange of liquid or vapors on the device is likely [208]. To achieve valves that enable simple and low-cost fabrication, on-demand release, and long term (12-18 months) storage, a few factors play a crucial role in the performance of the valves: material, fabrication, and implementation.

For vapor-tight storage of liquid reagents, the material is possibly the most important factor. Even a well-made valve may not retain liquid for long if the material is poorly chosen. The most common categories of materials used for liquid reagent storage are:

1. **Glass**—This is the most ideal material for reagent storage because it is inert in the presence of most reagents. Perfectly fabricated glass containers can retain liquid safely for years. However, the fragility of glass makes it a challenge to implement in all systems. Release can also be difficult with microfluidic glass containers due to the need to release on-demand, automatically, and safely. Hoffman *et al.* had previously released reagents by manual interference [96]. A more elegant method for reagent release is demanded.

2. **Polymer**—This material category includes various plastics and waxes. These materials tend to be more porous and have shorter shelf lives. In addition, implementation can

be challenging, resulting in low robustness. A successful valve implementation was by Johnson & Johnson, where a roller opens single-use, normally closed valves [209, 210]. Tubes of reagents operated by robots are more common, but cannot be implemented on a disc.

3. **Metal**—This may be the most common material for reagent storage due to the practicality of foil or metalized pouches. Foil pouches can store liquids for long periods of time when manufactured properly and can be easily opened by piercing. Innovative use of foil pouches for liquid reagent and release has been demonstrated by van Oordt *et al.*, who sealed the pouches by ultrasonic welding and performed automated reagent release by centrifugal force [95].

Fabrication and implementation can add to the cost and complexity of a method. For example, multifunctional wax valves (see Section 2.2) are difficult to fabricate, and both multifunctional wax valves and the laser-operated valves by Garcia-Cordero *et al.* require a heat source to operate, adding to the hardware cost [46, 92]. For implementation, the same valves by Garcia-Cordero *et al.* and the Laser Irradiated Ferrowax Microvalves (LIFM) by Park *et al.* require stopping disc and serially aligning of the heat source to each spot to be heated [71]. This requirement adds complexity to the hardware system, so that a visual recognition feature or a rotary encoder to track of the disc position may be required, increasing cost and operation time.

A novel method has been implemented to store and release liquid reagents using glass capsules. This method seeks to increase shelf-life and reduce complexity in implementation. The principle of the method is to break open glass capsules on-demand by increasing the spin frequency of the disc above a certain threshold, which increases the centrifugal force of a heavy object sitting on top of the glass capsule (Figure B.1). The heavy object can be small ceramic or stainless steel balls that do not interfere with any on-disc reactions. Above the critical spin frequency threshold, the stress caused by the centrifugal force exerted on the glass capsule overcomes the strength of the glass capsule, breaking it open and releasing the liquid inside. This method is fully automated, and the high critical spin frequency ensures that typical on-disc assay steps will not prematurely open the glass capsule.

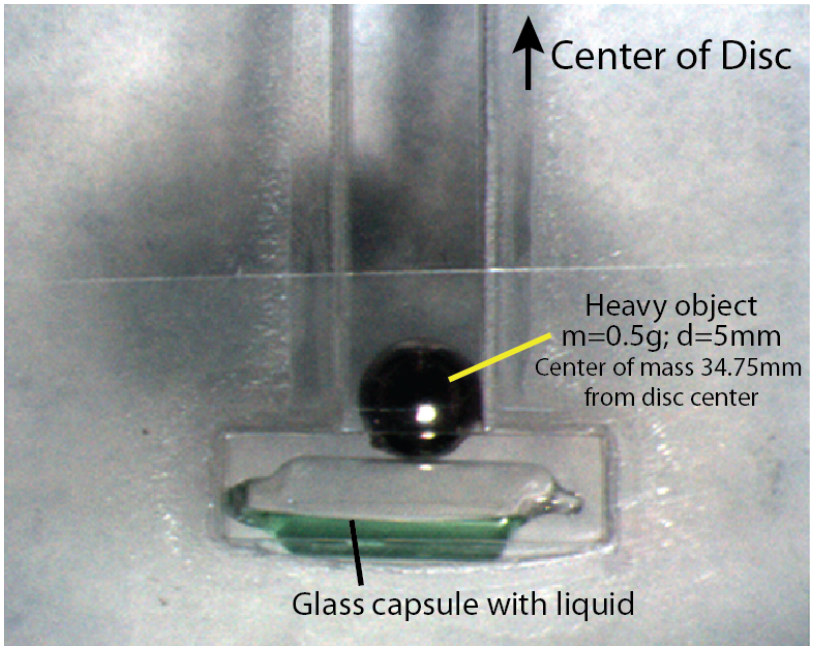

Figure B.1: The glass capsule liquid reagent storage and release method set up in a disc. The metal weight is 0.5 g in mass. The glass capsule has a wall thickness of 50 μm.

B.1 Experimental Methods

A fluidic disc was fabricated to hold glass capsules that are 4.1 mm in diameter, between 11 and 15 mm in length, and 50 μm in wall thickness. These glass capsules are placed in chamber so that they are perpendicular to the radial distance of the disc. The "heavy object" is a metal ball of 5 mm in diameter and 0.5 g in mass, which is placed adjacent and just inward of the glass capsule. The center of the ball is located 34.75 mm from the center of the disc.

The disc was spun at 4,000 RPM and ramped up by 200 RPM at a time until the glass capsule was broken by the metal ball. After each ramping step, the spin frequency was maintained for about 5 seconds. Three preliminary trials were performed and critical breaking spin frequencies of 5,000 RPM, 6,000 RPM, and 5,600 RPM were recorded.

B.2 Physics and Theory

This liquid storage-release system leverages the centrifugal force exerted by a heavy object to break the glass capsule. Figure B.2a shows a free body diagram of the system on a rotating

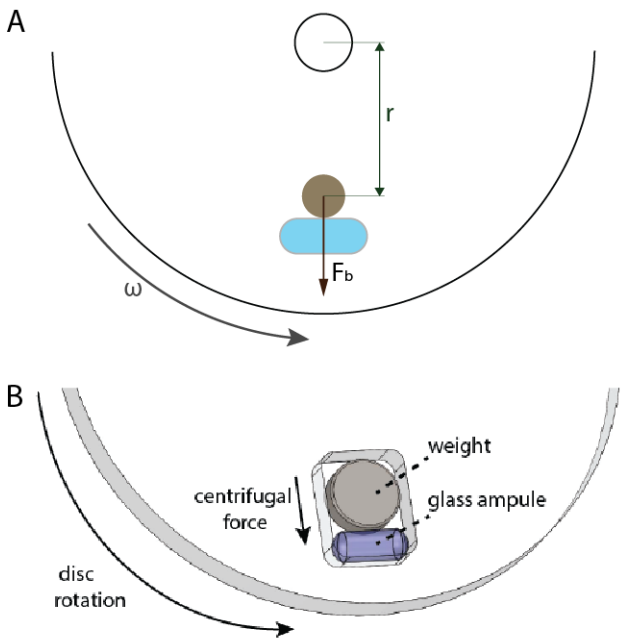

Figure B.2: The setup for the glass capsule liquid reagent storage and release method is shown. A free body diagram shows the centrifugal force (F_n) exerted by the heavy object on the glass capsule (A). Illustration of the setup (B).

centrifugal microfluidic disc. The force exerted on the glass capsule by the heavy object under centrifugal force is equal to:

$$F_b = m_b \times r \times \vec{\omega} \times \vec{\omega} \tag{B.1}$$

where m_b is the mass of the heavy object, r is the distance from the center of the disc to the center of mass of the heavy object, and $\vec{\omega}$ is the angular velocity of the disc.

The glass capsule breaks when the stress exerted on the capsule exceeds its compressive strength. For a horizontally placed glass capsule, a distributed reaction load is exerted by the bottom wall of the chamber on the glass capsule opposite of the direction of the centrifugal force. The stresses due to the reaction and centrifugal force appear as bending and shear stress terms. The bending stress is:

$$\sigma_{x,max} = \frac{Mc}{I} \tag{B.2}$$

where M is the moment of inertial of the glass capsule:

$$M = \frac{1}{2} F_b \left(\frac{l}{2}\right)^2 = \left(\frac{1}{8}\right) l^2 (m_b \times r \times \vec{\omega} \times \vec{\omega}) \tag{B.3}$$

and l, I, and c are the length of the glass capsule, moment of inertia of the glass capsule, and the maximum distance from the point of stress to the neutral axis of the capsule, respectively. Shear stress is significant in short, cylindrical structures and must be taken into the account:

$$\tau_{xy,max} = \frac{VQ}{It} \tag{B.4}$$

where V is the normal component of the shear force acting on the capsule, Q is the first moment with respect of the neutral axis of the glass capsule, and t is the thickness of the capsule wall. The maximum shear force that the heavy object can exert on the glass capsule is:

$$V_{max} = \frac{1}{2}F_b l \tag{B.5}$$

The glass capsule breaks when the maximum stress applied on the capsule exceeds its fracture strength. The maximum stress is calculated as follows:

$$\sigma_{max} = \frac{1}{2}\sigma_x \pm \sqrt{\left(\frac{\sigma_x}{2}\right)^2 - \tau_{xy}^2} \tag{B.6}$$

B.3 Discussion

While the spread of the critical disc angular velocity for breaking the glass capsule is quite large, the mass of the heavy object can be chosen so that the minimum critical angular velocity can be higher or lower as desired. A higher critical angular velocity, which can be achieved using a heavy object with a smaller mass, will allow more flexibility in the types of fluidic steps that can be performed before the liquid in the glass capsule needs to be released. A lower critical angular velocity, which can be achieved using a heavy object with a larger mass, will alleviate the cost of the system. For example, by breaking the glass capsule at a lower critical angular velocity, a less powerful, and hence, less expensive, motor for spinning the disc is required.

Shipping of stored reagents is often a concern, especially with glass containers which is very fragile. Due to the high centrifugal force required to break the glass capsule, it will be less likely to break when it is being manually handled; however, this can never be guaranteed. Thus, for shipping the disc, the heavy object can be wrapped in any cushioning material,

such as cotton or a thin layer of foam. Cushioning between the two components will reduce the impact between them if, for instance, the disc is dropped.

The production, filling, and sealing of the glass capsules can be expensive, as manufacturers often do not consider filling orders of fewer than 100,000 in quantity. Even so, glass is generally the most non-porous and non-reactive method to store liquid reagents. It was observed in 10 glass capsules that unless the tube was improperly sealed, the stored liquid experienced no loss after 1.5 years. It is hoped that the technique discussed in this section provides a solution for easy, on-demand release of stored liquid reagents with long shelf-life.